Structural Engineering Report 151

BEHAVIOUR AND ULTIMATE STRENGTH OF PARTIAL JOINT PENETRATION GROOVE WELDS

by

DARREL P. GAGNON

D. J. LAURIE KENNEDY

JULY, 1987

RECENT STRUCTURAL ENGINEERING REPORTS

Department of Civil Engineering

University of Alberta

120. *Concrete Masonry Prism Response due to Loads Parallel and Perpendicular to Bed Joints* by R. Lee, J. Longworth and J. Warwaruk.

121. *Standardized Flexible End Plate Connections for Steel Beams* by G.J. Kriviak and D.J.L. Kennedy, December 1984.

122. *The Effects of Restrained Shrinkage on Concrete Slabs* by K.S.S. Tam and A. Scanlon, December 1984.

123. *Prestressed Concrete Beams with Large Rectangular Web Openings* by T. do M.J. Alves and A. Scanlon, December 1984.

124. *Tests on Eccentrically Loaded Fillet Welds* by G.L. Kulak and P.A. Timler, December 1984.

125. *Analysis of Field Measured Deflections Scotia Place Office Tower* by A. Scanlon and E. Ho, December 1984.

126. *Ultimate Behaviour of Continuous Deep Reinforced Concrete Beams* by D.R. Ricketts and J.G. MacGregor, January 1985.

127. *The Interaction of Masonry Veneer and Steel Studs in Curtain Wall Construction* by W.M. McGinley, J. Warwaruk, J. Longworth and M. Hatzinikolas, May 1985.

128. *Evaluation of Existing Bridge Structure by Nondestructive Test Methods* by L. Mikhailovsky and A. Scanlon, May 1985.

129. *Finite Element Modelling of Buried Structures* by D.K. Playdon and S.H. Simmonds, October 1985.

130. *Behaviour and Ultimate Strength of Transversely Loaded Continuous Steel Plates* by K.P. Ratzlaff and D.J.L. Kennedy, November 1985.

131. *Inelastic Lateral Buckling of Steel Beam-Columns* by P.E. Cuk, M.A. Bradford and N.S. Trahair, December 1985.

132. *Design Strengths of Steel Beam-Columns* by N.S. Trahair, December 1985.

133. *Behaviour of Fillet Welds as a Function of the Angle of Loading* by G.S. Miazga and D.J.L. Kennedy, March 1986.

134. *Inelastic Seismic Response of Precast Concrete Large Panel Coupled Shear Wall Systems* by M.R. Kianoush and A. Scanlon, March 1986.

135. *Finite Element Prediction of Bin Loads* by A.H. Askari and A.E. Elwi, June 1986.

136. *Shear Behavior of Large Diameter Fabricated Steel Cylinders* by J. Mok and A.E. Elwi, June 1986.

137. *Local Buckling Rules for Structural Steel Members* by S. Bild and G.L. Kulak, May 1986.

138. *Finite Element Prediction of Reinforced Concrete Behavior* by S. Balakrishnan and D.W. Murray, July 1986.

139. *Behavior and Strength of Masonry Wall/Slab Joints* by T.M. Olatunji and J. Warwaruk, July 1986.

140. *Bayesian Analysis of In-Situ Test Data for Estimating the Compressive Strength of Concrete in Existing Structures* by G.J. Kriviak and A. Scanlon, July 1986.

141. *Shear-Moment Transfer in Slab-Column Connections* by S.D.B. Alexander and S.H. Simmonds, July 1986.

142. *Minimum Thickness Requirements for Deflection Control of Two-Way Slab Systems* by D.P. Thompson and A. Scanlon, November 1986.

143. *Shrinkage and Flexural Tests of Two Full-Scale Composite Trusses* by A. Brattland and D.J.L. Kennedy, December 1986.

144. *Combined Flexure and Torsion of I-Shaped Steel Beams* by R.G. Driver and D.J.L. Kennedy, March 1987.

145. *Cyclic and Static Behaviour of Thin Panel Steel Plate Shear Walls* by E.W. Tromposch and G.L. Kulak, April 1987.

146. *Postbuckling Behavior of Thin Steel Cylinders Under Transverse Shear* by V.G. Roman and A.E. Elwi, May 1987.

147. *Incipient Flow in Silos - A Numerical Approach* by R.A. Link and A.E. Elwi, May 1987.

148. *Design of Web-Flange Beam or Girder Splices* by D. Green and G.L. Kulak, May 1987.

149. *Spreadsheet Solution of Elastic Plate Bending Problems* by G.E. Small and S.H. Simmonds, July 1987.

150. *Behaviour of Transversely Loaded Continuous Steel-Concrete Composite Plates* by S.J. Kennedy and J.J. Cheng, July 1987.

151. *Behaviour and Ultimate Strength of Partial Joint Penetration Groove Welds* by D.P. Gagnon and D.J.L. Kennedy, July 1987.

Structural Engineering Report 151

THE BEHAVIOUR AND ULTIMATE STRENGTH OF PARTIAL JOINT PENETRATION GROOVE WELDS

by

Darrel P. Gagnon

and

D.J. Laurie Kennedy

Department of Civil Engineering

University of Alberta

Edmonton, Alberta

July 1987

Abstract

Partial joint penetration groove welds may be used where it is not necessary to develop the full tensile capacity of the cross-section or where it is not feasible to make a full joint penetration groove weld because welding can be done from one side only.

The limited experimental data in the literature on partial penetration welds indicate that weld strengths are proportional to the tensile capacity of the base metal and the area of the weld normal to the load. Despite this design standards base the strength on the shear capacity of the weld. A series of 75 tests on 25mm thick grade 300W or grade 350A steel plates, with welds made with matching electrodes and with 20 to 100% penetration, were conducted. Eccentrically loaded welds are as strong as concentrically loaded welds due to the inherent ductility of the welds that allows a relatively uniform stress state to develop before fracture. Welds are stronger than the plate on an unit area basis. This weld strength increases with decreasing penetration and is attributed to the lateral restraint. Overall specimen ductility is limited unless the weld is of sufficient penetration to cause general yielding of the plate before weld fracture.

Two proposals basing weld strength on the percent penetration multiplied by the ultimate tensile resistance of the plate are presented. Appropriate resistance factors for use with these proposals are also given.

Acknowledgements

This research was conducted under the supervision of Dr. D.J.L. Kennedy. His thoughtful guidance and unlimited patience are greatly appreciated.

I would like to thank S. Kennedy for the valuable assistance he provided throughout this study and the technical assistance of L. Burden and R. Helfrich during the experimental program.

Special thanks to C. Machon for the support and encouragement provided during the completion of this study.

Funding for this research was provided by the Canadian Steel Construction Council and supplemented with funds granted to Dr. Kennedy by the Natural Sciences and Engineering Research Council of Canada. Personal funding was received from the Alberta Region of the Canadian Institute of Steel Construction.

Table of Contents

List of Tables

List of Figures

List of Symbols

a	=	lack of penetration (Lawrence and Cox)
a'	=	upper limit of "a" for fracture to occur in plate (Lawrence and Cox)
a''	=	upper limit of "a" for general yielding to occur in plate before weld fractures
A_b	=	area of base metal normal to tensile load for partial joint penetration groove welds in tension
A_m	=	area of effective throat of weld
A_p	=	area of plate
A_w	=	area of weld
A_{wn}	=	net area of weld taking defects into account
A_θ	=	area of any plane at an angle θ from the weld throat
b	=	thickness of specimen (Lawrence and Cox) study
B	=	width of specimen (Lawrence and Cox) study
d	=	depth of penetration
e	=	the eccentricity of the applied load with respect to center of resistance of weld
E	=	modulus of elasticity
f	=	length of fillet weld leg

F_u = minimum specified ultimate strength of steel

F_y = minimum specified yield strength of steel

I = moment of Inertia

ℓ = half-length of specimen

M_e = moment in the plate at grips; subscript 1 indicates weld is elastic, subscript 2 indicates weld is plastic

M_p = moment in the plate at weld; with subscripts 1 and 2 as for M_e

M_w = moment in the weld; with subscripts 1 and 2 as for M_e

p = degree of weld penetration

P = applied axial load

P_m = permitted axial load based on von Mises criterion (Lawrence and Cox) study

P_t = permitted axial load based on Tresca criterion (Lawrence and Cox) study

P_u = unfactored limit load (Lawrence and Cox)

s = depth of preparation

t = thickness of plate

T_r = factored tensile resistance

T_{r1} = factored tensile resistance of partial penetration groove weld based on [6.2a]

T_{r2} = factored tensile resistance of partial penetration groove weld based on [6.3a]

V = coefficient of variation; shear force

V_r = factored shear resistance

V_{G1} = coefficient of variation of mean to nominal percent penetration

V_{G2} = coefficient of variation of plate dimensions

V_M = coefficient of variation of strength of material

V_P = coefficient of variation of test-to-predicted ratio

V_R = coefficient of variation of mean-to-nominal value of the resistance

w = width of the specimen (plate of weld)

X_u = minimum specified ultimate strength of weld metal

Y = comparative stress (von Mises-Hencky criterion)

α = angle of preset of plates before welding

α_R = separation coefficient

β = safety index

δ = lateral deflection of plate at weld

Δ = initial out-of-straightness of specimen

ϵ_x = strain in the x direction

ϵ_y = strain in the y direction

ϵ_z = strain in the z direction

θ = angle of plane with weld throat

μ = mean value

ν = poisson's ratio

ν_p = poisson's ratio in inelastic range

σ = standard deviation; stress

σ_{fw} = ultimate strength of a full penetration weld

σ_{pw} = ultimate strength of a partial joint penetration groove weld based on plate area

σ_u = measured ultimate strength

σ_{uw} = ultimate strength of a partial joint penetration groove weld based on gross weld area

σ_{uwn} = ultimate strength of a partial joint penetration groove weld based on net weld area

σ_x = stress in the x direction

σ_{x1} = stress under plane strain conditions

σ_{x2} = stress under uniaxial plane strain conditions

σ_{x3} = stress under biaxial plane strain conditions

σ_y = stress in y direction

σ_{yp} = comparative yield stress used in von Mises-Hencky criterion

σ_z = stress in z direction

σ_θ = normal stress on plane θ

$\sigma_{1,2,3}$ = stresses in principal directions

τ = shear stress

τ_o = maximum shear stress (Lawrence and Cox)

τ_{oM} = maximum shear stress based on von Mises criterion (Lawrence and Cox)

τ_{oT} = maximum shear stress based on Tresca criterion (Lawrence and Cox)

τ_θ = shear stress on plane at angle θ

ϕ = resistance factor

ϕ_w = resistance factor for welds

ϕ_1 = resistance factor for [6.2a]

ϕ_2 = resistance factor for [6.3a]

ρ_{G1} = mean-to-nominal ratio of percent weld penetration

ρ_{G2} = mean-to-predicted ratio of plate dimensions

ρ_M = mean-to-predicted ratio for the strength of the material

ρ_P = Test-to-predicted ratio for the tests

ρ_R = mean-to-nominal ratio of resistance

ω = rotation of plate at weld

1. INTRODUCTION

1.1 General

Partial joint penetration groove welds have direct application where it is not necessary to develop the full tensile capacity of the cross-section as may be the case in splicing columns subjected to tensile forces that are considerably less than the compressive forces. As well, where it is not feasible to make a full joint penetration groove weld, because welding can be done from one side only, the strength of a partial joint penetration groove weld may be all that is required.

Limited experimental data indicate that partial penetration welds are at least as strong proportionately as full penetration welds. However, the overall behaviour of partial joint penetration groove welds taking into consideration the strength of the plates joined, the eccentricity that may result because of the partial penetration, and the lateral restraint that may develop in the weld, has not been investigated.

Furthermore, although current design standards such as CSA Standard W59-1984 "Welded Steel Construction" (Metal-Arc Welding) (CSA, 1984) relate the strength of the weld to that of the plate material, they also limit the strength to the shear strength of the weld metal. Clearly the overall behaviour of partial joint penetration groove welds should be observed and analyzed so that rational design rules can

be established.

1.2 Objectives

The objectives of this thesis are:

1. to develop a method to predict the ultimate tensile strength of partial joint penetration groove welds,
2. to verify such a method by a suitable testing program, and
3. to make appropriate design recommendations.

1.3 Scope

A series of 75 partial joint penetration groove weld specimens were tested in tension. Five degrees of penetration and two strengths of steel were examined. Weld specimens were tested singly and in pairs to examine the effects of different loading conditions when the weld was able to move laterally to align itself with the load and when such movement was prevented. The proposed design recommendations derived from the results of these tests and the test results of others are compared with the current design standards.

2. LITERATURE REVIEW

2.1 General

Only limited work has been carried out on the behaviour of partial joint penetration groove welds subjected to tension. Most researchers have stated that little previous work could be found. Some studies on fatigue behaviour have been conducted and other investigators considered incomplete joint penetration as a defect.

Section 2.2 contains reviews of texts and papers while developments in Canadian standards are given in section 2.3.

2.2 Review of Texts and Papers

2.2.1 Texts

Kulak et al (1985) state that a partial penetration groove weld is less effective than a full penetration groove weld only because it provides a lesser cross-sectional area than that of a full penetration weld. Salmon and Johnson (1980) show how the nominal throat thickness is calculated for use with the allowable stresses given in Table 8.4.1 of AWS (1979). The allowable stresses for partial joint penetration groove welds are based on the tensile yield capacity of the effective base metal and the shear capacity of the throat when tension is normal to the effective area. Gray and Spence (1982) state that the strength of partial penetration welds should be based on the "weld ligament"

only. They also state that in many standards, even where fatigue is unlikely, the use of partial penetration welds is discouraged for primary tensile loads, presumably because they are prone to cracking in manufacture, or the risk of fracture in service is increased due to decreased ductility.

2.2.2 Papers

Biskup (1969) reported on a series of 12 tests, conducted by the Canadian Welding Bureau, to investigate the influence of weld defects, such as slag inclusions and lack of fusion, on the static tensile strength of groove welds. In all but two tests fracture occurred on or near a fusion face. On average, the strength of the defective weld, based on the net weld area, was 1.02 times that for a defect free weld. Biskup concluded that, for static loads, defects decrease the ultimate capacity of the joints in proportion to the area occupied by them and that the weld metal, of greater strength than the base metal, and reinforcement are both effective in compensating for lost strength.

Satoh et al. (1974), tested T-joints formed with partial joint penetration groove welds with varying degrees of penetration and fillet weld reinforcement as shown in Fig. 2.1. In general, the strength of the connection increased as the depth of penetration and amount of fillet weld reinforcement increased and also as the ratio of depth of penetration to fillet weld size increased. Fracture occurred along the fusion face of the base plate when the

depth of penetration was greater than the fillet weld leg length. When the fillet weld leg length was greater than the depth of penetration the fracture tended to occur on the fillet weld throat. The capacity of welds with no fillet weld reinforcement, when based on the net area of the weld in tension, varied from 1.02 to 1.16 times that for a full penetration weld.

Honig and Carlson (1976), studied the effects of cluster porosity on the tensile properties of A514 steel butt weldments. The tests showed that if a defect was below 3% of the total area it had no effect on the strength or ductility of the member. Once this defect size was exceeded the member strength decreased in proportion to the size of the defect but the ductility decreased dramatically. They concluded that the restrictions on tolerable defects could be relaxed for working stress design but the severe loss of ductility would make this inadvisable (apparently on the mistaken assumption that load redistribution was required) for "Limit Stress Design".

Lawrence and Cox (1976) investigated the effect of incomplete joint penetration, again considered as a defect, on the tensile behaviour of high strength steel welds. A series of welds with up to 39% lack of penetration were tested. Five additional conditions also investigated included: welds where the incomplete joint penetration was inclined relative to the tensile load, welds that had the crack tips sharpened by fatigue cycling, welds that were

produced with varying heat inputs, specimens with different edge preparations and welds that contained less than full length incomplete joint penetrations.

Using a uniaxial stress formulation where the major principal stress is twice the maximum shear stress and for a plate of width B, thickness b and lack of penetration a, as shown in Fig. 2.2, they proposed a limit load of,

$$[2.1] \qquad P_u = 2\tau_o B(b-a)$$

Using the von Mises failure criterion, the critical shear stress is

$$[2.2] \qquad \tau_{oM} = \frac{\sigma_u}{\sqrt{3}}$$

and using the Tresca failure criterion, the critical shear stress is

$$[2.3] \qquad \tau_{oT} = \frac{\sigma_u}{2}$$

Substituting these criteria into [2.1] give

$$[2.4] \qquad P_M = \frac{2}{\sqrt{3}} \sigma_u B(b-a)$$

and

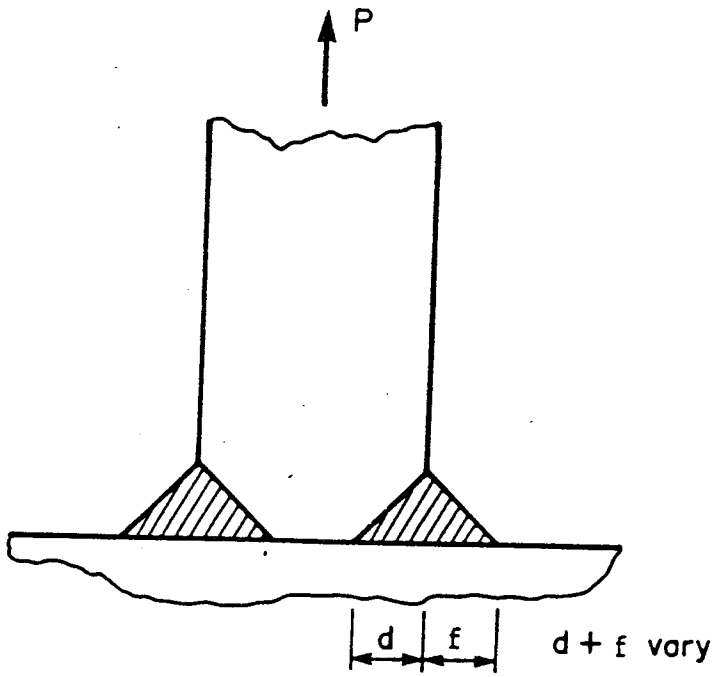

Figure 2.1 Type of Weld Tested by Satoh et. al. (1974)

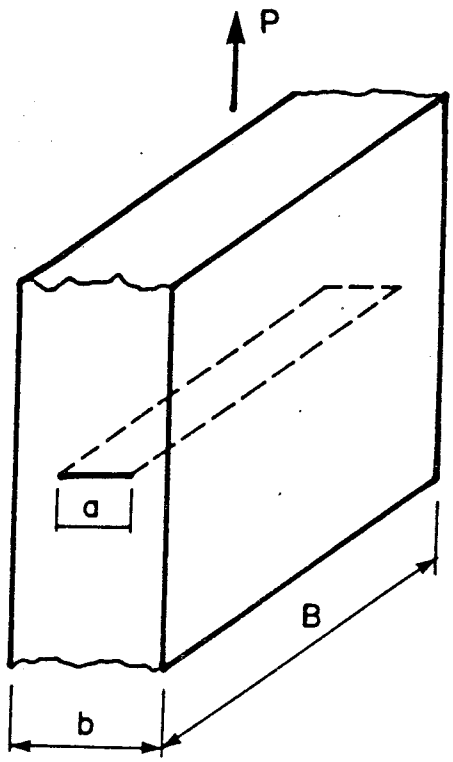

Figure 2.2 Model of Welds Tested by Lawrence and Cox (1976)

[2.5] $$P_T = \sigma_u B(b-a)$$

respectively. These expressions can be written in terms of stresses by dividing by the gross or net sections.

For the investigation by Lawrence and Cox the ultimate strength of the base metal was 0.87 times that of the weld metal and therefore either prediction could be a reasonable basis for the weld strength even though Lawrence and Cox used the weld metal strength in [2.4] and [2.5]. Test data tended to lie between the two strengths predicted by the von Mises and Tresca failure criteria. Failure planes followed the line of fusion in these tests. Though tensile strengths decreased generally in proportion to the lack of penetration the overall ductility dropped markedly when the ultimate capacity of the joint fell below the yield strength of the plate. Lawrence and Cox proposed three different behavioural regions based on the presence of ductility or the lack of it. The first region is when the ultimate capacity of the joint is greater than that of the plate leading to a ductile failure in the plate. The second region occurs when the strength of the joint is less than that of the plate but greater than the yield strength of the plate. Failure occurs in the weld but only after the plate yields. The third region occurs when the strength of the joint is less than the yield strength of the plate and failure occurs in the weld with little deformation of the specimen. The lack of penetration, a', marking the boundary between the first and

second regions is therefore given by

$$[2.6] \qquad \frac{a'}{b} = 1 - \frac{\sigma_u}{\sigma_{uw}}$$

while the boundary between the second and third regions is defined by a lack of penetration, a'', given by

$$[2.7] \qquad \frac{a''}{b} = 1 - \frac{\sigma_y}{\sigma_{uw}}$$

The tests with inclined defects, fatigue cracks and varying weld preparations were not different in behaviour from the main tests. When varying heat inputs were used there was a notable decrease in capacity for non-optimum heat inputs. When the length of the defect exceeded 60% of the plate width the specimen behaved as if the defect was 100% of the plate width. It was noted that several welds had other defects which reduced strength in proportion to the lost area.

Popov and Stephen (1977) performed a limited number of tests to investigate the strength of partial joint penetration groove welds in heavy column sections to simulate the condition of columns in a braced steel frame that may go into tension during a seismic disturbance. Welds with up to 77% lack of penetration were tested. All welds gave satisfactory strengths with the ultimate tensile stress sustained by the weld at failure increasing with increasing

lack of penetration. When some welds were cycled three times to the maximum compressive capacity of the testing machine (17800 kN) and to the approximate yield load of the welds in tension the ultimate strength was not significantly affected and the loading curves showed negligible hysteresis loops. All failures were sudden and the welds exhibited little ductility. These tests are the only ones found in the literature directed specifically towards establishing the strength of partial joint penetration groove welds.

Bent (1983), in a theoretical study, noted that CSA standard W59 (CSA 1982) considers partial joint penetration groove welds to be similar to fillet welds and therefore penalizes the former unnecessarily. The standard does not identify the stress states on the planes considered to be critical. Bent conducted a finite element study that showed that the maximum stress concentration for partial joint penetration groove welds was only 52% of that for a similar sized fillet weld under the same loading conditions. He proposed that the strength of partial joint penetration groove welds be determined on the basis of the stress state on critical planes that resulted from the particular loading. A distinction was made between parallel and tranverse loadings and the resulting planes of maximum shear and normal stresses are determined for both the weld and base metal. He did not, however, propose using a failure theory such as the von Mises criterion, to take into account the effective stress on these planes. He proposed that the

allowable shear stresses in the weld and base metals be $0.3X_u$ and $0.4F_y$ respectively, but that the allowable tensile stress in both weld and base metal be $0.6F_y$. The permissible tensile or shearing load on the critical plane is found as a component of the total load on the specimen. He also cautioned against welding from one side only though he did not provide experimental evidence for this concern.

To apply Bent's criteria, established for welds consisting of combined partial joint penetration groove welds with various angles of preparation and fillet welds joining two plates to form a "T", to the welds studied in this investigation the fillet weld size would be taken to be zero and the preparation groove angle to be 45°. Fig. 2.3 shows the resulting plane of maximum normal stress, plane 1, and of maximum shear stress, plane 2. The maximum normal stress on plane 1 is

$$[2.8] \qquad \sigma = \frac{P}{A_w}$$

and the maximum shear stress on plane 2 is

$$[2.9] \qquad \tau = \frac{P\cos 45° \sin 45°}{A_w} = 0.5\frac{P}{A_w}$$

Assuming grade 300W steel and E480 electrodes the allowable shear stresses would be 150 MPa and 120 MPa in the weld and steel respectively and the allowable tension stress 180 MPa.

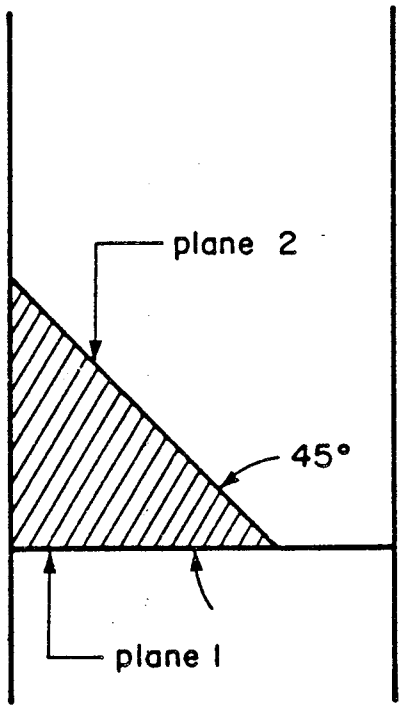

Figure 2.3 Bent's failure planes for a Non-reinforced Weld (Bent, 1983)

The ratios of the allowable shear stresses to the allowable tension stress are 0.83 and 0.67 which are both larger than that predicted by [2.9]. Therefore, Bent's method suggests that tension on the weld throat is critical.

2.3 Codes and Standards

2.3.1 General

CSA Standard W59-1984 (Welded Steel Construction) (CSA, 1984) governs the use of arc welding in Canada for steel structures. Provisions for the limit states design of partial joint penetration groove welds have existed in Canadian standards since 1974.

2.3.2 CSA Standard S16.1-1974

The equations for the design of welds with tension normal to the weld axis given in CSA Standard S16.1-1974, Steel Structures for Buildings - Limit States Design, (CSA, 1974) are:

[2.10] $$V_r = 0.66 \phi A_m F_y$$

for the base metal and

[2.11] $$V_r = 0.50 \phi A_w X_u$$

for the weld metal with the provision, of course, that the lesser resistance be used. In both cases ϕ is taken as 0.9. These are the same equations used to design for shear on the effective throat as shown in Fig. 2.4. As they describe shear resistances they do not reflect the fact that the welds are actually loaded in tension. For butt joint welds made with matching electrodes, the resistance of the base metal given by [2.10] controls for all steels except grades 380, 480 and 700.

2.3.3 CSA Standard W59-M1982

CSA Standard W59-1982 recognized that a partial joint penetration groove weld may be loaded in tension and added the category of 'tension normal to axis of weld'. The resistance for this category is taken as the least of

[2.12a] $$T_r = \phi F_y A_m$$

and

[2.12b] $$T_r = 0.85 \phi F_u A_m$$

for the base metal, and

[2.13] $$V_r = 0.50 \phi X_u A_w$$

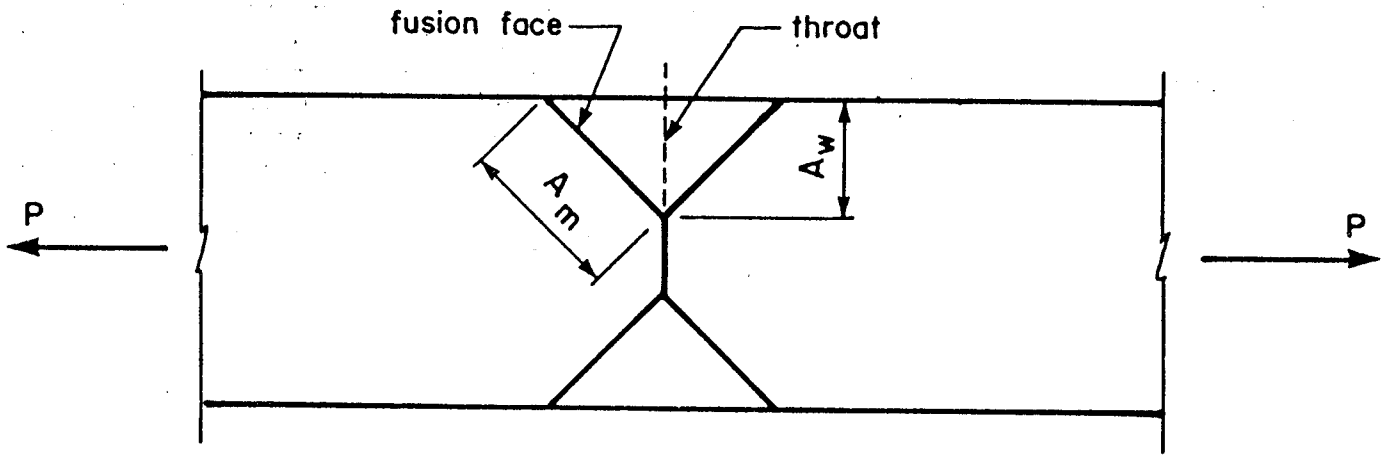

Figure 2.4 Planes on which shear strength is computed by CSA Standard W59 (1977)

for the weld metal in which ϕ=0.90 throughout. Equations [2.12a] and [2.12b] give tensile resistances for the base metal although [2.13] still describes a shear resistance on the weld itself. The area of the partial joint penetration groove weld, A_m, is defined as the size of the effective throat of weld multiplied by the length of weld. The 1982 provisions increased the design capacity of the joint as compared to the 1974 provision in most situations with the weld metal capacity generally governing.

2.3.4 CSA Standard W59-M1984

An editorial change in this edition of the standard gives the shear resistance as

$$[2.14] \qquad V_r = 0.67\ \phi_w\ X_u\ A_w$$

rather than that of [2.11]. The product of 0.50ϕ with ϕ=0.90 in [2.11] is, however, the same as $0.67\phi_w$ with ϕ_w=0.67 in [2.14]. The change therefore explicitly recognized that the shear resistance was at least $0.67X_u$ and that 0.67 may be an appropriate resistance factor for welds. Also, in the equation for the tensile resistance of the base metal the symbol A_b has been used to replace A_m to avoid confusion with the planes used in shear design. The symbol A_b is defined as the applicable area of base metal normal to tensile load for partial joint penetration groove welds in

tension. This means that the applicable area of base metal is equal to the minimum area of weld metal perpendicular to the load.

The shear resistance of the weld metal [2.14] still generally governs the design.

2.4 Discussion

Although experimental evidence indicates that partial joint penetration groove welds fail in tension on the cross section perpendicular to the load, welding standards still give resistances as if the throat area were loaded in shear.

3. EXPERIMENTAL PROGRAM

3.1 General

The objectives of the experimental program were to examine the ultimate strength and mode of failure of partial joint penetration groove welds as a function of the degree of penetration. The effect of eccentric loading of the welds was also to be investigated. Seventy-five specimens with five degrees of weld penetration and two types of base metal, some loaded singly and others in pairs, were tested. Twenty-two additional ancillary tests were performed on steel plate and weld metal coupons.

3.2 Test Specimens

To investigate the behaviour of partial joint penetration groove welds over the full spectrum of joint penetration, nominal penetrations of 20, 40, 60, 80 and 100% were tested. Table 3.1 shows the number and type of specimens.

For economic reasons only one type of weld preparation was studied. As a survey of Canadian steel fabricators indicated that most would use a single 45° bevel for the preparation and the shielded metal arc welding (SMAW) process, this preparation, as indicated in Fig. 3.1, and process were used.

Test specimens were proportioned for testing in the Materials Testing Systems (MTS) testing facilities at the

Table 3.1 Distribution of Tests

Type of Specimen	300W Base Metal		350A Base Metal		Totals
	Single	Pair	Single	Pair	
5mm Welds	6	4	4	2	16
10mm Welds	6	4	4	2	16
15mm Welds	6	4	4	2	16
20mm Welds	6	4	4	2	16
Full Penetration	6	-	5	-	11
Plate Coupons	6	-	6	-	12
Weld Metal Coupons	5	-	5	-	10
Totals	41	16	32	8	97

I.F. Morrison Structural Laboratory of the University of Alberta. A typical test set-up is shown in Fig. 3.2 and the dimensions in millimetres of typical test specimens are indicated in Fig. 3.3. Widths of 160, 160, 160, 145 and 120 mm were used for the specimens with nominal 5, 10, 15, 20 and 25 mm welds respectively. The 25 mm (full penetration) welds were back gouged and rewelded.

The specimens were initially designed to be loaded through pins but, because of the moments perpendicular to the plane of the plate resulting from the eccentric loading of the welds, the pin hole detail was deleted and the specimens were designed to be placed in the self-aligning hydraulic grips. This change also reduced the amount of material and machining required.

The test specimens were proportioned to make use of the full width of the self-aligning hydraulic grips and to permit the testing of two specimens back-to-back. A reduced section was used on all specimens that had 80% or more penetration to avoid failure in the grips. As the general dimensions of the specimens did not conform to standards such as those given in ASTM A370-77 a finite element analysis was performed to establish whether or not the stresses were relatively uniform at the cross-section along the weld. This analysis showed that within 100mm of either side of the weld, the elastic variation of stresses was less than 1%. This was considered to be satisfactory.

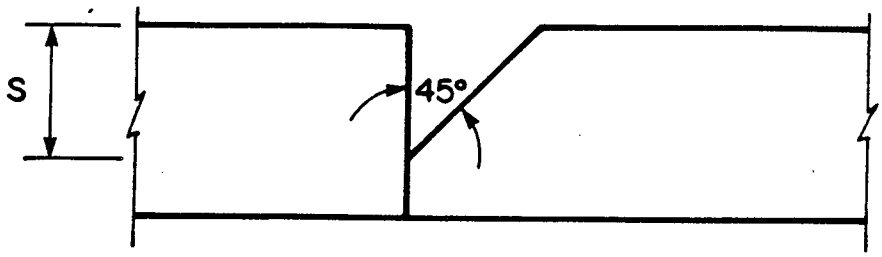

Figure 3.1 Weld Preparation Selected

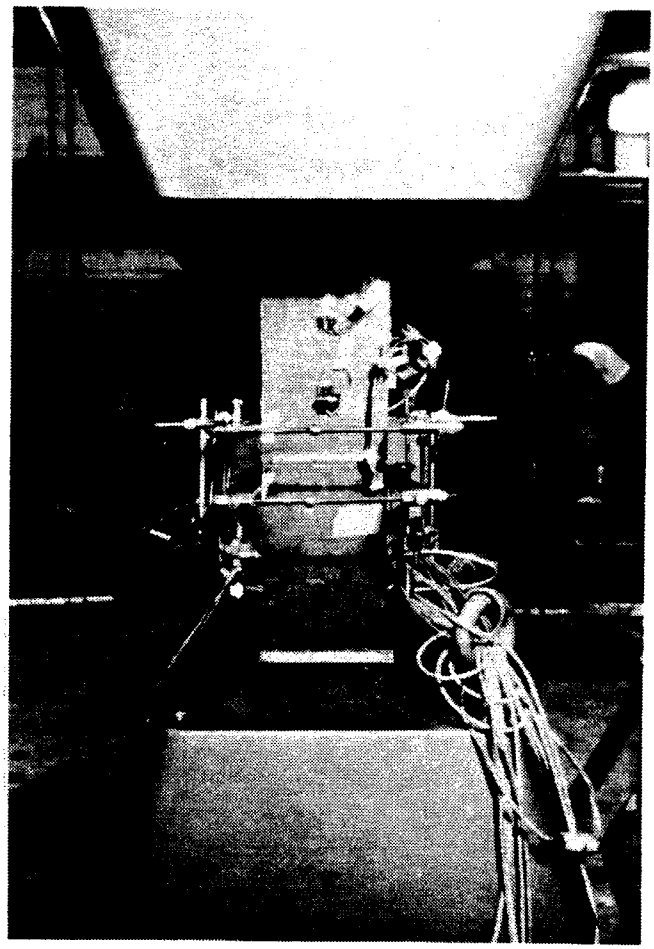

Figure 3.2 Typical Test Setup

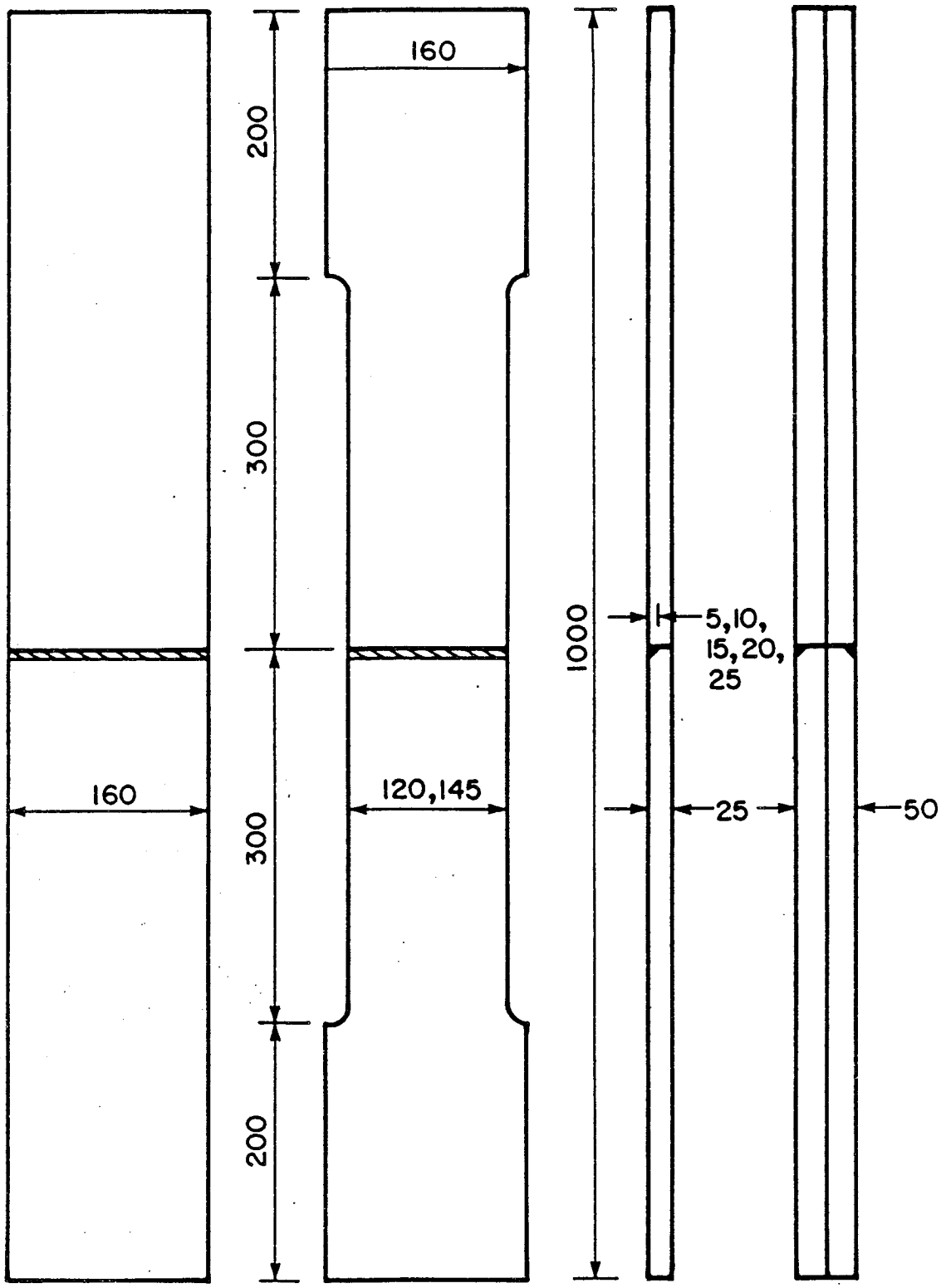

Figure 3.3 Dimensions of Typical Test Specimens

3.3 Single and Double Specimens

In a steel plate specimen with a partial joint penetration groove weld, the weld is eccentric with respect to the steel plate on either side. This eccentricity will produce moments in both the weld and plates causing the plates to deflect laterally, if not completely restrained, as the weld tends to align itself with the load. To assess the possible effect of this eccentric loading on the behaviour of the weld, the welds were tested singly and in pairs. The single specimens tended to align themselves in the tests and reduce the eccentricity. While overall concentric loading was obtained by testing two specimens together, back to back, the individual welds were still eccentrically loaded as discussed in chapter 5.

3.4 Plate Material

The steel plates used were CSA Standard CAN3-G40.21-M81, "Structural Quality Steels", (CSA, 1981), grades 300W and 350A with a thickness of 25mm. All specimens of each grade came from a single heat. Both the 300W plate, manufactured by Algoma Steel, and the 350A plate, manufactured by Stelco, were supplied by, C. W. Carry Ltd., a local fabricator. Table 3.2, giving the mill test values and the chemical requirements of CSA Standard CAN3-G40.21-M81, show that both steels met the specifications.

Table 3.2 Chemical Composition of Plates

Grade & Supplier	Data Source	C %	Mn %	S %	P %	Si %
300W	Max or range specified in CSA G40.21-M81	0.22	0.5-1.50	0.05	0.04	0.40
Algoma	Mill Report Heat 5947L	0.16	1.12	0.009	0.015	0.24
350A	Max or range specified in CSA G40.21-M81	0.20	0.75-1.35	0.04	0.03	0.15-0.40
Stelco	Mill Report Heat 620803	0.15	1.30	0.007	0.008	0.26

3.5 Electrodes

Because E480XX electrodes match both 300W and 350A grade steels as specified by CSA Standard W59, (CSA, 1984) E48018 electrodes (3.2mm in diameter) were used. CSA Standard W48.1-M1980 (CSA, 1980) specifies an ultimate strength of 500-650 MPa, a minimum yield strength of 410 MPa and a minimum elongation in 50mm of 22% for the E48018 electrodes.

3.6 Plate Preparation

The location of each specimen was marked on the plate supplied and recorded for later reference. Each specimen was flame-cut, using an automatic flame-cutter to produce uniform specimens, with the longitudinal axis parallel to the direction of rolling.

The end of one of each pair of plates was prepared with a 45° bevel by flame-cutting. The depth of the preparation was specified to be 3mm deeper than the required weld depth as specified by CSA Standard W59, (CSA, 1984). Any ridges or bumps on the bevels were ground off and the depth of the preparation was measured.

3.7 Welding Procedure

All welds, except for the full penetration groove welds, were produced by welding from one side only. On cooling a welding-induced rotational distortion about the axis of the weld occurs that may lead to out-of-straight

specimens. To minimize this problem a series of trial welds were produced, where the plates were preset at a given angle opposite to the anticipated distortion. The best value of the preset angle, α, the angle each side of plate made with a flat surface, as shown in Fig. 3.4, was determined for each size of weld. These angles and other welding parameters are given in Table 3.3. The trial specimens were used in the testing program.

Each specimen was produced by:

1. aligning the plates in the jig of Fig. 3.4 and presetting the angle,
2. clamping the plates in position,
3. tack-welding V-shaped run-on and run-off tabs to the plates as shown in Fig. 3.5,
4. making the root pass in one continous pass and inspecting visually for any defects,
5. cleaning the slag from the weld surface for the next pass,
6. completing remaining passes with starts and stops as required,
7. once the weld cooled, unclamping the specimen and machining off the run-off tabs.

The full penetration groove welds were formed in the same manner but were back gouged, (using a 490 Torch), and welded from the back.

The 5 mm and 10 mm weld series were fabricated first and, after testing, because general yielding of the plates

Table 3.3 Welding Parameters

Weld Size (mm)	Preset Angle (degrees)	Weld Passes	Current (Amps)
5	0.2	2	150
10	0.4	3	150
15	0.6	5	150
20	0.8	6	150
25	0.7	8	150
Range specified in CSA W48.1-M80			110-160

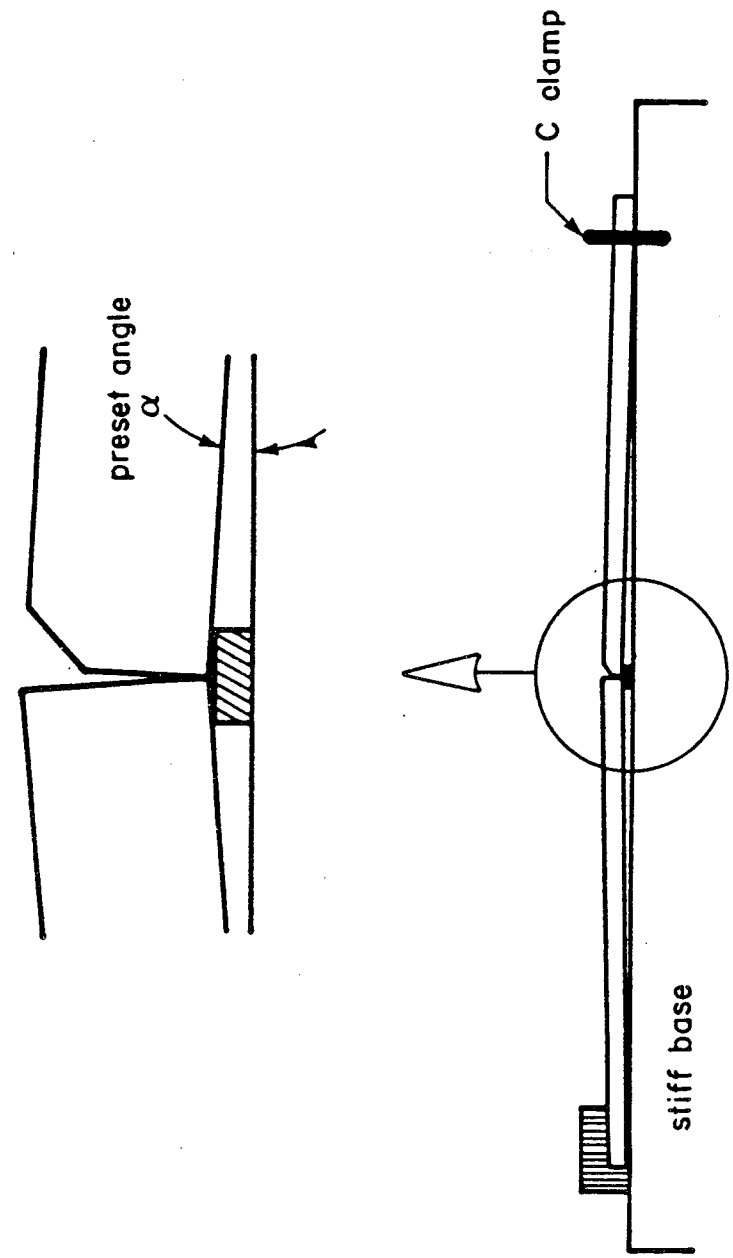

Figure 3.4 Jig Used to Preset Angle

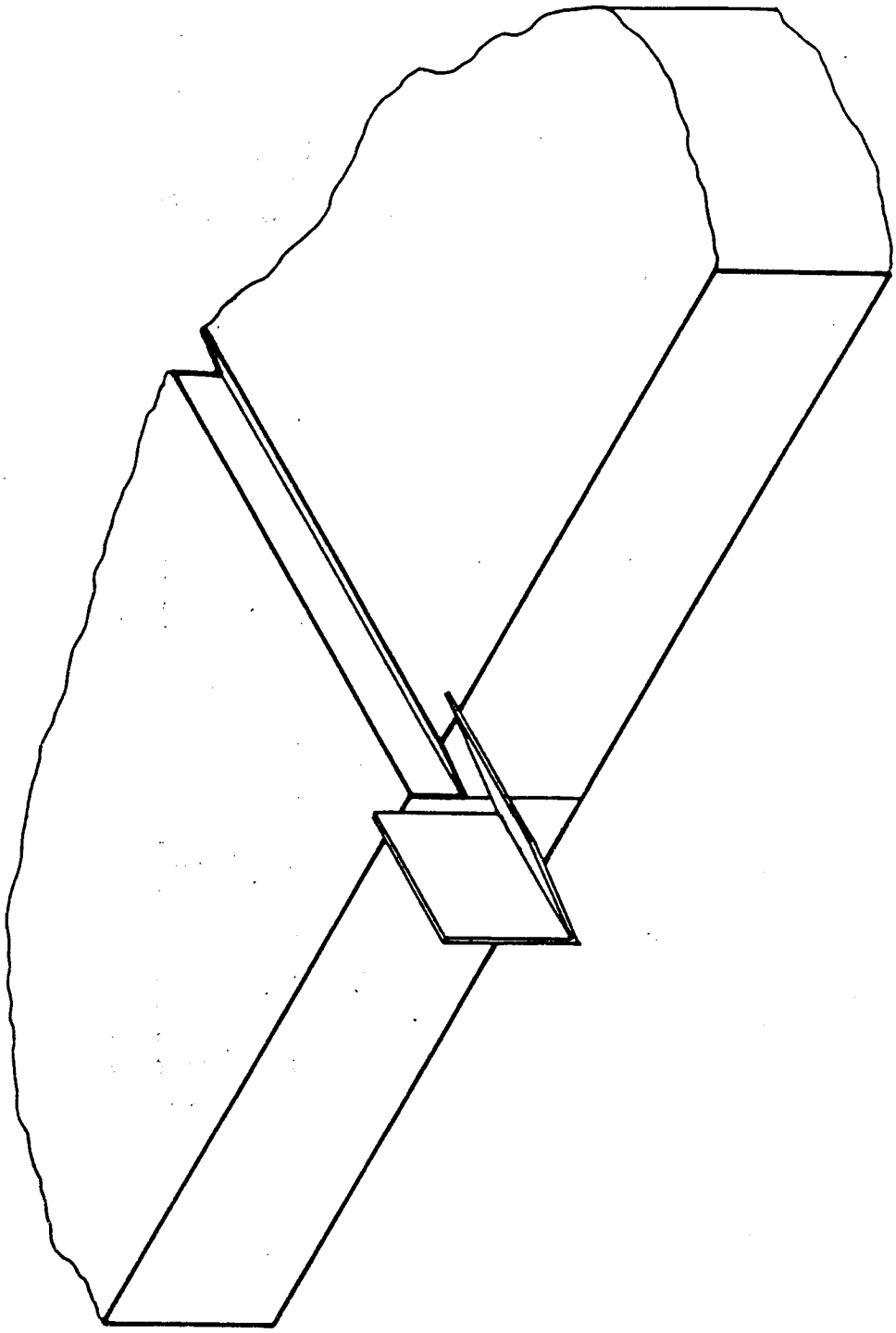

Figure 3.5 Run-off Tabs

had not occurred, the welds were cut out and the plates reused by rebevelling and welding for the 15 and 20 mm weld tests.

All welds were produced by one welder using the SMAW process at C.W. Carry Ltd. Edmonton, Alberta.

3.8 Final Preparation of Test Specimens

To ensure uniform edge conditions at the welds the 5 mm, 10 mm and 15 mm test specimens were machined to a depth of two millimeters on each side after flame-cutting and welding. Specimens constructed with 20 mm or full penetration groove welds were reduced in width by machining to 145 mm and 120 mm respectively in order to prevent failure of the specimen in the grips.

The out-of-straightness of each specimen was measured by placing each side in turn against a series of dial gauges as shown in Fig. 3.6 and averaging the readings. The elastic deflection of the plates was considered to be negligible. Measurements of the weld reinforcement were also taken and any unusual features were noted. Based on the out-of-straightness data, specimens were selected for testing in pairs.

3.9 Test Setup

All tests were conducted in the 6000kN Material Testing Systems (MTS) test system at the University of Alberta.

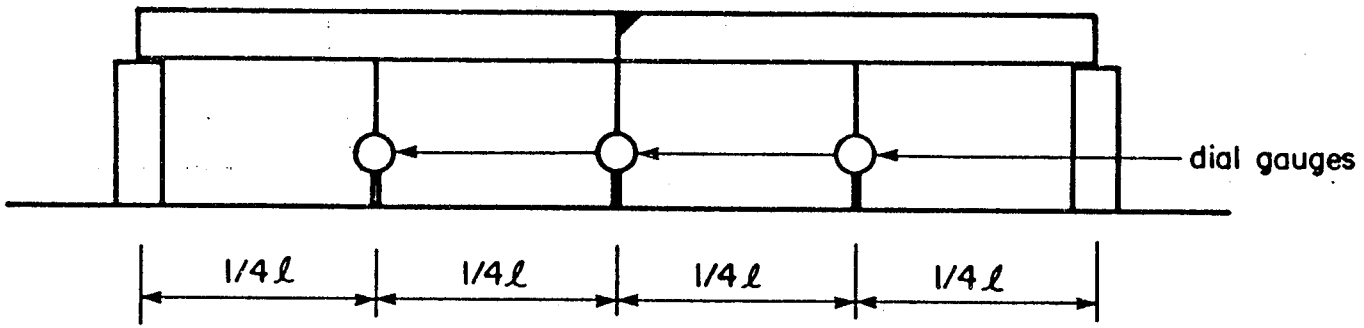

Figure 3.6 Method for Measuring Out-of-straightness of Specimens

At least four KFC-5-C1-11 electronic resistance strain gauges were mounted on each test specimen as shown in Fig. 3.7. When positioned in pairs on opposite sides of the plate bending and axial strains could be determined. These gauges have a gauge length of 5 mm, a gauge factor of 2.10 and a resistance of 120 ohms. Immediately prior to each test the strain gauges were calibrated at a set input voltage which was monitored throughout the test. No significant changes in the input voltages were observed.

Specimens were placed in the 4000kN capacity self-aligning hydraulic grips of the MTS machine and 10% of the anticipated maximum load was applied before the alignment was locked. Due to the initial out-of-straightness of some specimens it is possible that the gripping procedure could have produced some bending strains in the specimen before testing began. Therefore, several tests were conducted to determine if the gripping procedure produced any moments in the specimen after the alignment load had been removed. This was accomplished by taking strain gauge readings before, during and after the gripping procedure. No significant bending strains were observed.

Six linear variable differential transformers (LVDTs) were used to measure deformations over a 75 mm gauge length centered on the weld. A Hewlett Packard Model 24DCDT-250 LVDT, with a linear operating range of 13 mm, was positioned on the centerline of each face of the specimen as shown in Fig. 3.8 and four additional Hewlett Packard Model

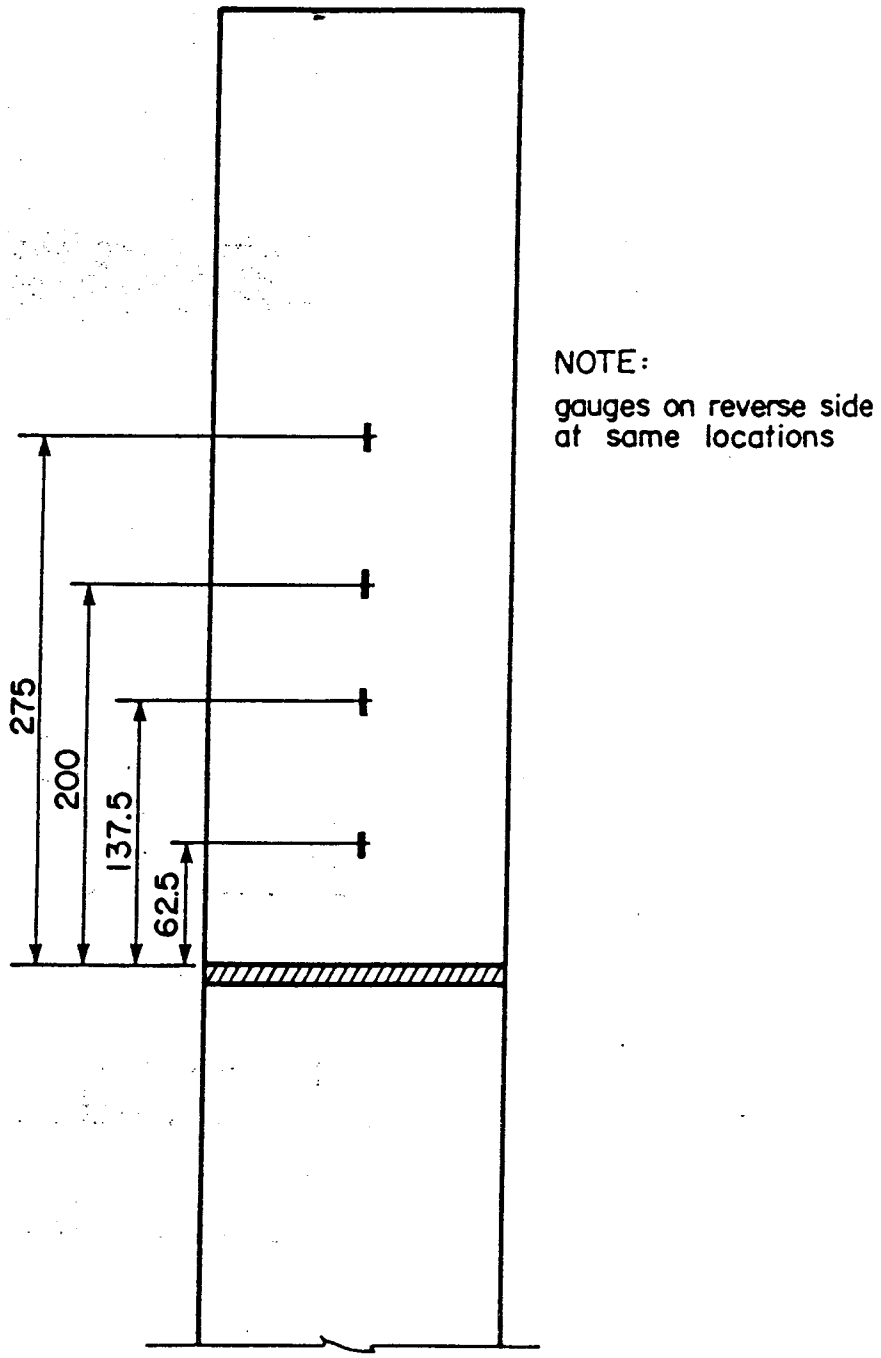

Figure 3.7 Strain Gauge Locations

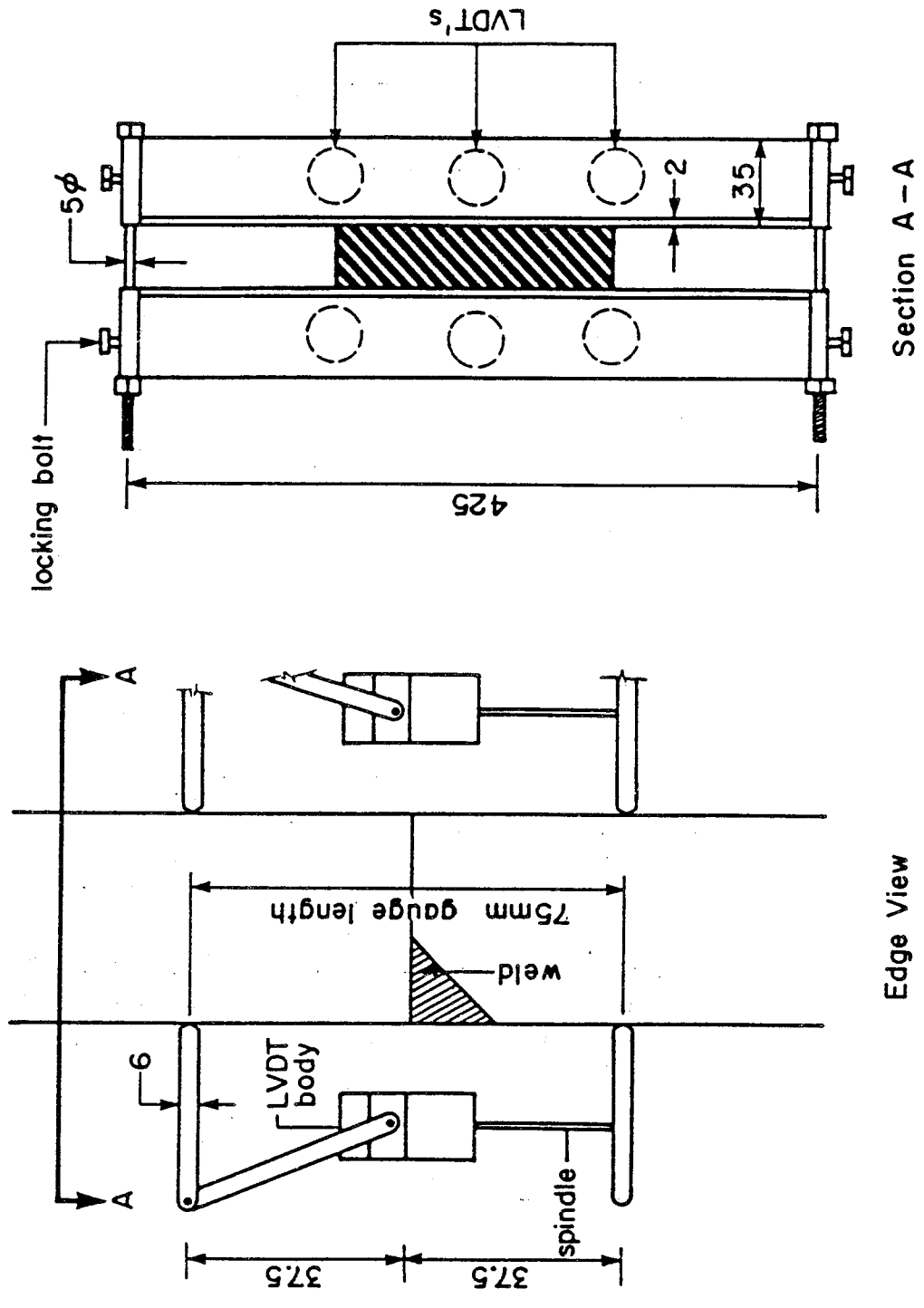

Figure 3.8 LVDT Mounting Device

24DCDT-100 LVDTs with a linear range of 5 mm, (not shown in Fig. 3.8) were placed at each corner to detect any variations in strains or rotation of the mounts. One additional LVDT was used to measure lateral deflections of the specimen at midheight.

Each LVDT was calibrated before and after the test program to determine the linear operating range. There were no significant differences between the two calibrations.

The two mounting devices, Fig. 3.8, held the LVDT's in place. Each mounting device consisted of two plates with a machined V-shaped edge placed against the specimen and held in place by a clamping force provided by the threaded rods at the ends of the plates. The spindles of the LVDTs fixed to the upper mount were in bearing against the lower mount. The lateral contraction of the specimen during loading in tests with 80% or greater weld penetration resulted in a gradual loss of the clamping force and therefore the clamping rods had to be retightened. Displacement readings were taken immediately before and after tightening and the data adjusted for any differences observed.

The stroke control mode of the MTS system was used to load the specimens. The system applies whatever load is necessary to elongate the specimen to a set value. Testing in this mode allows loads to be established at zero strain rate and on the descending portion of the curve. The load carried by the specimens and their overall elongation were measured by the MTS system by means of an internal load cell

and displacement transducer.

The dedicated 256 channel Data General S/120 data aquistion computer system in the structural laboratory was used to monitor all measurements throughout the test. Each output signal from the MTS, the LVDTs and strain gauges was assigned an individual channel. Between 8 and 20 channels were used for each test and permanent readings were taken at discrete intervals and stored on magnetic tape.

3.10 Test Procedure

The specimens were placed in the hydraulic grips and loaded to 10% of the anticipated maximum load when the alignment of the grips was locked. The load was reduced to zero, initial readings were recorded and the load was reapplied in increments of one-twentieth of the expected ultimate load. A complete set of readings were taken at each load increment. When the weld or plate yielded the size of the increments was decreased. After fracture, the specimen was removed from the machine, labelled and the fracture surface was sawn off for later examination.

3.11 Fracture Observations

It was anticipated that all partial joint penetration groove welds would fail in the weld. From the fracture surfaces the initial depth of the weld and uniformity of weld penetration could be determined. The angle of the fracture plane through the weld root was measured. The

fracture surfaces were examined to determine whether they had a silky (ductile) or crystalline (brittle) appearance and also for the presence of weld defects. Photographs were taken of various fracture surfaces.

3.12 Ancillary Tests

3.12.1 Plate Coupons

Six full thickness tension coupons of the 300W and 350A steels were tested to determine the stress-strain characteristics. The coupons were flame-cut parallel to the rolling direction of the plate and machined to final dimensions of 1000 mm long by 25 mm thick with a reduced width between the grips of 120 mm. To obtain data for another experiment the coupons had extensive instrumentation in the form of high elongation strain gauges, capable of straining up to 20% and LVDTs mounted with a 450 mm gauge length. The stress-strain curves were consistent as indicated by the low coefficients of variation in Tables 4.1 and 4.2.

3.12.2 Weld Coupons

As failure had occurred in the base plate away from the weld it was possible to obtain all-weld metal coupons from the full penetration groove welds specimens after testing. Ten all-weld metal coupons were prepared in accordance with CSA Standard W48.1-M80 (CSA, 1980). Cross-sectional

dimensions were measured using a digital micrometer. Strain gauges were mounted on opposite sides to determine axial and bending strains. The coupons were tested in an MTS testing system with a 1000 kN capacity.

4. TEST RESULTS

4.1 Ancillary Test Results

4.1.1 Tension Tests on Plates

Tests results for coupons of the grade 300W steel and 350A steel are given in Tables 4.1 and 4.2 respectively. Typical stress-strain curves for each grade of steel are shown in Fig. 4.1. The modulus of elasticity was determined, based on strain gauge readings, using the method of least squares, as given in ASTM E111-61 (1961). Strain readings up to the ultimate load were obtained with the high elongation strain gauges.

Minimum strength and elongation requirements as specified in CSA Standard CAN3-G40.21-M81 (1981) were exceeded substantially for both grades of steel. In particular mean test/specified ratios of the yield strength, ultimate strength and final elongation of 1.16, 1.11 and 1.75 respectively for the grade 300W steel and 1.10, 1.12 and 1.55 respectively for grade 350A steel were obtained. The coefficients of variation, particularly as related to the strength parameters, ranging from 0.4% to 2.5%, are relatively small.

4.1.2 Full Penetration Groove Weld Tests

Because the plates with full penetration groove welds invariably failed in the plate, some 120 to 165 mm from the

Table 4.1 Grade 300W Steel Tension Coupons Results

Coupon No.	E X10E3 (MPa)	Yield Strain X10E-6	Yield Stress (MPa)	Ult. Strain X10E-6	Ult. Stress (MPa)	Frac. Strain (%)
1	212.1	1655	351	0.22	501	34
2	208.0	1654	344	0.18	501	-
3	201.8	1744	352	0.23	502	36
4	208.5	1688	352	0.23	501	36
5	192.9	1783	344	0.17	498	37
6	214.7	1630	350	0.23	497	34
μ	206.3	1692	349	0.21	500	35
σ	7.9	59	3.7	0.030	2.0	1.3
V (%)	3.8	3.5	1.1	14.2	0.4	3.7
Min or range requirements from CSA G40.21-M81.			300		450-620	20

Table 4.2 Grade 350A Steel Tension Coupon Results

Coupon No.	E X10E3 (MPa)	Yield Strain X10E-6	Yield Stress (MPa)	Ult. Strain X10E-6	Ult. Stress (MPa)	Frac. Strain (%)
1	208.2	1811	377	0.15	537	25
2	221.9	1699	377	0.20	530	30
3	208.6	1850	386	0.15	539	-
4	-	-	388	0.20	544	29
5	198.3	1896	376	0.25	528	39
6	205.1	1955	401	0.21	556	34
μ	208.4	1837	384	0.19	539	31
σ	8.6	87	9.7	0.038	10.1	5.3
V (%)	4.1	4.7	2.5	20.0	1.9	17.1
Min or range requirements from CSA G40.21-M81.			350		480-650	20

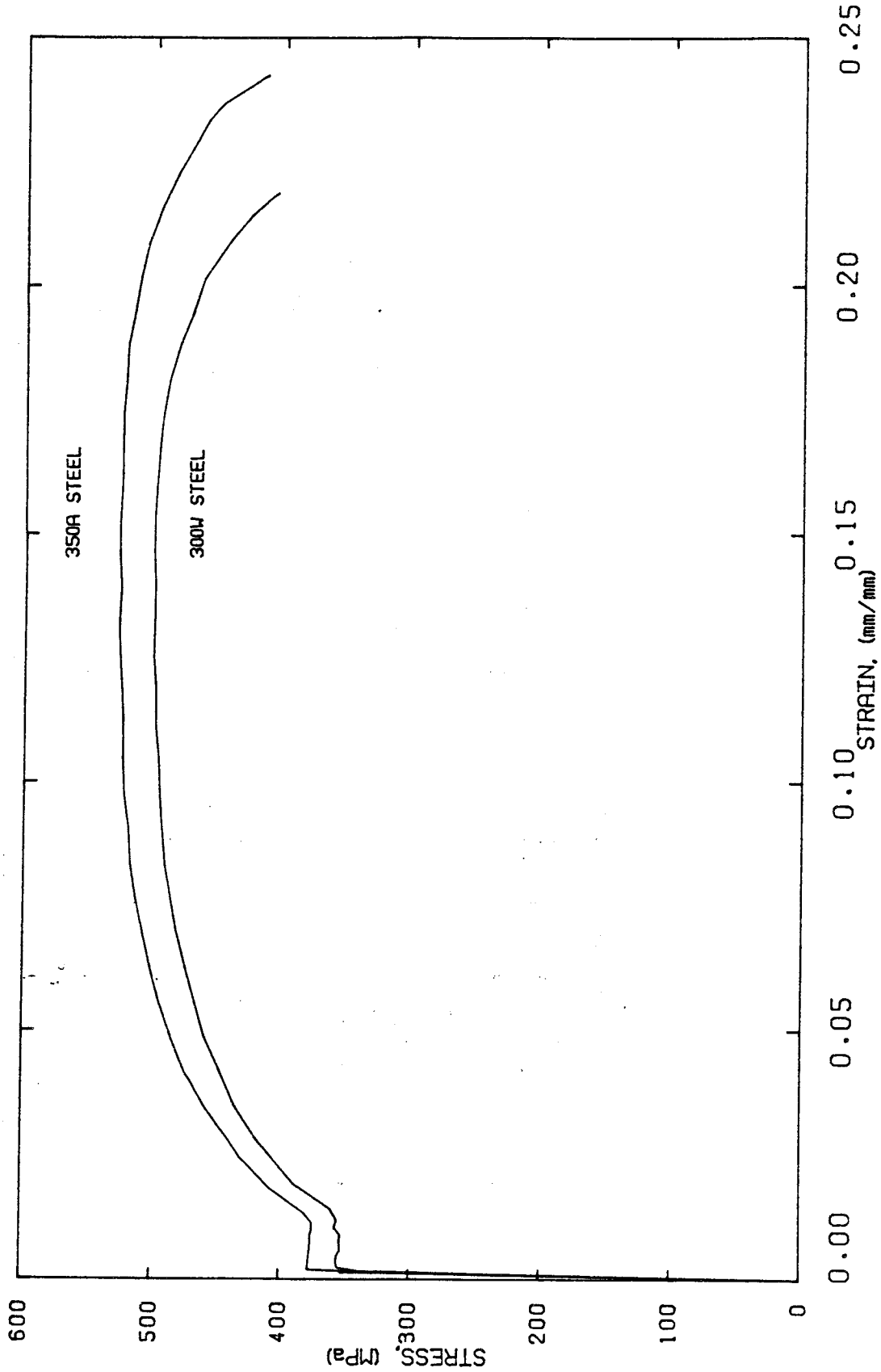

Figure 4.1 Typical Stress-Strain Curves for Steels

weld, these tests can be considered to be tension tests of the plate material. The relevent data for these tests are shown in Tables 4.3 and 4.4. Some data were not recorded as there were no high elongation strain gauges used and the LVDTs did not span the fracture zones.

These test results do not differ significantly from those of the non-welded full thickness tension coupons. When combined with the full-thickness coupon data they give test/specified ratios and coefficents of variations respectively of 1.15 and 1.9% for σ_y, 1.11 and 1.1% for σ_u of the 300W steel and 1.08 and 3.4% for σ_y, 1.11 and 2.9% for σ_u of the 350A steel.

4.1.3 All-Weld Metal Tension Coupons

The results of tests on ten all-weld metal coupons, as described in section 3.11.2, are given in Table 4.5 and a typical stress-strain curve is given in Fig. 4.2.

The minimum strength requirement as specified in CSA Standard W48.1-M80 (CSA, 1980) was exceeded on the average by 1.16 times with a coefficent of variation of 3.6%.

4.2 Partial Penetration Groove Weld Test Results

4.2.1 General

All test specimens failed in the welds. Failures varied from slow incremental fracturing as the plates tore apart to almost instantaneous fracture. The specimens tested in pairs

Table 4.3 Grade 300W Steel Full Penetration Weld Data

Coupon No.	E X10E3 (MPa)	Yield Strain X10E-6	Yield Stress (MPa)	Ult. Strain X10E-6	Ult. Stress (MPa)	Frac. Strain (%)
1	215.0	1563	336	-	488	-
2	201.0	1711	344	-	500	-
3	202.0	1663	336	-	494	-
4	206.1	1640	338	-	506	-
5	201.4	1698	342	-	502	-
6	202.2	1662	336	-	488	-
μ	204.6	1656	339	-	496	-
σ	5.4	52	3.5	-	7.5	-
V (%)	2.6	3.2	1.0		1.5	
Min or range requirements from CSA G40.21-M81.			300		450-620	20

Table 4.4 Grade 350A Steel Full Penetration Weld Data

Coupon No.	E X10E3 (MPa)	Yield Strain X10E-6	Yield Stress (MPa)	Ult. Strain X10E-6	Ult. Stress (MPa)	Frac. Strain (%)
1	200.0	1845	369	-	534	-
2	199.0	1884	375	-	538	-
3	201.0	1891	380	-	536	-
4	200.5	1825	366	-	494	-
5	198.2	1776	352	-	523	-
μ	199.6	1844	368	-	525	-
σ	1.1	47	11.0	-	18.0	-
V (%)	0.6	2.5	3.0		3.4	
Min or range requirements from CSA G40.21-M81.			350		480-650	20

Table 4.5 All Weld-Metal Tension Coupon Data

Specimen	Ultimate Load (kN)	Area (mm^2)	σ_u (MPa)
1	42.9	77.1	557
2	43.5	77.9	558
3	45.4	78.4	579
4	44.6	78.2	570
5	43.6	78.2	557
6	48.0	78.1	615
7	45.0	77.8	578
8	45.9	77.9	590
9	45.2	77.0	587
10	47.1	77.4	608
μ (MPa)			580
σ (MPa)			20.6
V (%)			3.6
Requirements of W48.1 M80			500

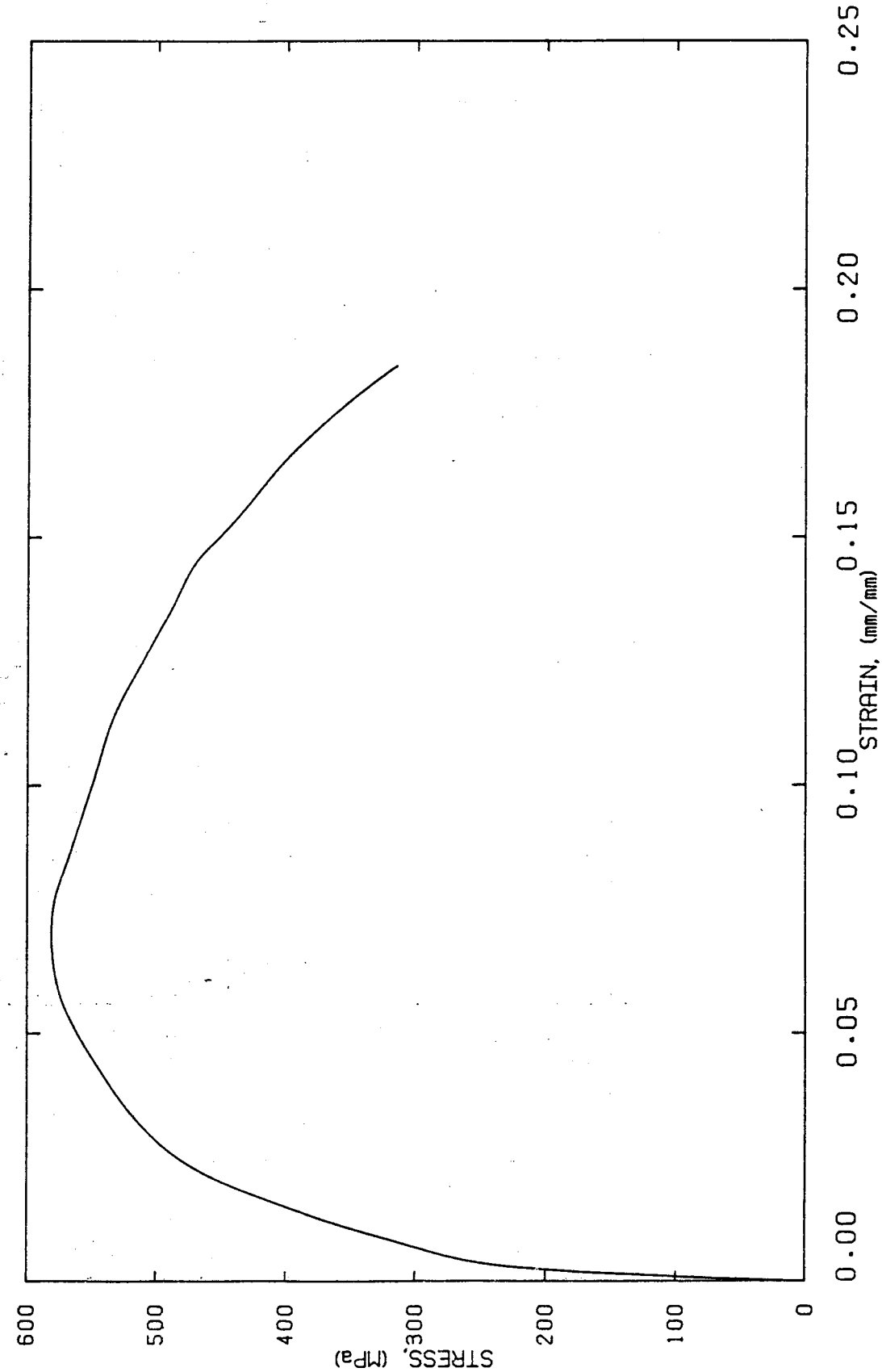

Figure 4.2 Typical Stress-Strain Curve for Weld Metal

did not always fail simultaneously. When the degree of penetration was relatively small the plates themselves behaved elastically. With greater degrees of penetration the plates yielded and for the case of 100% penetration the plates fractured as described in section 4.1.

The specimen designation gives in order, the nominal penetration in millimeters (05, 10, 15, 20 and 25), the grade of steel, (with W signifing grade 300W and A, grade 350A), whether the specimens were tested singly (S) or in pairs (P) and the sequential number of testing for that type as shown in Tables 4.6 to 4.10.

4.2.2 Weld Dimensions

The dimensions of each weld and base plate were measured using digital calipers with a sensitivity of $\pm$0.005 mm. The amount of weld penetration was computed from a minimum of six readings across the width of the plate by deducting the non-fused depth, measured after fracture, from the total orginal plate thickness. Tables 4.6 to 4.10 give average values for weld penetration along with base plate area, depth of preparation, weld area, area of weld defects and initial out-of-straightness of the specimen. Weld defects were measured using calipers or templates. Negative out-of-straightness indicates that the weld was on the concave side of the bow and positive values on the convex. For tests involving a pair of specimens the values for plate and weld areas are for two specimens. The weld penetration

Table 4.6 Dimensions of Welds and Specimens, 5 mm Series

Test No.	Plate Dimensions				Weld Depth				Gross Weld Area mm2	Area of Defects (mm^2)	Initial O-O-S (mm)
	Width (mm)	Thick (mm)	Area (mm^2)	Depth of Preparation	μ (mm)	σ (mm)	V (%)	Mean Nominal			
O5WS1	158.0	25.8	4076	7.5	5.46	0.83	15.1	1.09	863	2	-0.28
O5WS2	158.3	25.9	3970	7.5	5.27	0.29	5.5	1.05	834	1	-1.06
O5WS3	158.4	25.8	4087	8.0	6.47	0.88	13.5	1.29	1025	4	0.36
O5WS4	158.2	25.8	4082	7.0	5.98	0.53	8.9	1.20	946	2	2.55
O5WS5	158.2	25.8	4082	7.0	6.98	0.68	9.8	1.40	1104	21	2.84
O5WS6	158.5	25.8	4089	7.0	6.38	0.75	11.8	1.28	1011	3	0.36
O5AS1	158.5	26.0	4118	5.5	5.26	0.87	16.6	1.05	834	1	-1.73
O5AS2	158.2	25.8	4082	6.5	4.94	0.44	8.9	0.99	782	10	-1.76
O5AS3	158.1	26.0	4111	5.5	5.05	0.58	11.4	1.01	798	3	-0.12
O5AS4	158.5	25.7	4067	6.5	5.04	0.34	6.7	1.01	799	4	-0.17
O5WP1	158.2	25.9	8194	7.3	6.19	0.65	10.5	1.24	1959	19	0.0
O5WP2	158.0	25.9	8168	6.5	6.03	0.79	13.1	1.21	1905	28	0.0
O5WP3	156.4	25.8	8070	7.0	5.86	0.63	10.8	1.17	1832	12	0.0
O5WP4	158.1	25.9	8190	7.0	5.52	0.67	12.1	1.10	1745	40	0.0
O5AP1	158.6	25.9	8216	5.5	4.84	0.56	11.6	0.97	1535	10	0.0
O5AP2	158.7	26.0	8252	7.0	6.25	0.49	7.9	1.25	1984	36	0.0

Table 4.7 Dimensions of Welds and Specimens, 10 mm Series

Test No.	Plate Dimensions				Weld Depth				Gross Weld Area mm^2	Area of Defects (mm^2)	Initial O-O-S (mm)
	Width (mm)	Thick (mm)	Area (mm^2)	Depth of Preparation	μ (mm)	σ (mm)	V (%)	Mean Nominal			
10WS1	157.7	25.7	4053	11.0	10.4	2.42	23.3	1.04	1640	8	3.14
10WS2	158.7	25.7	4079	10.0	8.67	0.54	6.2	0.87	1376	13	1.65
10WS3	157.9	25.9	4090	10.0	8.03	0.62	7.7	0.80	1268	10	1.95
10WS4	158.0	25.7	4061	10.0	9.43	0.62	6.6	0.94	1490	2	3.19
10WS5	158.1	25.7	4063	10.0	8.08	0.41	5.1	0.81	1277	4	2.03
10WS6	159.2	25.9	4123	10.0	7.94	0.66	8.3	0.79	1264	11	3.53
10AS1	158.6	25.8	4092	12.0	10.9	0.61	5.6	1.09	1729	13	-1.19
10AS2	158.6	25.8	4092	12.0	10.4	0.61	5.9	1.04	1649	22	-0.90
10AS3	158.6	25.8	4092	13.0	11.6	1.09	9.4	1.16	1840	7	1.66
10AS4	156.3	25.8	4033	13.0	11.3	1.07	9.5	1.13	1766	15	-2.82
10WP1	158.2	25.8	8164	10.5	10.1	0.82	8.2	1.01	3196	20	0.0
10WP2	158.5	25.7	8146	9.5	8.48	0.35	4.2	0.85	2688	19	0.0
10WP3	158.2	25.7	8132	10.0	9.08	0.39	4.3	0.91	2872	24	0.0
10WP4	158.0	25.7	8122	10.0	9.35	0.40	4.3	0.94	2954	14	0.0
10AP1	157.6	25.9	8164	11.0	10.4	1.01	9.7	1.04	3278	16	0.0
10AP2	158.4	25.8	8174	11.5	10.3	0.45	4.4	1.03	3260	24	0.0

Table 4.8 Dimensions of Welds and Specimens, 15 mm Series

Test No.	Plate Dimensions				Weld Depth				Gross Weld Area mm^2	Area of Defects (mm^2)	Initial O-O-S (mm)
	Width (mm)	Thick (mm)	Area (mm^2)	Depth of Preparation	μ (mm)	σ (mm)	V (%)	Mean Nominal			
15WS1	156.7	25.6	4012	13.1	11.6	1.04	9.0	0.77	1818	12	-2.00
15WS2	157.4	25.8	4061	15.1	12.7	1.24	9.8	0.85	1999	56	4.36
15WS3	157.4	25.9	4077	18.4	14.7	1.35	9.2	0.98	2314	36	-3.34
15WS4	157.0	25.8	4051	16.0	15.2	1.20	7.9	1.01	2386	12	-1.57
15WS5	157.1	25.9	4069	16.9	15.7	0.66	4.2	1.05	2466	96	0.00
15WS6	156.0	25.9	4040	16.1	13.1	1.47	8.7	0.88	2049	103	-0.78
15AS1	157.5	26.0	4095	16.8	14.5	0.64	4.4	0.97	2284	72	-0.92
15AS2	156.8	26.0	4077	16.2	14.0	1.11	7.9	0.93	2195	56	-0.57
15AS3	157.5	26.0	4095	17.0	15.3	0.74	4.8	1.02	2410	33	-0.45
15AS4	157.3	26.0	4090	13.8	9.9	0.57	5.8	0.66	1557	7	1.50
15WP1	157.0	25.9	8122	15.2	12.6	1.19	9.4	0.84	3946	90	0.0
15WP2	155.4	25.9	8050	16.1	13.3	0.94	7.1	0.88	4124	67	0.0
15WP3	157.3	25.8	8116	15.3	13.0	1.06	8.2	0.87	4090	55	0.0
15WP4	156.7	25.9	8118	16.1	12.4	0.43	3.3	0.85	4014	66	0.0
15AP1	157.1	25.9	8138	15.4	13.6	1.08	8.0	0.91	4284	92	0.0
15AP2	157.2	26.0	8174	16.2	14.1	2.35	16.7	0.94	4436	61	0.0

Table 4.9 Dimensions of Welds and Specimens, 20 mm Series

Test No.	Plate Dimensions				Weld Depth				Gross Weld Area mm^2	Area of Defects (mm^2)	Initial O-O-S (mm)
	Width (mm)	Thick (mm)	Area (mm^2)	Depth of Preparation	μ (mm)	σ (mm)	V (%)	Mean Nominal			
20WS1	145.0	25.5	3698	20.2	17.8	1.24	7.0	0.89	2581	24	4.70
20WS2	145.0	25.9	3756	20.9	16.6	0.67	4.1	0.83	2407	40	-
20WS3	145.0	25.9	3756	21.6	19.4	1.18	6.1	0.97	2819	30	0.89
20WS4	145.1	25.8	3744	21.4	19.9	0.85	4.3	1.00	2881	82	-2.25
20WS5	145.0	25.7	3727	20.7	18.4	0.33	1.8	0.92	2674	71	2.28
20WS6	145.1	25.8	3744	21.6	18.9	0.96	5.1	0.94	2736	41	2.35
20AS1	144.7	25.8	3733	20.8	18.7	2.02	10.8	0.94	2706	117	-0.02
20AS2	145.0	25.8	3741	20.8	19.0	1.36	7.2	0.95	2755	28	1.03
20AS3	145.0	25.8	3741	20.1	19.0	2.36	12.4	0.95	2755	124	-0.49
20AS4	144.9	25.8	3738	20.6	15.6	1.35	8.7	0.78	2264	12	1.90
20WP1	145.1	25.9	7516	20.8	18.1	0.96	5.3	0.91	5248	71	0.0
20WP2	145.1	25.7	7458	19.3	17.1	1.27	7.4	0.86	4556	53	0.0
20WP3	145.0	25.6	7424	20.5	16.3	0.82	5.0	0.82	4736	162	0.0
20WP4	145.0	25.8	7482	20.2	17.3	1.95	1.1	0.87	5022	99	0.0
20AP1	145.0	25.8	7482	20.6	17.1	1.26	7.4	0.86	4960	105	0.0
20AP2	145.1	25.8	7488	20.4	19.1	1.78	9.3	0.96	5540	172	0.0

Table 4.10 Dimensions of Welds and Specimens, 25 mm Series

Test No.	Plate Dimensions				Weld Depth				Gross Weld Area mm^2	Area of Defects (mm^2)	Initial O-O-S (mm)
	Width (mm)	Thick (mm)	Area (mm^2)	Depth of Preparation	μ (mm)	σ (mm)	V (%)	Mean Nominal			
25W1	120.7	25.7	3096	25.7	25.7	0.0	0.0	1.03	3096	N.A.	4.80
25W2	120.0	25.5	3060	25.5	25.5	0.0	0.0	1.02	3060	N.A.	0.34
25W3	119.7	25.9	3100	25.9	25.9	0.0	0.0	1.04	3100	N.A.	-1.01
25W4	120.6	25.8	3111	25.8	25.8	0.0	0.0	1.03	3111	N.A.	1.06
25W5	121.0	25.6	3098	25.6	25.6	0.0	0.0	1.02	3098	N.A.	-3.28
25W6	119.5	25.9	3095	25.9	25.9	0.0	0.0	1.04	3095	N.A.	0.85
25A1	120.7	25.9	3120	25.9	25.9	0.0	0.0	1.04	3120	N.A.	4.60
25A2	119.0	25.8	3070	25.8	25.8	0.0	0.0	1.03	3070	N.A.	-1.36
25A3	117.5	25.8	3032	25.8	25.8	0.0	0.0	1.03	3032	N.A.	-0.30
25A4	120.8	25.8	3117	25.8	25.8	0.0	0.0	1.03	3117	N.A.	-2.36
25A5	120.6	25.9	3124	25.9	25.9	0.0	0.0	1.04	3124	N.A.	3.06

Table 4.11 Summary of Weld Dimensions

	Weld Penetrations				
Nominal	5	10	15	20	25
Mean (mm)	5.72	9.65	13.48	18.02	25.78
Standard Dev. (mm)	0.64	1.19	1.50	1.24	0.14
Mean measured/nom.	1.14	0.965	0.899	0.901	1.031
Standard Dev.	0.128	0.119	0.100	0.062	0.056
Coeff. of Var. (%)	11.1	12.3	11.1	6.87	0.53

data are summarzied in Table 4.11.

4.2.3 Fracture Surface Observations

Failure of all partial joint penetration groove welds occurred on or near the fusion face of the plate with the square preparation. This fusion face for 5 mm welds lay in the base metal at an angle approaching 45° to the square preparation because of melting of the base metal. As the depth of penetration increased this angle decreased until for the 15 and 20 mm welds the angle approached zero. The fracture appearance, angle of fracture and the amount of defects present varied with depth of penetration.

The 5 mm welds all had a silky smooth appearance giving evidence of a ductile shear failure. Fracture appears to have begun at the weld root and propogated along the fusion face of the plate. In most cases the fracture surface was at angle of about 45° with the plate surface following the line where the base metal had been melted. Figures 4.3a and 4.3b, show a typical fracture surface. There were few or no defects evident in the 5 mm welds.

Fracture surfaces of the 10 mm weld specimens were predominately silky smooth in appearance with a few small clevage areas. In general the fracture surfaces were nearly perpendicular to the plate surfaces as shown in Figs. 4.4a and 4.4b. Some localized yielding could be seen in the adjoining base plate on either side of the weld.

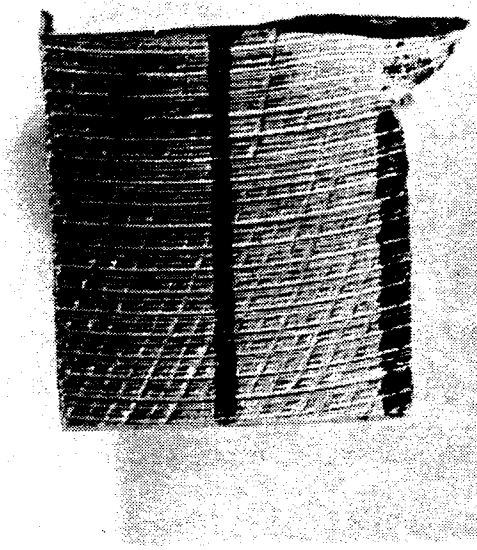

a) Profile of fracture

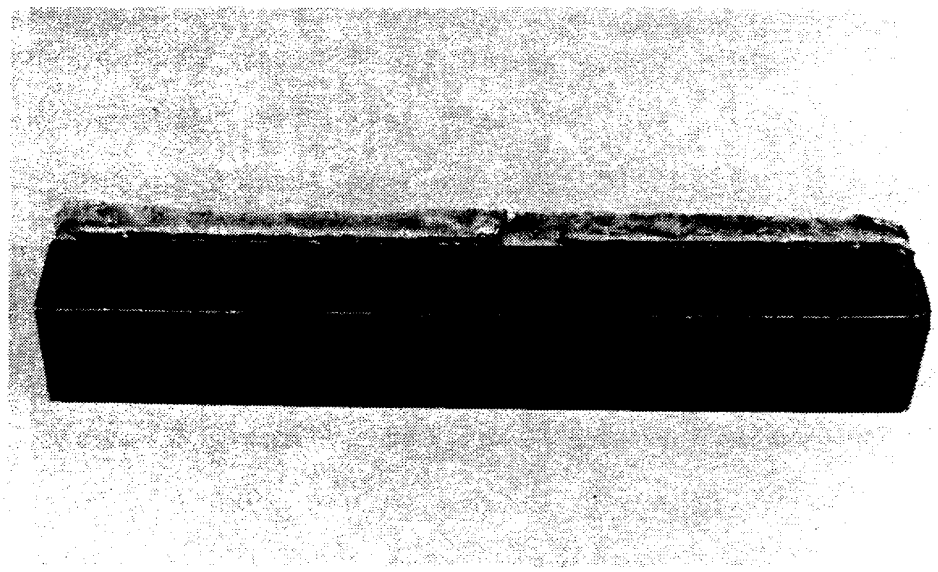

b) Fracture face

Figure 4.3 Fracture Surfaces of 5 mm Weld

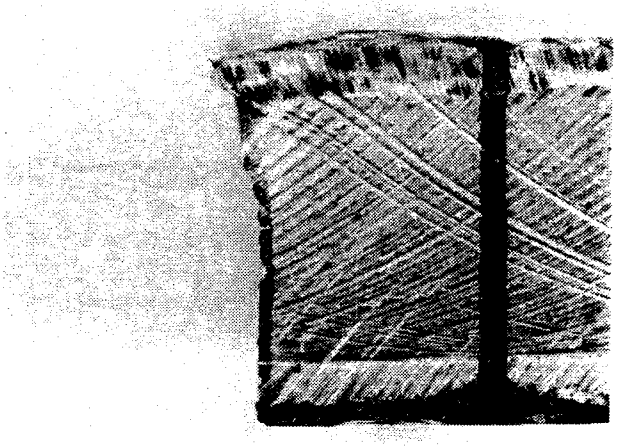

a) Profile of fracture

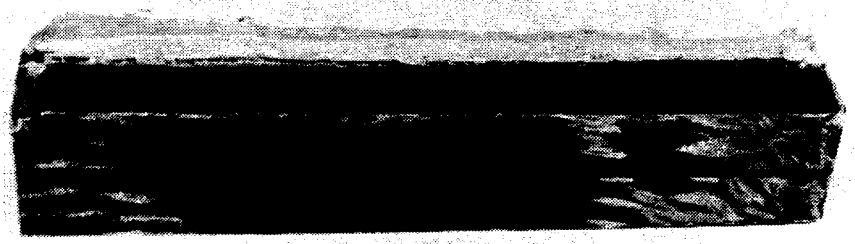

b) Fracture face

Figure 4.4 Fracture Surfaces of 10 mm Weld

In the 15 mm weld series the appearance of the fracture surfaces were in general half silky smooth and half grainy or crystalline. Although the grainy fracture surfaces indicate the final failure was brittle all welds showed considerable ductility. Most of the fracture surfaces were at right angles to the plate surfaces but in some cases the fracture extended into the plate as shown in Figs. 4.5a and 4.5b. Some porosity or inclusions amounting to up to 4.5% of the area of the weld were present in about one half of the welds of this size.

Although the fracture was very ductile, as was evident from the rotations and deformations that occurred as discussed subsequently, the fracture surfaces of the 20 mm welds were predominately grainy in appearance and were at right angles to the plate surface as shown in Figures 4.6a and 4.6b. Porosity and inclusions were present amounting to up to 4.5% of the weld area in twelve of the sixteen specimens, as shown in Fig. 4.7.

The 25mm or full penetration weld specimens failed in the plate as discussed in section 4.1.2.

The fracture surface observations showed that for partial joint penetration groove welds failure always occurred on or near the fusion face of the plate with no or square preparation. All welds exhibited ductile behaviour. However, because of the small amount of weld metal that deforms the overall deformation of the specimen may be limited. Data related to weld defects are presented in

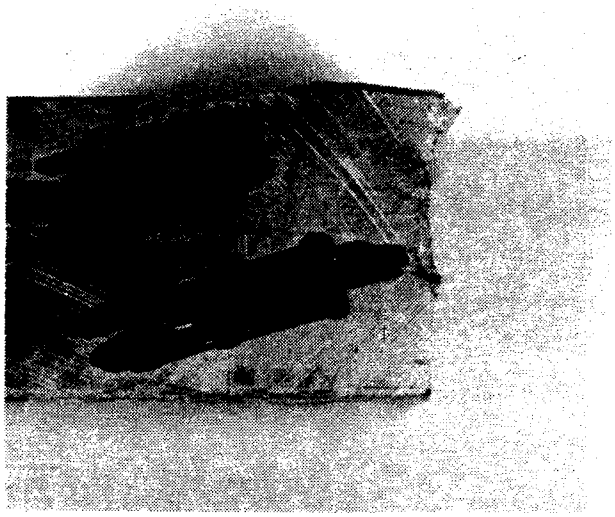

a) Profile of fracture

b) Fracture face

Figure 4.5 Fracture Surfaces of 15 mm Weld

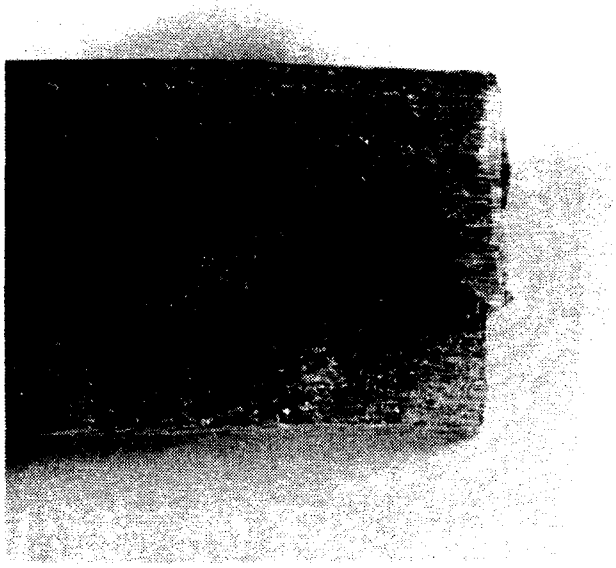

a) Profile of fracture

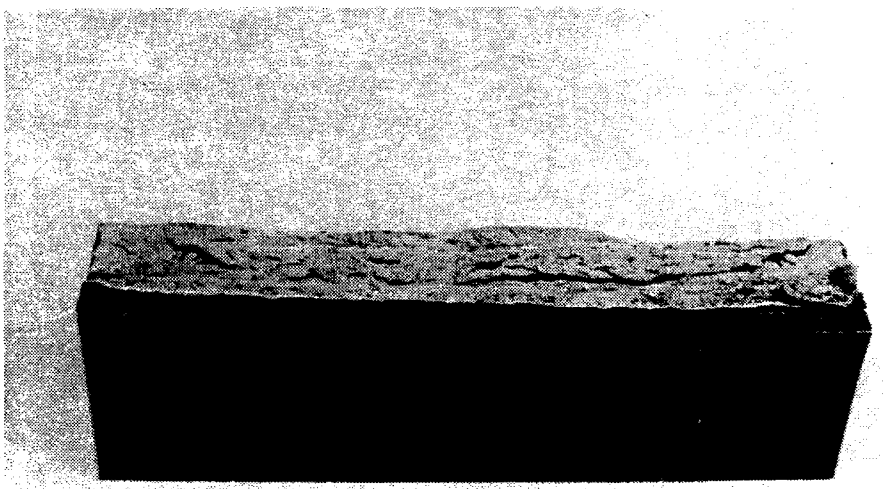

b) Fracture face

Figure 4.6 Fracture Surfaces of 20 mm Welds

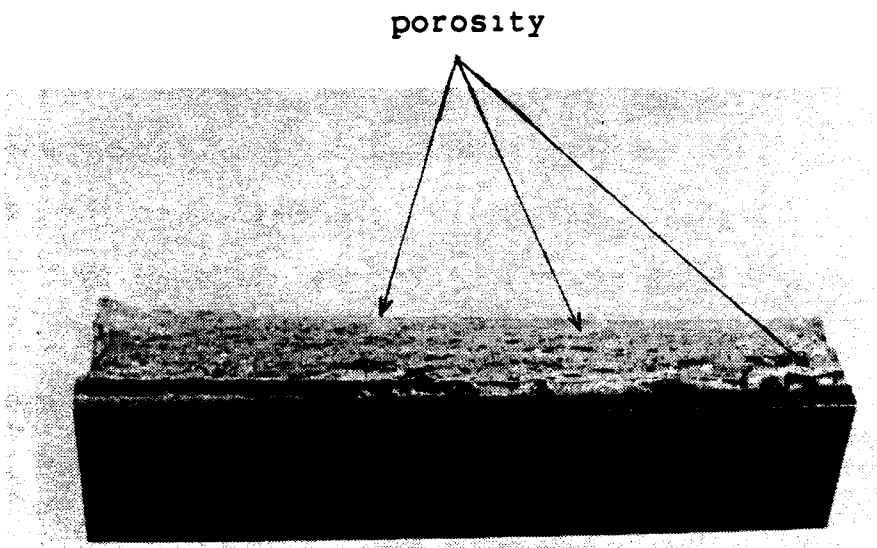

Figure 4.7 Secondary Defects in Welds

Tables 4.6 to 4.9. These data show that the average area of defects for the 5 mm welds was 0.8% and ranged from 0.1 to 2.3% of the weld area, for the 10 mm welds, 0.7% and ranged from 0.1 to 1.3%, for the 15 mm welds, about 2.0% and ranged from 0.4 to 4.5 and for the 20 mm welds, about 2.1% and ranged from 0.5 to 4.5%.

4.2.4 Ultimate Weld Strength

The ultimate strengths of the partial joint penetration groove welds have been computed in 3 different ways, first by dividing the ultimate load the weld sustained by the gross area of the plate, second by dividing by the gross area of the weld assuming no defects and third by dividing by the net area of the weld taking the area of defects into account. In each case the results are normalized by dividing by the mean ultimate strength of the full penetration groove welds made from the same grade of base metal, as given in Tables 4.3 and 4.4. The weld strength data are given in Tables 4.12 to 4.15 and summarized in Table 4.16. The percent penetration is the ratio of gross weld area to plate area.

4.2.5 Deformations in Welds

For the specimens tested singly, deformations across the welds, lateral deflections of the specimens at the weld, and rotations of the plates with respect to one another due to deformations in the weld are given in Tables 4.17 to 4.20

Table 4.12 Ultimate Strengths of 5 mm Welds

			Ultimate Strength, Based on					
			Plate Area		Gross Weld Area		Net Weld Area	
TEST No.	Weld Penetration (%)	Ultimate Load (kN)	$\sigma_{pw}=\frac{P}{A_p}$	$\frac{\sigma_{pw}}{\sigma_{fw}}$	$\sigma_{uw}=\frac{P}{A_w}$	$\frac{\sigma_{uw}}{\sigma_{fw}}$	$\sigma_{uwn}=\frac{P}{A_{wn}}$	$\frac{\sigma_{uwn}}{\sigma_{fw}}$
O5WS1	21.2	556.5	136.5	0.275	644.8	1.30	646.3	1.30
O5WS2	21.0	545.0	137.3	0.277	653.3	1.32	654.3	1.32
O5WS3	25.1	599.2	146.6	0.245	584.6	1.18	586.9	1.18
O5WS4	23.2	630.8	154.4	0.312	666.8	1.34	667.9	1.35
O5WS5	27.1	663.4	162.5	0.328	600.9	1.21	612.4	1.23
O5WS6	24.7	644.5	157.6	0.318	637.5	1.29	639.4	1.29
O5AS1	20.3	539.6	131.0	0.250	647.0	1.23	647.8	1.23
O5AS2	19.2	589.1	144.3	0.275	753.3	1.43	763.1	1.45
O5AS3	19.4	570.8	138.8	0.265	715.3	1.36	718.0	1.37
O5AS4	19.7	664.0	163.3	0.311	831.0	1.58	835.2	1.59
O5WP1	23.9	1185	144.6	0.292	604.9	1.22	610.8	1.23
O5WP2	23.3	1281	156.8	0.316	672.4	1.36	682.5	1.38
O5WP3	22.7	1169	144.9	0.292	638.1	1.29	642.3	1.30
O5WP4	21.3	1122	137.0	0.276	643.0	1.30	658.1	1.33
O5AP1	18.7	1255	152.8	0.291	817.6	1.56	823.0	1.57
O5AP2	24.0	1387	168.1	0.320	699.1	1.33	712.0	1.36

Note: Stresses in MPa

Table 4.13 Ultimate Strengths of 10 mm Welds

		Ultimate Strength, based on						
			Plate Area		Gross Weld Area		Net Weld Area	
TEST No.	Weld Penetration (%)	Ultimate Load (kN)	$\sigma_{pw}=\frac{P}{A_p}$	$\frac{\sigma_{pw}}{\sigma_{fw}}$	$\sigma_{uw}=\frac{P}{A_w}$	$\frac{\sigma_{uw}}{\sigma_{fw}}$	$\sigma_{uwn}=\frac{P}{A_{wn}}$	$\frac{\sigma_{uwn}}{\sigma_{fw}}$
10WS1	40.5	887	218.9	0.441	540.9	1.09	543.5	1.10
10WS2	33.7	816	200.0	0.403	593.0	1.20	598.7	1.21
10WS3	31.0	781	191.0	0.385	615.9	1.24	620.8	1.25
10WS4	36.7	858	211.3	0.426	575.8	1.16	576.6	1.16
10WS5	31.4	814	200.3	0.404	637.4	1.29	639.4	1.29
10WS6	30.7	798	193.5	0.390	631.3	1.27	636.9	1.28
10AS1	42.3	1030	251.7	0.479	595.7	1.13	600.2	1.14
10AS2	40.3	979	239.2	0.456	593.7	1.13	601.7	1.15
10AS3	45.0	1069	261.2	0.498	581.0	1.11	583.2	1.11
10AS4	43.8	1057	262.1	0.499	598.5	1.14	603.7	1.15
10WP1	39.2	1843	225.7	0.455	576.7	1.16	580.3	1.17
10WP2	33.0	1630	200.1	0.403	606.4	1.22	610.7	1.23
10WP3	35.3	1764	216.9	0.437	614.2	1.24	619.4	1.25
10WP4	36.4	1782	219.4	0.442	603.2	1.22	606.1	1.22
10AP1	40.2	1982	242.8	0.462	604.6	1.15	607.6	1.16
10AP2	39.9	2020	247.1	0.471	619.6	1.18	624.2	1.19

Note: Stresses in MPa

Table 4.14 Ultimate Strengths of 15 mm Welds

			Ultimate Strength, based on					
			Plate Area		Gross Plate Area		Net Plate Area	
TEST No.	Weld Penetration (%)	Ultimate Load (kN)	$\sigma_{pv}=\frac{P}{A_p}$	$\frac{\sigma_{pv}}{\sigma_{tw}}$	$\sigma_{uv}=\frac{P}{A_v}$	$\frac{\sigma_{uv}}{\sigma_{tw}}$	$\sigma_{uvn}=\frac{P}{A_{vn}}$	$\frac{\sigma_{uvn}}{\sigma_{tw}}$
15WS1	45.3	1049	261.5	0.527	577.0	1.16	580.8	1.17
15WS2	49.2	1094	269.4	0.543	547.3	1.10	563.0	1.14
15WS3	56.8	1189	291.6	0.588	513.8	1.04	521.9	1.05
15WS4	58.9	1224	302.1	0.609	513.0	1.03	515.6	1.04
15WS5	60.6	1299	319.2	0.644	526.8	1.06	548.1	1.11
15WS6	50.7	1110	274.8	0.554	541.7	1.09	570.4	1.15
15AS1	55.8	1285	313.8	0.598	562.6	1.07	580.9	1.11
15AS2	53.8	1277	313.2	0.597	581.8	1.11	597.0	1.14
15AS3	58.9	1371	334.8	0.638	568.9	1.08	576.8	1.10
15AS4	38.1	1042	254.8	0.485	669.2	1.27	672.3	1.28
15WP1	48.6	2283	281.1	0.567	578.6	1.17	592.1	1.19
15WP2	51.2	2295	285.1	0.575	556.5	1.12	565.7	1.14
15WP3	50.4	2353	289.9	0.585	575.3	1.16	583.1	1.18
15WP4	49.5	2265	279.0	0.563	564.3	1.14	573.7	1.16
15AP1	52.6	2678	329.1	0.627	625.1	1.19	638.8	1.22
15AP2	54.3	2606	318.8	0.607	587.5	1.12	595.7	1.13

Note: Stresses in MPa

Table 4.15 Ultimate Strengths of 20 mm Welds

			Ultimate Strength, based on					
			Plate Area		Gross Weld Area		Net Weld Area	
TEST No.	Weld Penetration (%)	Ultimate Load (Kn)	$\sigma_{pv}=\frac{P}{A_p}$	$\frac{\sigma_{pv}}{\sigma_{fv}}$	$\sigma_{uv}=\frac{P}{A_v}$	$\frac{\sigma_{uv}}{\sigma_{fv}}$	$\sigma_{uvn}=\frac{P}{A_{vn}}$	$\frac{\sigma_{uvn}}{\sigma_{fv}}$
20WS1	69.8	1391	376.1	0.758	538.9	1.09	544.0	1.10
20WS2	64.1	1271	338.4	0.682	528.0	1.06	537.0	1.08
20WS3	75.1	1553	413.5	0.834	550.9	1.11	556.8	1.12
20WS4	77.0	1640	438.0	0.883	569.2	1.15	585.9	1.18
20WS5	71.8	1426	382.6	0.771	533.3	1.08	547.8	1.10
20WS6	73.1	1422	379.8	0.766	519.7	1.05	527.6	1.06
20AS1	72.5	1452	389.0	0.741	536.6	1.02	560.8	1.07
20AS2	73.6	1635	437.0	0.833	593.5	1.13	599.6	1.14
20AS3	73.6	1519	406.0	0.773	551.4	1.05	577.3	1.10
20AS4	60.6	1363	364.6	0.695	602.0	1.15	605.2	1.15
20WP1	69.8	2764	367.7	0.741	526.7	1.06	533.9	1.08
20WP2	61.1	2482	332.8	0.671	544.8	1.10	551.2	1.11
20WP3	63.8	2641	342.3	0.690	536.5	1.08	577.4	1.16
20WP4	67.1	2486	332.3	0.670	495.0	0.998	505.0	1.02
20AP1	66.3	2927	391.2	0.745	590.1	1.12	602.9	1.15
20AP2	74.0	2851	380.7	0.725	514.6	0.98	531.1	1.01

Note: Stresses in MPa

Table 4.16 Summary of Ultimate Weld Strengths

Weld size, mm	5	10	15	20	25
μ % Pen.	22.2	37.5	52.2	69.6	100.0
σ	2.4	4.6	5.7	5.1	0.0
V (%)	11.0	12.3	10.9	7.4	0.0
μ $\frac{\sigma_{pw}}{\sigma_{tw}}$	0.289	0.441	0.582	0.749	1.00
σ	0.028	0.037	0.042	0.062	0.02
V (%)	9.7	8.4	7.2	8.3	0.02
μ $\frac{\sigma_{uw}}{\sigma_{tw}}$	1.33	1.18	1.13	1.08	1.00
σ	0.11	0.06	0.06	0.05	0.02
V (%)	8.5	5.0	5.6	4.7	0.02
μ $\frac{\sigma_{uwn}}{\sigma_{tw}}$	1.34	1.19	1.14	1.10	1.00
σ	0.12	0.06	0.06	0.05	0.02
V (%)	8.58	4.88	5.20	4.38	0.02

for both the ultimate and fracture loads. As the mounting devices tended to remain at right angles to the plate surfaces, any rotation in the weld causing rotation leads to LVDTs measurements that are too large. The data have been corrected to allow for this. The lateral deflections of the specimens at the weld have been adjusted for the initial out-of-straightness. Typical stress-strain curves, lateral deflection vs. stress on the weld area and rotation vs. stress curves are shown in Figures 4.8 to 4.9, 4.10 to 4.11 and 4.12 to 4.13 respectively.

No data are presented for the weld deformations of specimens tested in pairs as the opposing curvatures that developed in the specimens under load made it impossible to interpret the LVDT readings.

4.2.6 Deformations in the Plate

From the strain gauges mounted in pairs on opposite sides on the plate both axial and bending strains can be determined. Then by using the stress-strain relationships determined in the ancillary tests the bending moment can be determined at the gauge locations. Tables 4.21 to 4.24 give the bending moments at various distances from the weld that existed at ultimate load. Table 4.25 gives the same data at various load steps for several specimens where P is the maximum load for the particular specimen.

Table 4.17 Deformations at Weld, 5 mm Series

Specimen	Strain Across Weld on 75mm gauge length		Lateral Deflections at Weld (mm)		Rotations at weld (deg)	
	Ultimate	Fracture	Ultimate	Fracture	Ultimate	Fracture
05WS1	0.0114	0.0134	5.13	5.04	2.32	2.25
05WS2	0.0090	0.0104	5.02	5.05	2.33	2.29
05WS3	0.0110	0.0130	5.48	5.64	2.40	2.29
05WS4	0.0204	0.0232	5.95	5.81	2.55	2.53
05WS5	0.0161	0.0215	6.05	5.78	2.79	2.61
05WS6	0.0111	0.0205	5.37	4.89	2.37	2.10
05AS1	0.0052	0.0066	4.07	4.03	2.06	2.07
05AS2	0.0094	0.0129	4.41	4.11	2.15	2.10
05AS3	0.0118	0.0129	4.66	4.50	2.29	2.20
05AS4	0.0109	0.0151	5.60	5.48	2.52	2.41

Table 4.18 Deformations at Weld, 10 mm Series

Specimen	Strain Across Weld on 75mm gauge length		Lateral Deflections at Weld (mm)		Rotations at weld (deg)	
	Ultimate	Fracture	Ultimate	Fracture	Ultimate	Fracture
10WS1	0.0274	0.0280	6.85	7.97	2.47	2.61
10WS2	0.0206	0.0267	6.42	6.47	2.54	2.58
10WS3	0.0252	0.0343	6.65	6.34	2.37	2.27
10WS4	0.0188	0.0244	7.19	7.62	2.90	2.97
10WS5	0.0158	0.0234	6.93	6.99	2.76	2.79
10WS6	0.0140	0.0208	6.32	6.44	3.03	3.06
10AS1	0.0168	0.0267	5.17	6.40	2.16	2.50
10AS2	0.0129	0.0241	4.54	5.71	1.98	2.47
10AS3	0.0156	0.0244	4.78	6.25	2.56	2.99
10AS4	0.0124	0.0256	3.66	5.08	1.89	2.29

Table 4.19 Deformations at Weld, 15 mm Series

Specimen	Strain Across Weld on 75mm gauge length		Lateral Deflections at Weld (mm)		Rotations at weld (deg)	
	Ultimate	Fracture	Ultimate	Fracture	Ultimate	Fracture
15WS1	0.0124	-	3.97	-	3.84	-
15WS2	0.0155	0.0374	1.16	2.82	2.41	4.50
15WS3	0.0136	0.0457	3.21	5.42	2.67	5.65
15WS4 *	-	-	-	-	-	-
15WS5	0.0132	0.0150	0.46	0.49	1.45	1.61
15WS6	0.0122	0.0301	3.46	5.54	3.58	5.81
15AS1	0.0161	0.0335	2.86	4.41	3.16	4.82
15AS2	0.0180	0.0342	2.40	4.04	3.11	5.37
15AS3	0.0136	0.0276	1.91	3.84	3.88	7.06
15AS4	0.0132	0.0237	3.02	3.63	4.18	4.98

Table 4.20 Deformations at Weld, 20 mm Series

Specimen	Strain Across Weld on 75mm gauge length		Lateral Deflections at Weld (mm)		Rotations at weld (deg)	
	Ultimate	Fracture	Ultimate	Fracture	Ultimate	Fracture
20WS1	0.0212	0.0256	3.12	3.76	3.70	4.88
20WS2	0.0239	0.0255	1.30	1.39	1.97	2.11
20WS3	0.0378	0.0506	0.56	1.23	2.92	4.30
20WS4	0.0480	0.0855	-1.45	0.65	1.09	4.37
20WS5	0.0294	0.0465	1.88	3.91	3.71	6.42
20WS6	0.0266	0.0580	1.43	3.24	2.37	5.10
20AS1	0.0185	0.0357	0.68	2.04	0.92	3.08
20AS2	0.0316	0.0556	1.74	3.69	2.78	5.62
20AS3	0.0185	0.0470	0.64	0.82	2.56	3.41
20AS4	0.0127	0.0186	2.20	2.55	2.88	3.50

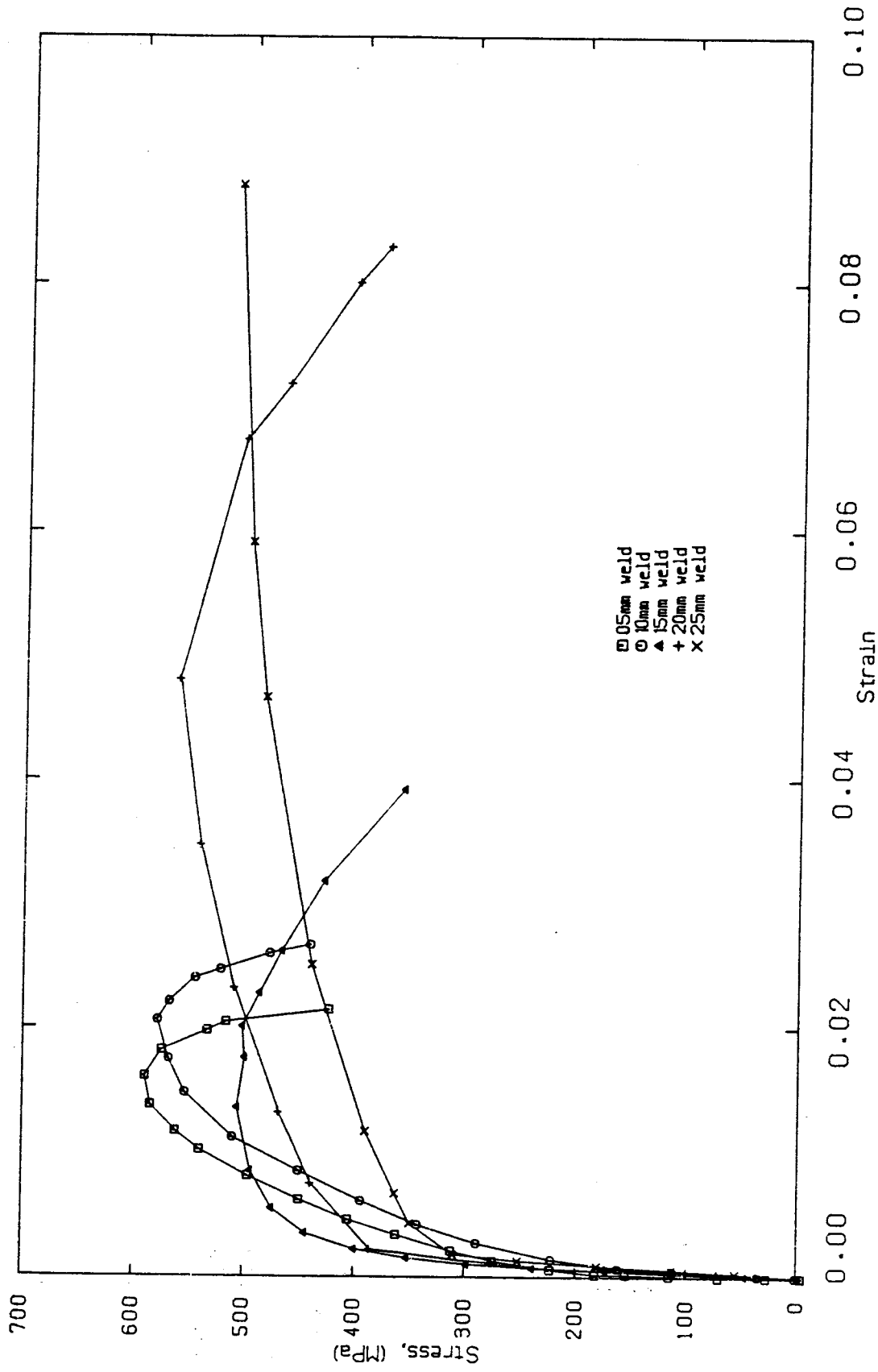

Figure 4.8 Stress-Strain Curves for 300W Steel Specimens

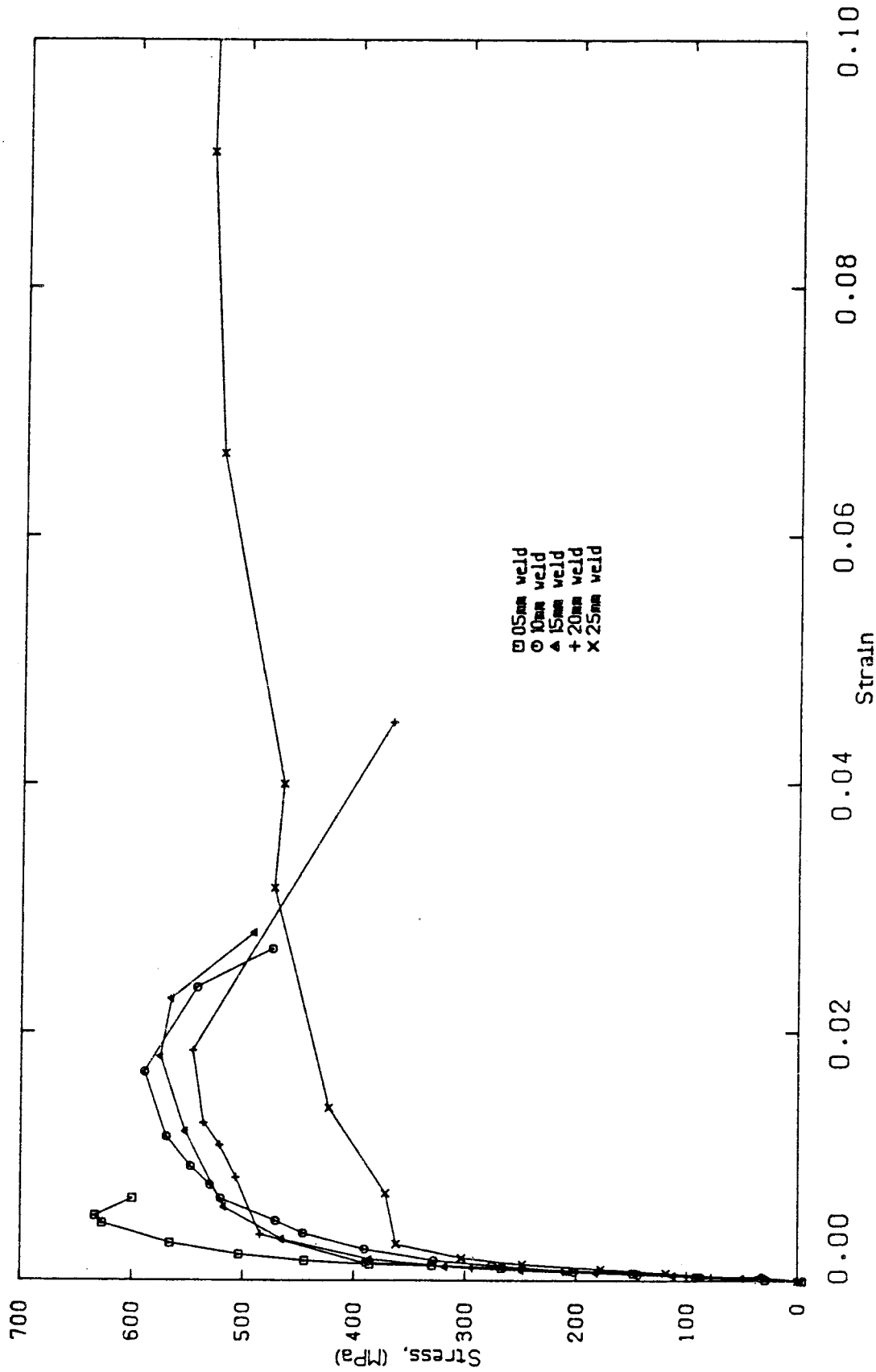

Figure 4.9 Stress-Strain Curves for 350A Steel Specimens

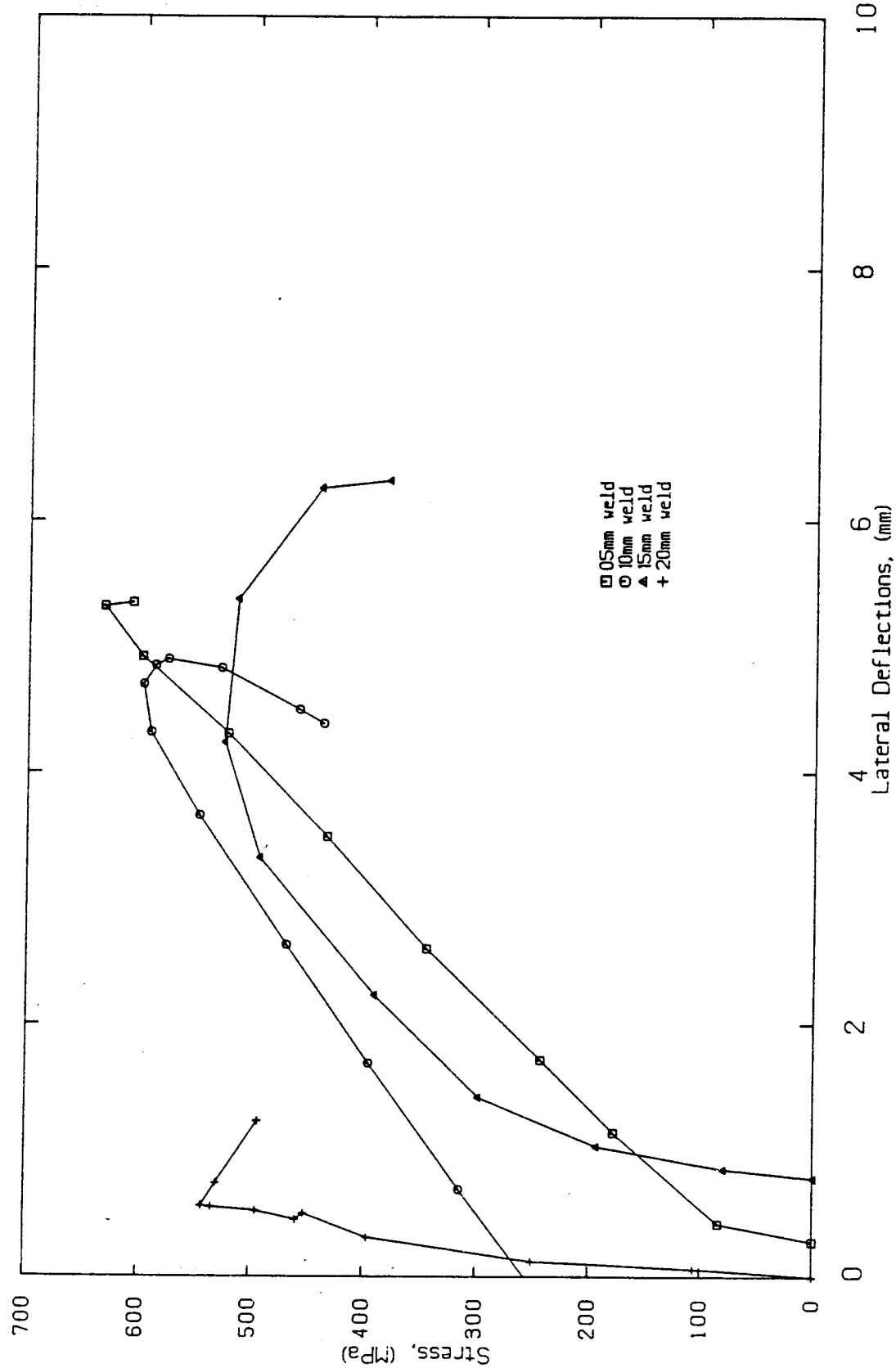

Figure 4.10 Lateral Deflections at Weld 300W Steel Specimens

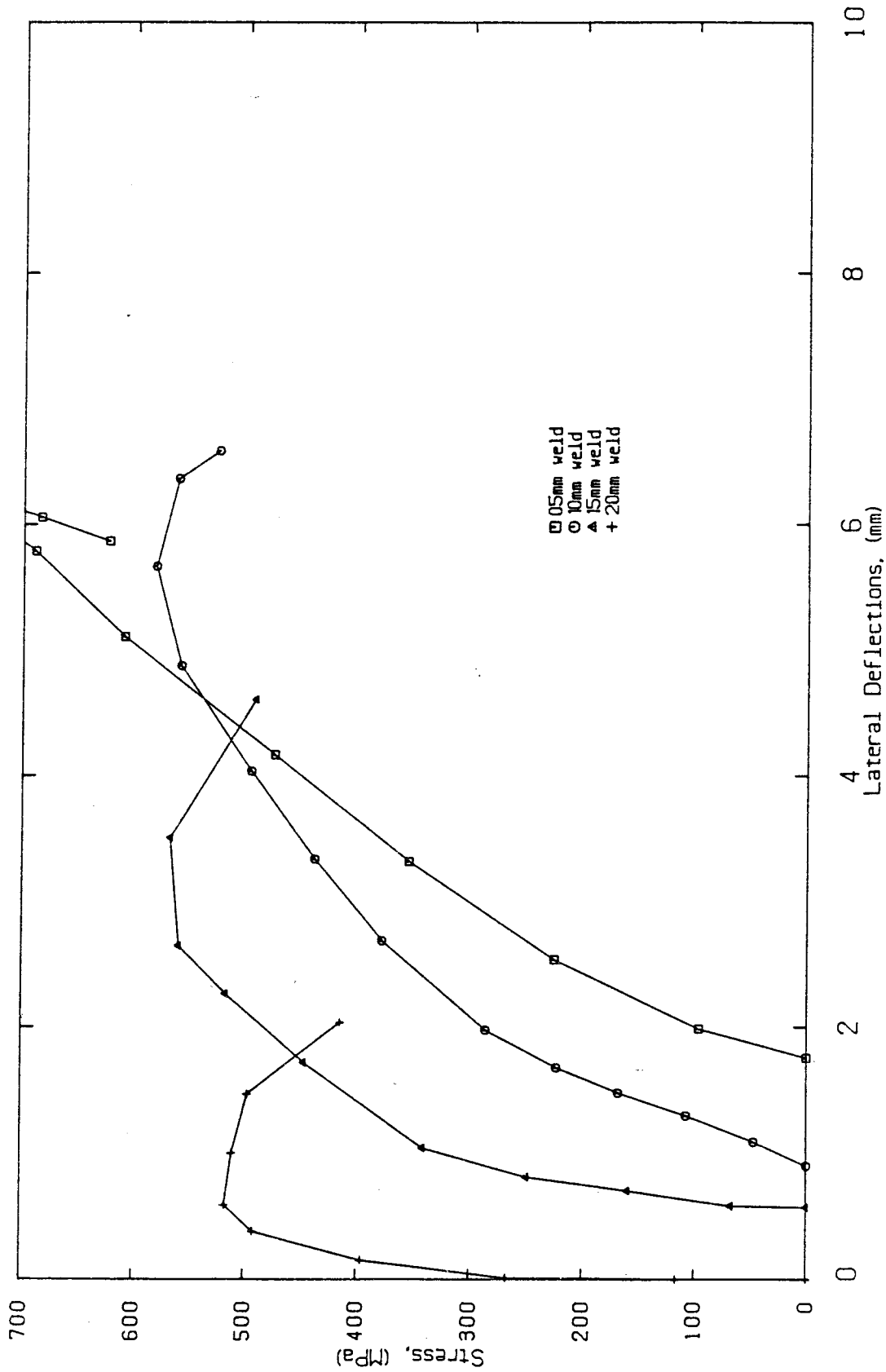

Figure 4.11 Lateral Deflections at Weld 350A Steel Specimens

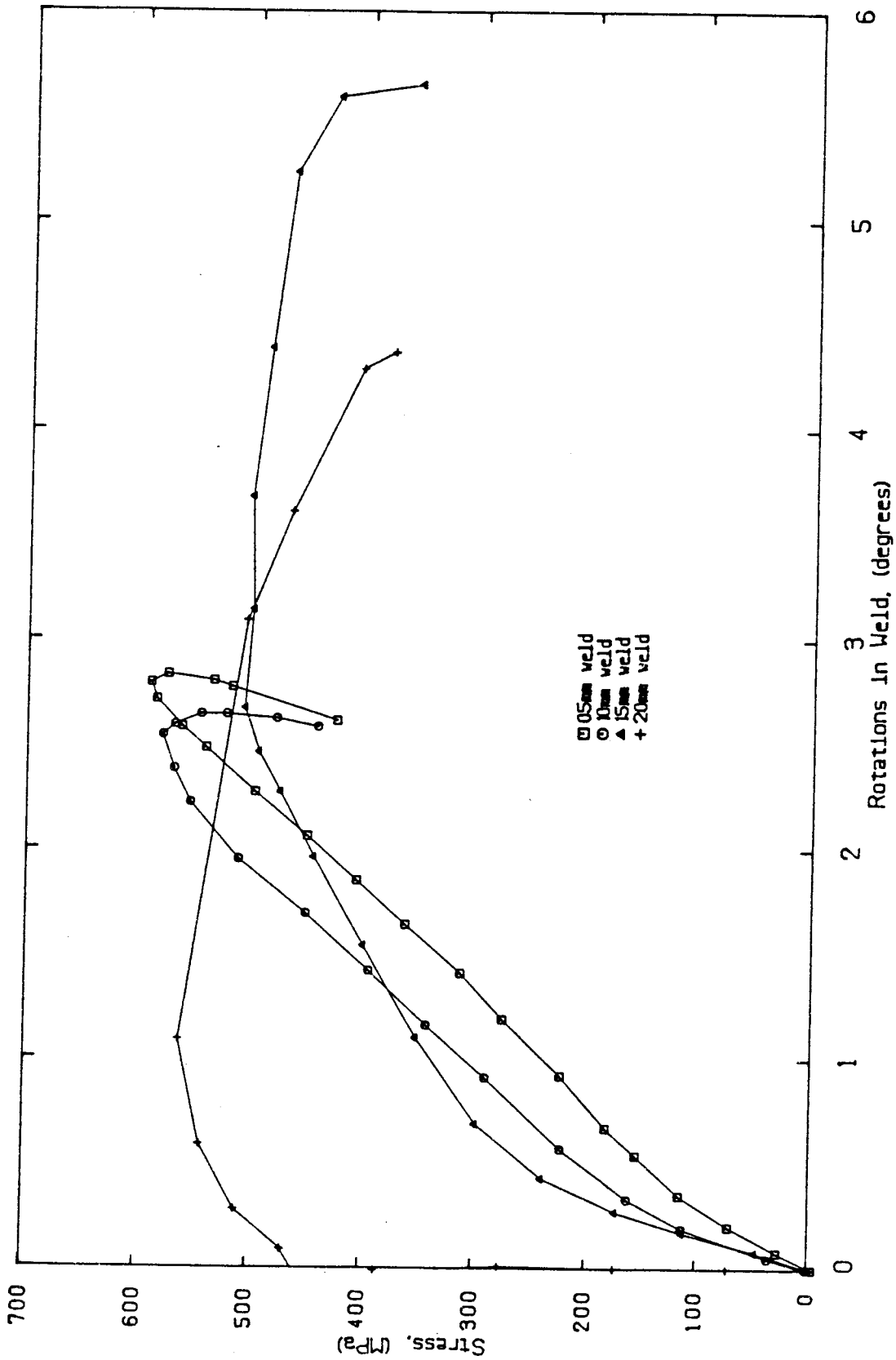

Figure 4.12 Rotations in Weld 300W Steel Specimens

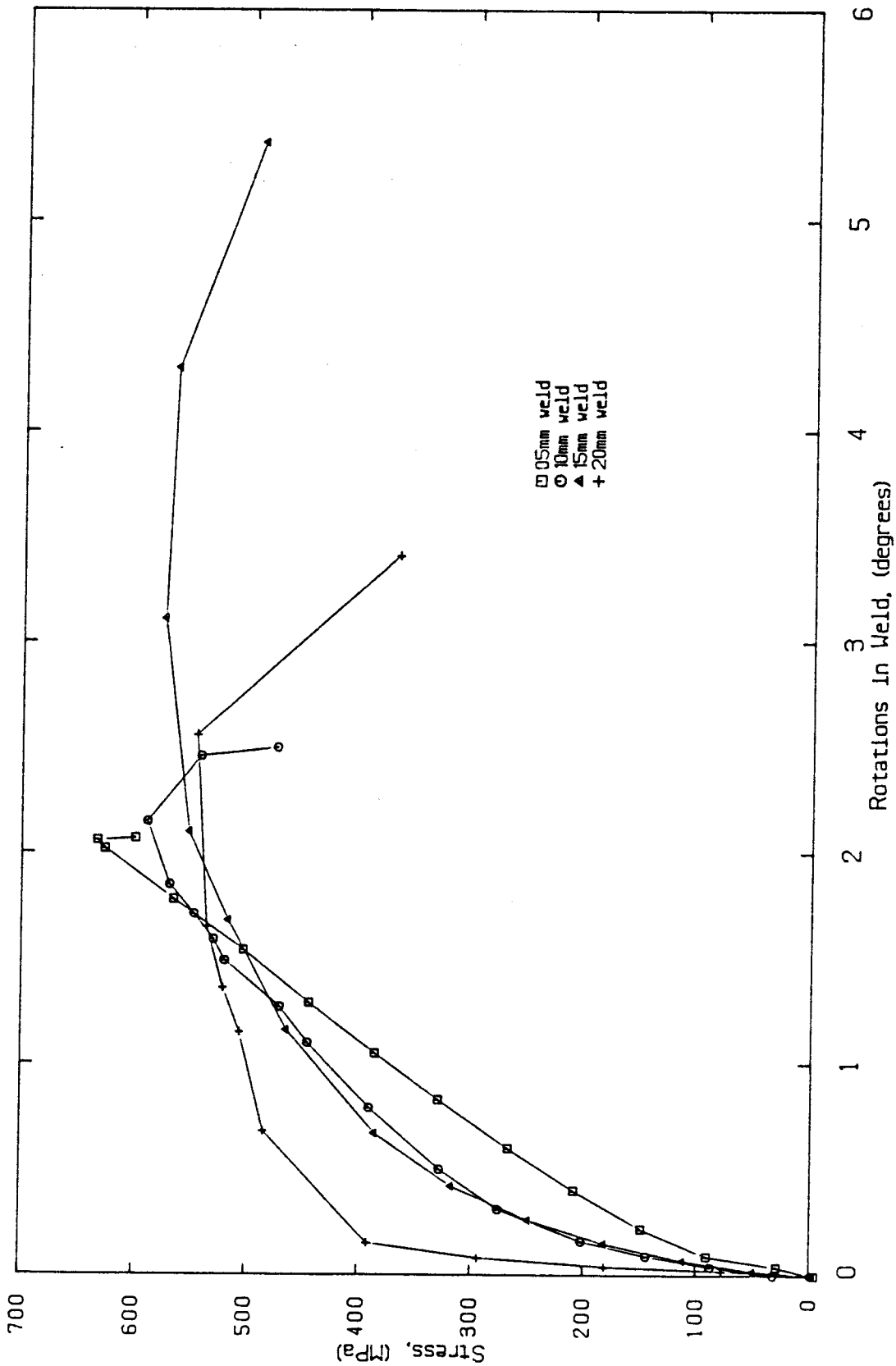

Figure 4.13 Rotations in Weld 350A Steel Specimens

Table 4.21 Bending Moments in Plates, 5 mm Series

Specimen	Bending moment at 62.5mm from weld (kNm)	Bending moment at 137.5mm from weld (kNm)
O5WS1	4.40	-
O5WS2	4.53	-
O5WS3	5.03	-
O5WS4	5.41	4.81
O5WS5	5.44	4.33
O5WS6	5.00	-
O5AS1	4.20	3.77
O5AS2	4.32	-
O5AS3	4.73	4.31
O5AS4	5.31	4.22
O5AP2	4.52	-

Table 4.22 Bending Moments in Plates, 10 mm Series

Specimen	Bending moment at 62.5mm from weld (kNm)	Bending moment at 137.5mm from weld (kNm)	Bending Moment at 200mm from weld (kNm)	Bending Moment at 275mm from weld (kNm)
10WS1	4.20	4.02	-	-
10WS2	5.32	3.74	-	-
10WS3	5.49	3.98	-	-
10WS4	5.07	3.79	-	-
10WS5	5.14	3.76	3.09	2.48
10WS6	5.11	3.85	3.13	2.47
10AS1	-	3.19	2.33	1.31
10AS2	4.96	3.17	2.49	1.77
10AS3	4.72	3.35	-	-
10AS4	4.00	4.44	-	-

Table 4.23 Bending Moments in Plates, 15 mm Series

Specimen	Bending moment at 75.0mm from weld (kNm)	Bending moment at 175.0mm from weld (kNm)
15WS1	4.16	2.63
15WS2	3.04	1.34
15WS3	2.02	1.55
15WS4	-	-
15WS5	1.82	1.01
15WS6	2.86	2.20
15AS1	2.39	1.66
15AS2	2.49	1.84
15AS3	1.96	1.41
15AS4	4.40	3.32
15WP1	2.08	-1.22
15WP2	1.29	-0.82
15WP3	1.58	-1.19
15WP4	1.83	-0.34
15AP1	1.09	-
15AP2	0.03	-0.63

Table 4.24 Bending Moments in Plates, 20 mm Series

Specimen	Bending moment at 75.0mm from weld (kNm)	Bending moment at 175.0mm from weld (kNm)
20WS1	0.0	0.0
20WS2	0.0	0.0
20WS3	0.0	0.0
20WS4	0.0	0.0
20WS5	0.0	0.0
20WS6	0.0	0.0
20AS1	0.0	0.0
20AS2	0.0	0.0
20AS3	0.0	0.0
20AS4	1.00	0.96
20WP1	0.0	0.0
20WP2	0.98	0.0
20WP3	0.0	0.0
20WP4	0.41	0.25
20AP1	0.0	0.10
20AP2	0.08	0.14

Table 4.25 Bending Moments in Specimens at Various Loads

Specimen and load steps	Distance from weld, mm, and bending moment, kNm			
05AS3	62.5 mm	137.5 mm		
0.25P	0.80	0.76		
0.50P	1.83	1.70		
0.75P	3.34	2.98		
1.00P	4.73	4.31		
10AS1	62.5 mm	137.5 mm	200.0 mm	275.0 mm
0.25P	0.14	0.00	-0.10	-0.18
0.50P	0.67	0.40	0.22	0.00
0.75P	2.76	1.75	1.30	0.77
1.00P	-	3.19	2.33	1.31
15AS2	75.0 mm	175.0 mm		
0.25P	0.12	0.18		
0.50P	0.40	0.48		
0.75P	1.05	0.95		
1.00P	2.49	1.84		
05AP2	62.5 mm			
0.25P	0.42			
0.50P	1.67			
0.75P	2.97			
1.00P	4.52			
15WP3	75.0 mm	175.0 mm		
0.25P	0.08	0.13		
0.50P	0.27	0.18		
0.75P	1.24	0.11		
1.00P	1.58	-1.19		

5. ANALYSIS OF TEST RESULTS

5.1 Specimen Equilibrium

5.1.1 General

The objective of the specimen equilibrium analysis is to derive models for both types of specimens, tested singly and in pairs, from which the forces acting on the weld can be determined. The analysis should be verifiable with test results.

5.1.2 Single Specimen

A free-body diagram of an initially straight single specimen is shown in Fig. 5.1a with an axial load, P, applied to the specimen. The eccentricity of the axial load with respect to the centre of resistance of the weld is, e. If the specimen is assumed to act as a rigid body the end moments are zero. From the free-body diagram of one-half the specimen in Fig. 5.1b the bending moment (moment of forces to one side of section about the centroid of the section) at any section of the plate and in the weld can be determined. The moment in the plate is zero and in the weld is

$$[5.1] \qquad M_w = Pe$$

as shown in Fig. 5.1c plotted on the compression side. The free-body diagram of the weld in Fig. 5.1d shows that the

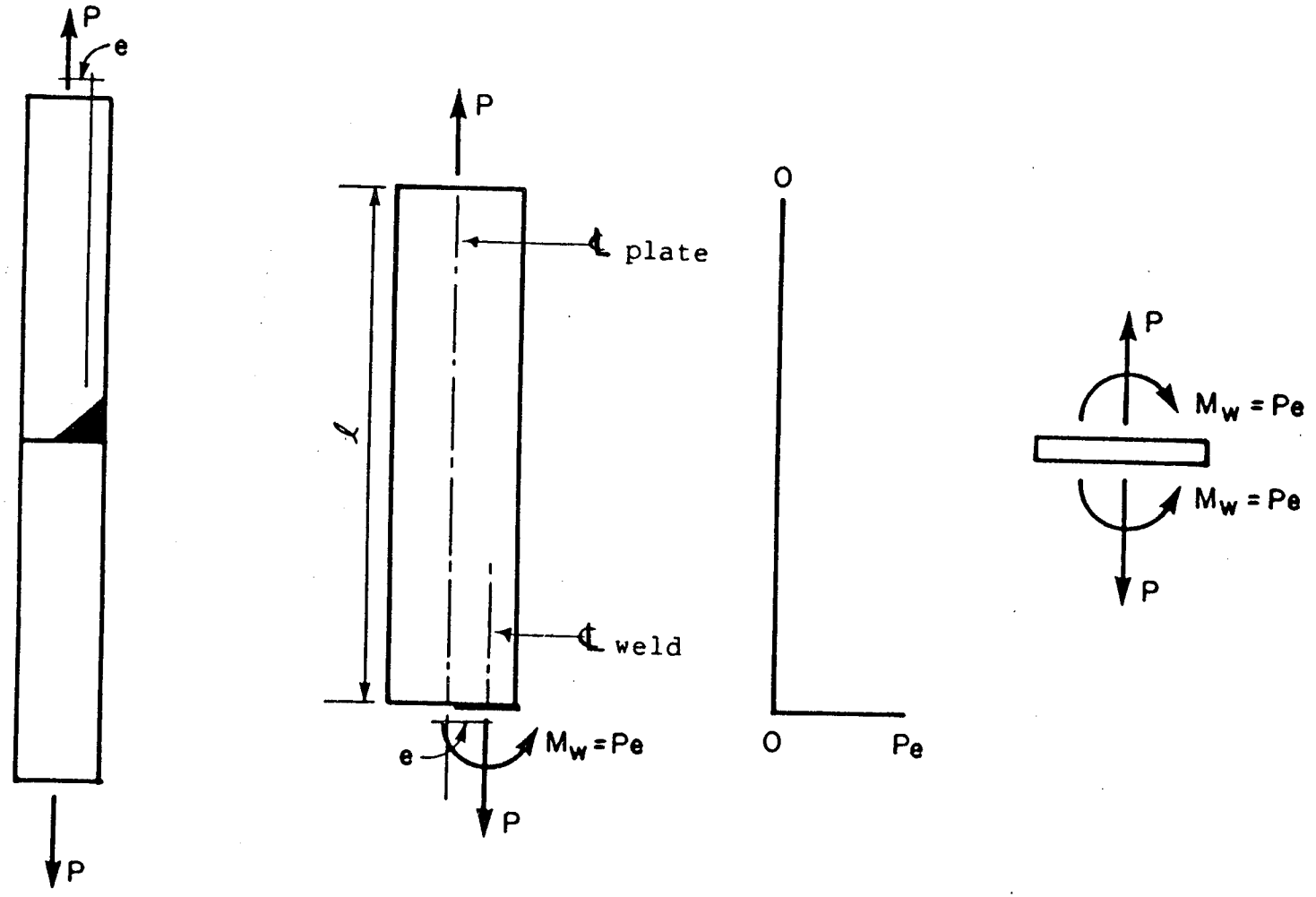

a) Free-body diagram of full specimen

b) Free-body diagram of half specimen

c) Bending moment diagram

d) Equilibrium of weld

Figure 5.1 Single Specimen

weld is acted upon by both the axial force P and the moment Pe.

Rotations in the weld occur and the plate tends to deflect, δ, laterally with the weld tending to align itself with the load, as the load, P, is increased. When lateral deflections occur end moments must be developed in the grips unless the grips are free to rotate. A free-body diagram of one-half of the deformed specimen, deflected δ, is shown in Fig. 5.2a. Deflections in the same direction as the eccentricity are taken to be positive. It is first assumed that the end moments, M_e, approach zero. The deflection δ decreases the eccentricity of the axial force on the weld to $(e - \delta)$ and the bending moment in the weld (with $M_e = 0$) is therefore

$$[5.2] \qquad M_{w1} = P(e - \delta)$$

The bending moment in the plate adjacent to the weld is

$$[5.3] \qquad M_{p1} = P\delta$$

and, as assumed, is zero in the grips. The bending-moment diagram (plotted on the compression side) under these assumptions is shown in Fig. 5.2b.

When the end moments are not zero, as must be the case when the specimen is held rigidly in the grips, the

bending-moment diagram is as shown in Fig. 5.2c. The end moment M_e reduces the moment in the weld as does the deflection.

As the load increases the weld will begin to yield in tension, first at the weld root, and finally across the entire throat. Under these conditions the weld has no moment capacity and must be loaded concentrically as shown in Fig. 5.3a, and the moment in the weld becomes

$$[5.4] \qquad M_{w2} = 0$$

The end moment in the plate is now increased to

$$[5.5] \qquad M_{e2} = P\ (e - \delta)$$

and the moment in the plate at the weld is

$$[5.6] \qquad M_{p2} = Pe$$

The bending-moment diagram is shown in Fig. 5.3b.

Tensile yielding may also occur in the plate reducing its moment capacity and this capacity reaches zero when the plate is fully yielded in tension.

Most plates had an initial out-of-straightness, Δ, due to the angular distortion about the axis of the weld caused by the welding procedure. This out-of-straightness is

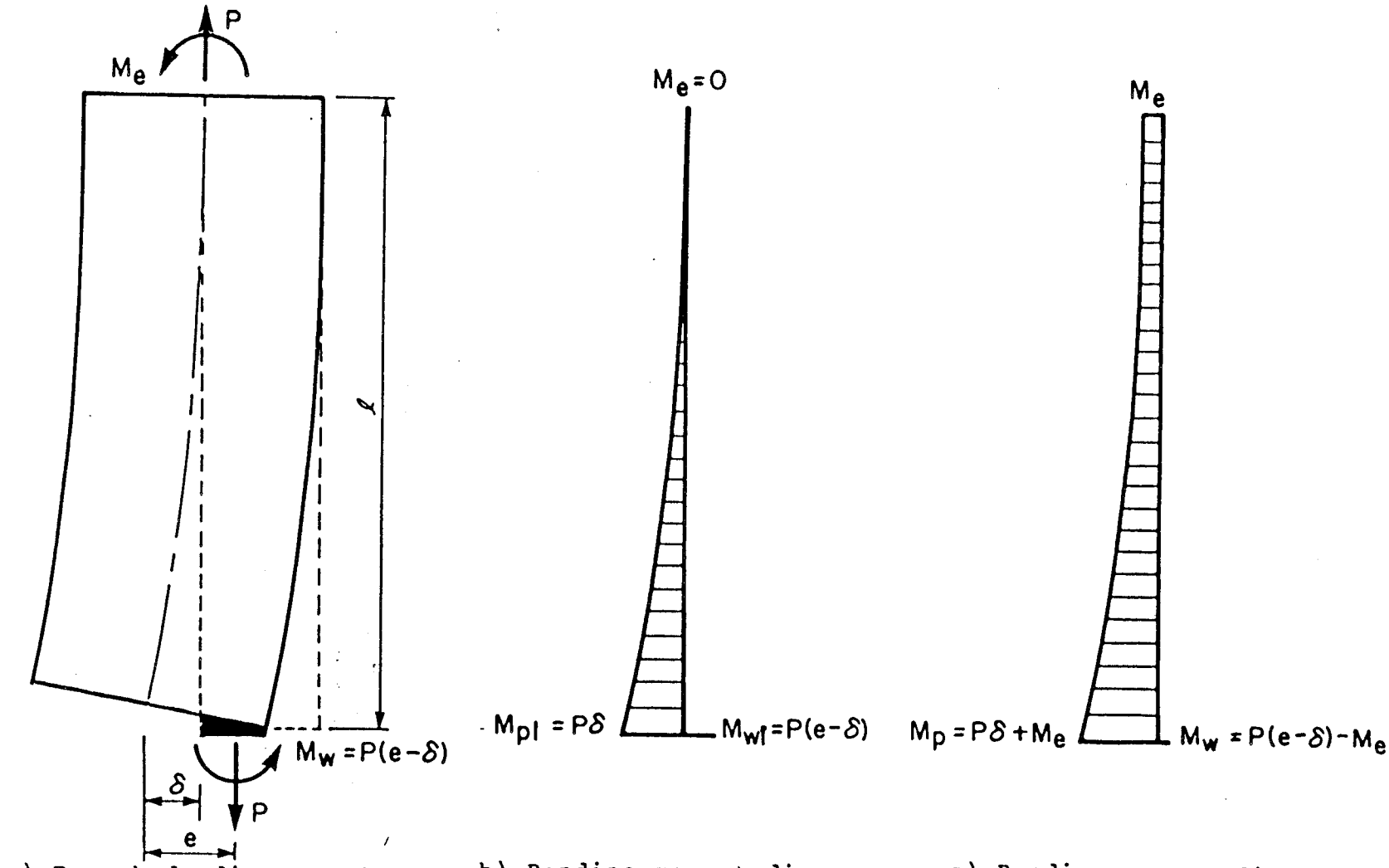

a) Free-body diagram of deflected 1/2 specimen

b) Bending moment diagram when $M_e=0$

c) Bending moment diagram when $M_e=M_e$

Figure 5.2 Bending Moment Diagrams for Single Specimens with Zero Initial Out of Straightness

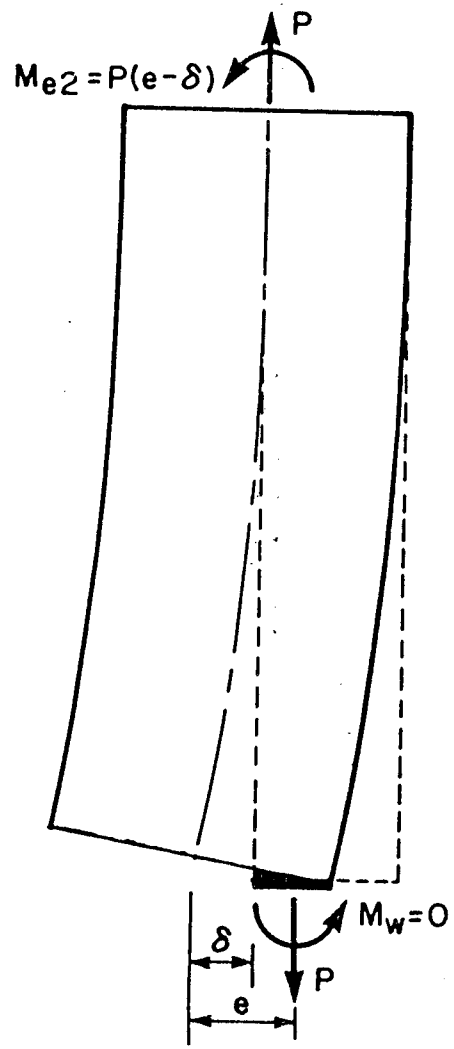

a) Free-body diagram of deflected shape

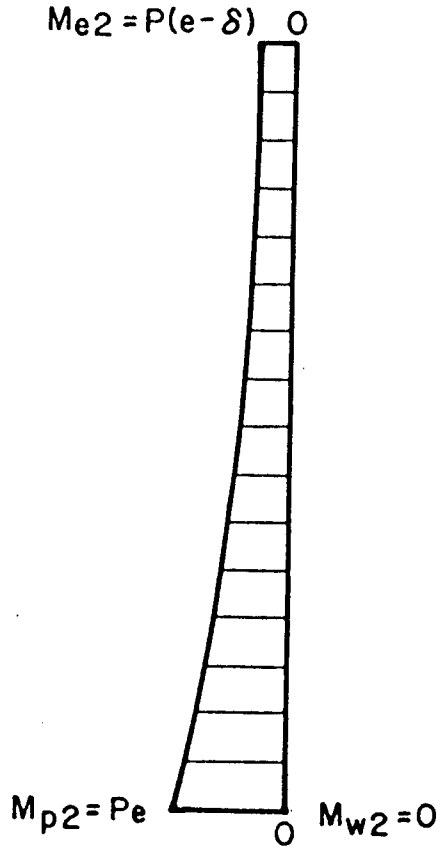

b) Bending moment diagram with fully yielded weld

Figure 5.3 Single Specimen with Fully Yielded Weld

considered to be positive if it increases the initial eccentricity of the weld as shown on Figures 5.2 and 5.3. Before the weld yields the out-of-straightness can increase or decrease the moment in the weld depending on its sign. Assuming the end moment is zero gives the moment diagram in Fig. 5.4a with a weld moment increased to

$$[5.7] \qquad M_{w1} = P\ (e + \Delta - \delta)$$

and the moment in the plate at the weld decreased to

$$[5.8] \qquad M_{p1} = P\ (\delta - \Delta)$$

When the weld is fully yielded in tension the moment in the weld is zero and the moment in the plate at the weld is

$$[5.6] \qquad M_{p2} = Pe$$

but the end moment is increased to

$$[5.9] \qquad M_{e2} = P\ (e + \Delta - \delta)$$

as shown in Fig. 5.4b. Of course the lateral deflection δ will tend to increase because of the presence of the initial out-of-straightness Δ just as it is greater when the initial eccentricity is greater.

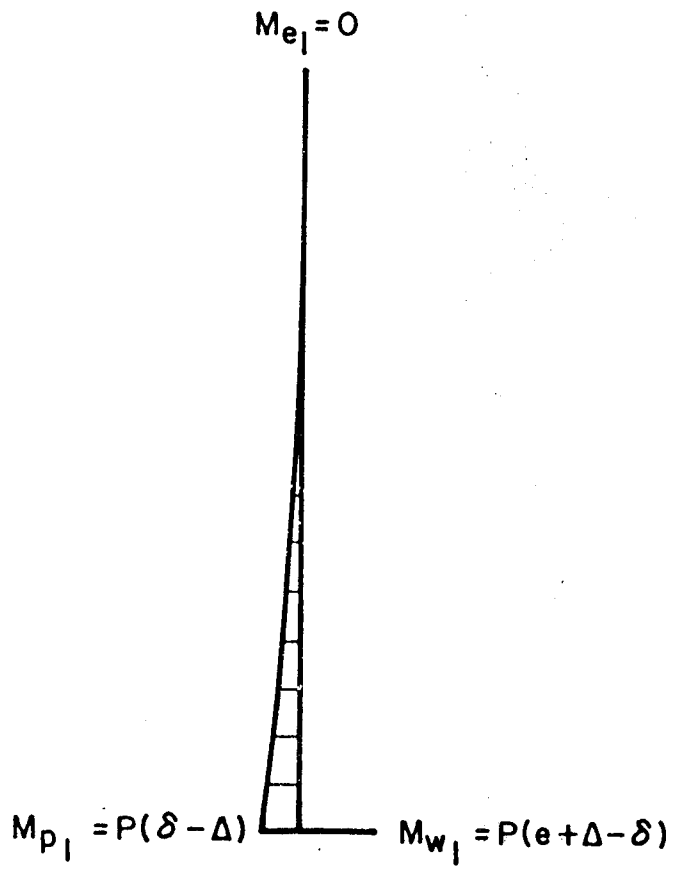

a) When $M_e = 0$

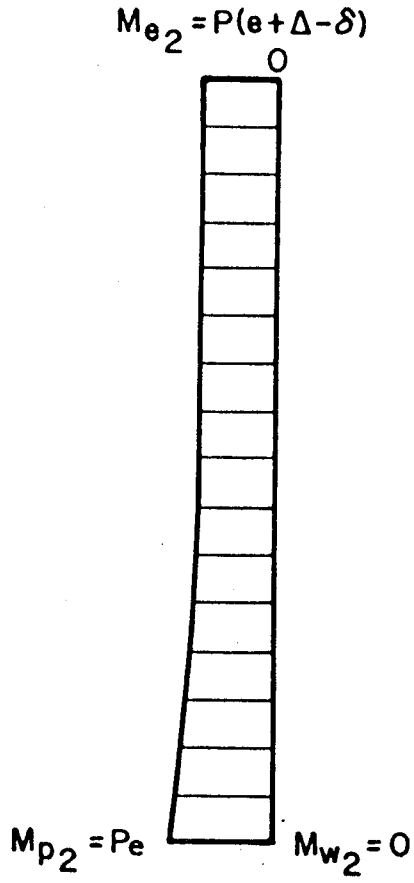

b) When weld is fully yielded

Figure 5.4 Bending Moment Diagrams for Initially Out-of-Straight Specimens

Therefore the model predicts that, in single specimens at ultimate load conditions, the welds are subject to tension only provided that the welds are sufficiently ductile to accommodate the rotations that must occur.

5.1.3 Pairs of Specimens

By testing specimens in pairs back-to-back with the welds on the outer faces, the lateral movement of the plates which reduces the moments in the welds is eliminated. Although overall, the pair of specimens is loaded concentrically, the moments in the welds are therefore greater than in the single specimens until yielding of the welds tends to reduce the bending moments. The rotations at the welds will therefore be greater than for the single welds at corresponding loads thus inducing greater moments in the plates. In Fig. 5.5 the bending distortions that occurred are evident. Fig. 5.6a shows a free-body diagram of 1/4 of a doubly symmetric specimen. For equilibrium

$$[5.10] \qquad \Sigma M = 0 = Pe + M_e - M_w - V\ell$$

When the weld yields fully $M_w = 0$ and therefore

$$[5.11] \qquad Pe + M_e - V\ell = 0$$

The plate is subject to a moment at the weld of Pe, and if

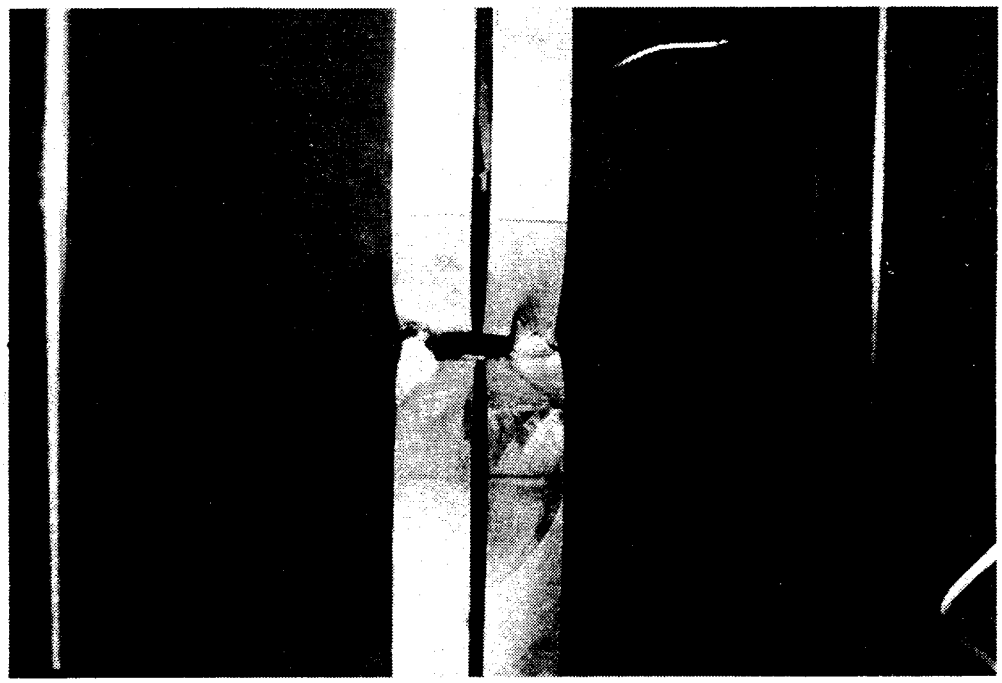

Figure 5.5 Bending in Pairs of Specimens

the plate is behaving elastically and fully fixed in the grips then

[5.12] $M_e = 0.5\ Pe$

and the moment diagram and deflected shape are as shown in Fig. 5.6b and 5.6c. Substituting [5.12] in [5.11] gives

[5.13] $V = \frac{3Pe}{2\ell}$

Testing the specimen in pairs back to back therefore introduces greater rotations in the welds and transverse shears in the plates that in the worst case, in these tests, was estimated to be about 5% of the axial load. For the larger size welds, not only is the eccentricity reduced relatively but also the condition may result that the plate adjacent to the weld yields fully before the weld fractures. When this is the case, the moments in the plate are zero and therefore the shears are zero.

5.1.4 Comparison with Test Results

The distribution of predicted bending moments in the plates for single specimens and specimens tested in pairs can be compared with test results for those tests in which strain gauges were mounted on both sides of the plate. From the strain readings both bending moments and axial forces

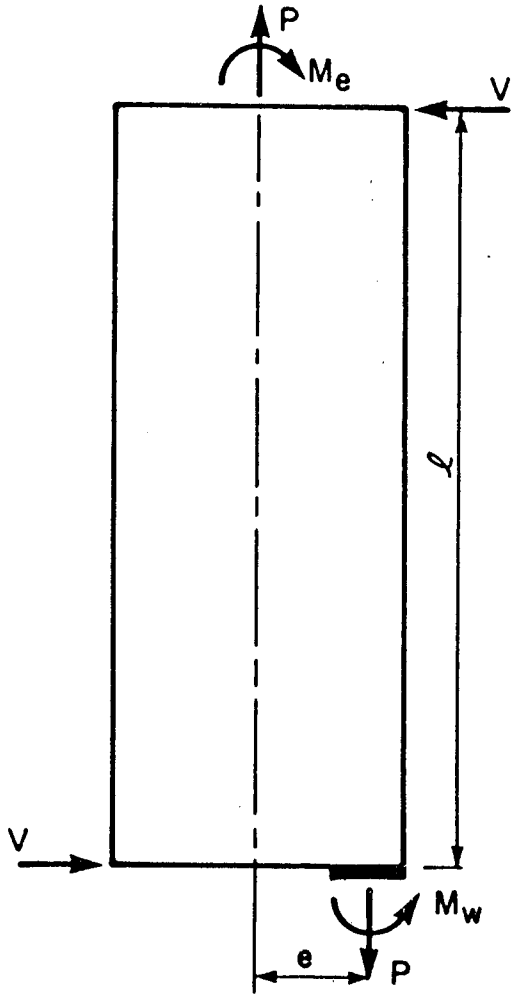

a) Free-body diagram

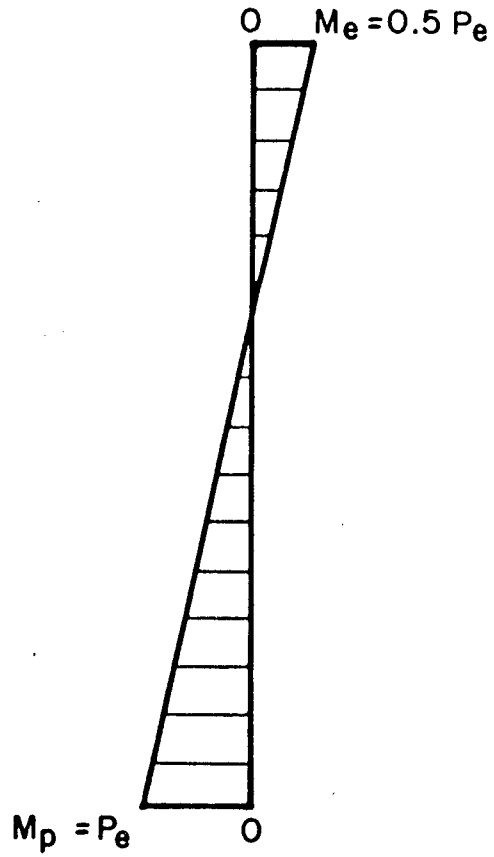

b) Bending moment diagram for plate when weld is plastic

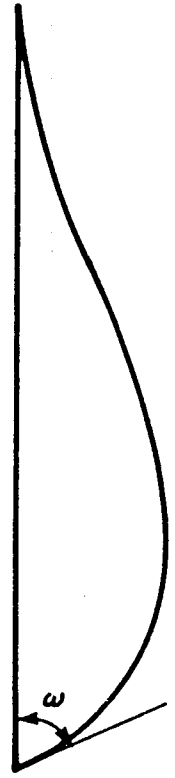

c) Deflected shape

Figure 5.6 Pair of Specimens

can be deduced.

Fig. 5.7 shows the distribution of bending moments in one-half of a single plate for test 05AS3 for loads from $0.25P_u$ to $1.0P_u$, where P_u is the ultimate load, in $0.25P_u$ increments. As the 5 mm weld is relatively small compared to the plate area the plates remained elastic throughout the test. The lower curve for each increment represents the case where the end moment in the grips is assumed to be zero and the upper curve represents the case when the weld is fully yielded. It is seen that the experimental points gradually migrate upwards as the load is increased and lie on or near the upper line for higher loads indicating that the weld has yielded.

Fig. 5.8 gives the distribution of bending moments for 4 load increments for specimen 10AS1 in the 10 mm series tested singly. As for the 5 mm single specimen the data for low loads lie near the line representing zero moment in the grips but migrate upwards to coincide with the curve representing full yielding of the weld. In Fig. 5.9 moment distributions are plotted at ultimate load for 3 different 10 mm specimens tested singly. At the weld the moments predicted for the fully yielded weld condition are in reasonable agreement with the test results while at the grip end the moments range from about 40 to 90% of the predicted moments for the 3 tests. When the weld is fully yielded the initial out-of-straightness affects the end moment and not the moment in the plate at the weld as discussed previously

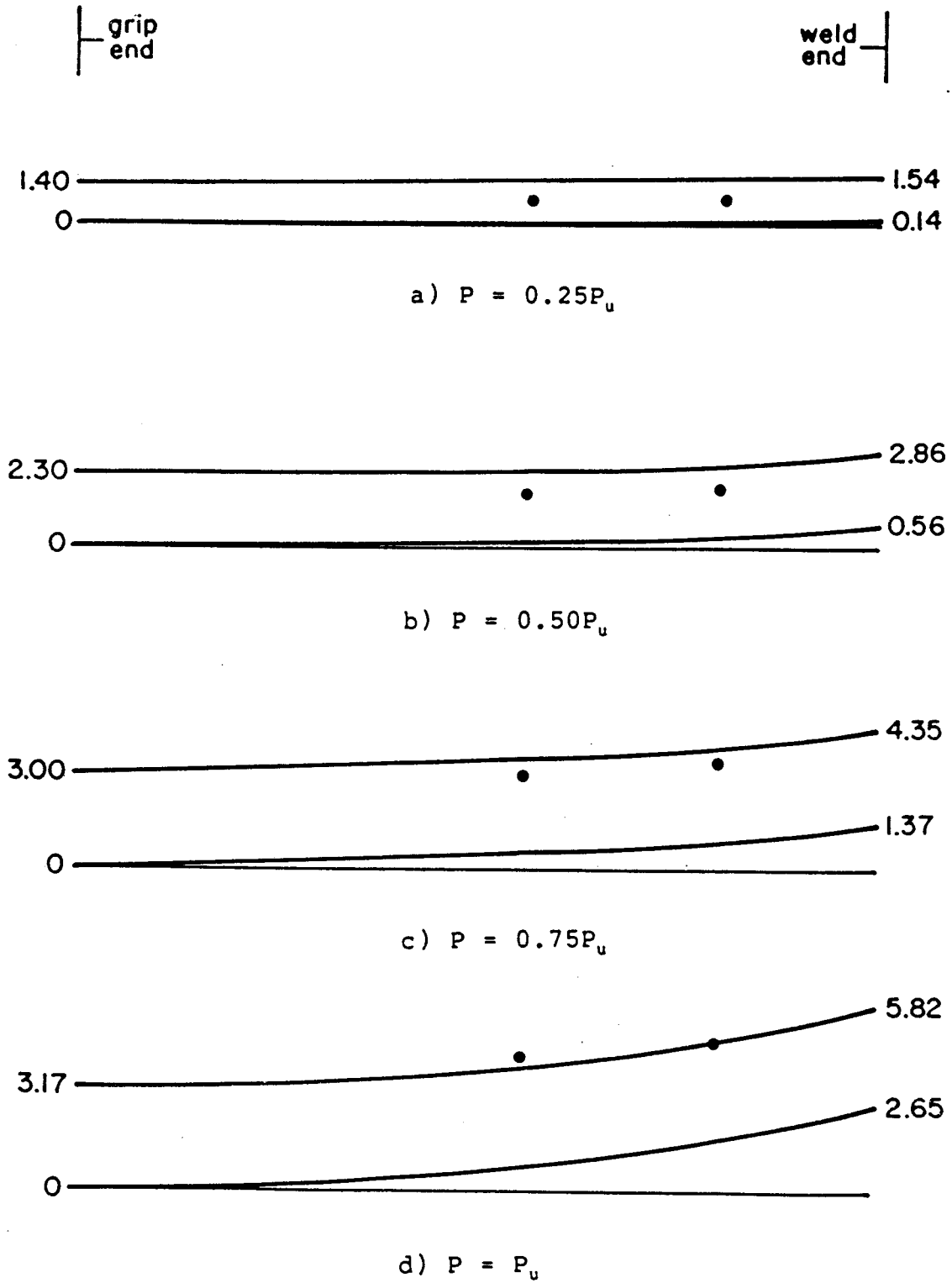

Figure 5.7 Distribution of Bending Moments in Test 05AS3

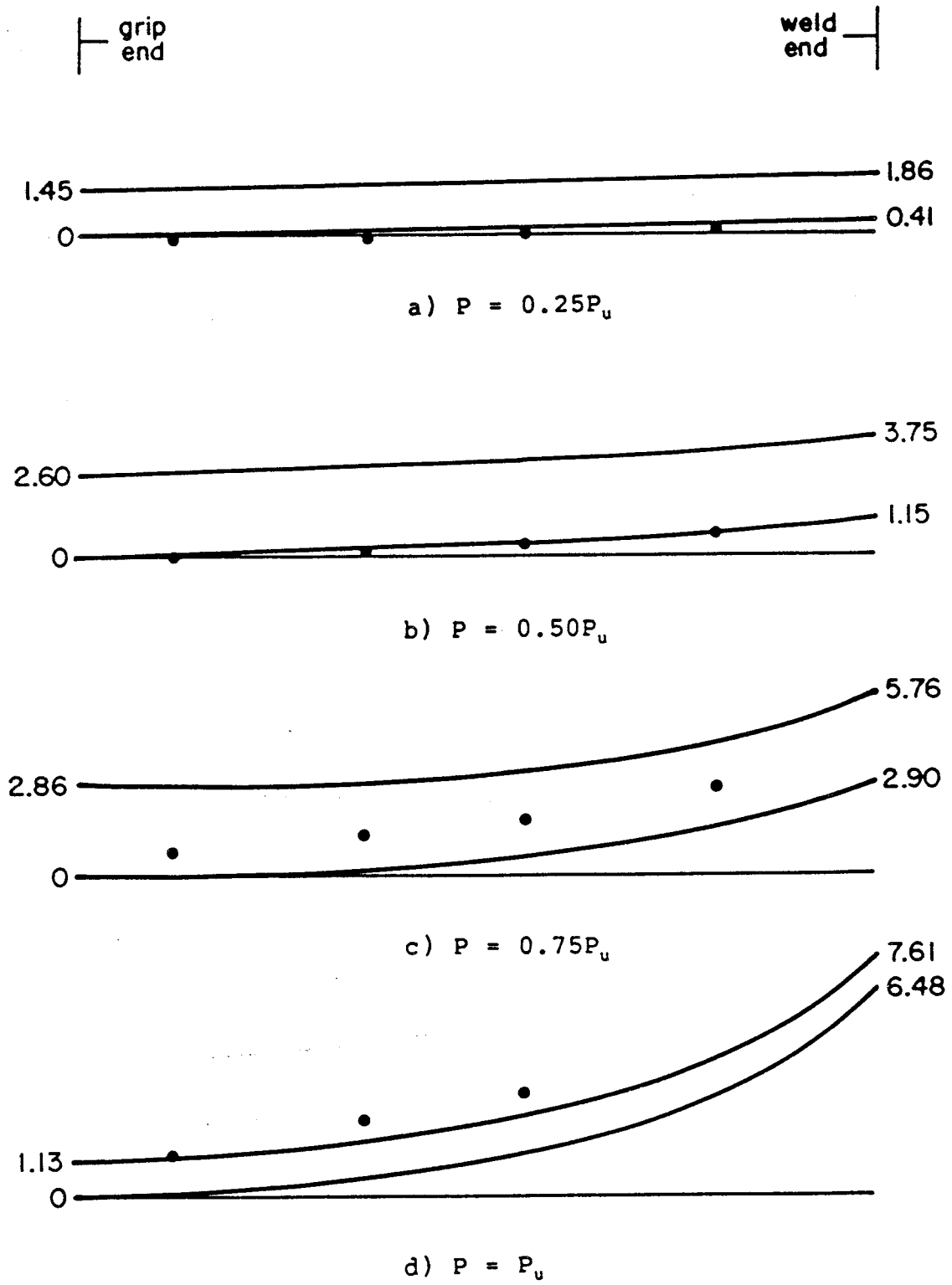

Figure 5.8 Distribution of Bending Moments in Tests 10AS1

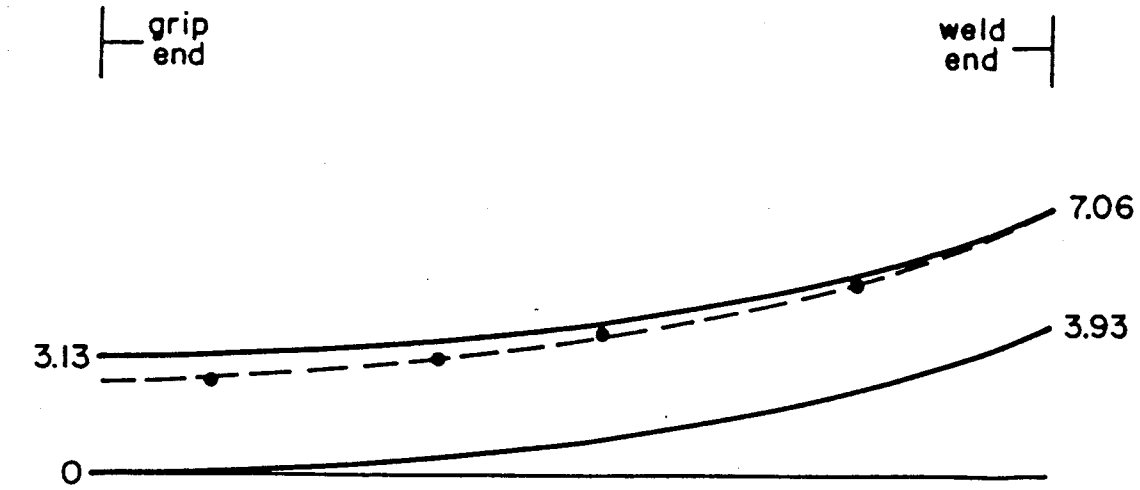

Specimen 10WS5 at P_u

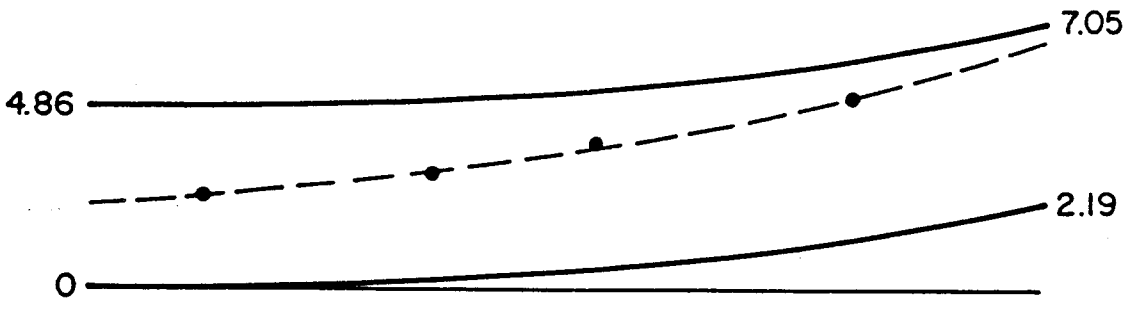

Specimen 10WS6 at P_u

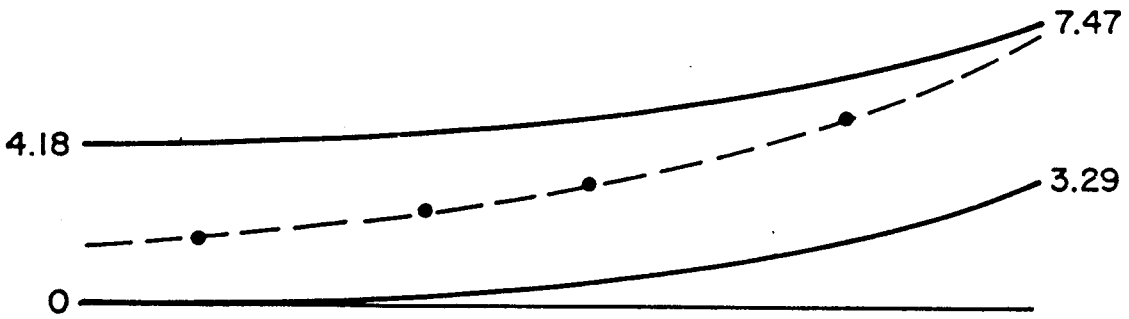

Specimen 10AS3 at P_u

Figure 5.9 Distribution of Bending Moments in Tests 10WS5, 10WS6 and 10AS3

and therefore it is postulated that the differences between the test and predicted results is due to inaccuracies in the measurements of initial out-of-straightness. A difference of 3.3 mm in out-of-straightness would account for the maxmium difference.

Fig. 5.10 shows the moment distribution data for four load levels on a 15 mm specimen tested singly. All data lie slightly above the lines based on zero end moments and never approach the line for the fully yielded weld condition. This is accounted for by the fact that in tests with 15 mm welds the weld area was such that partial yielding of the plate occurred before the weld was fully yielded.

Fig. 5.11 gives the distribution of bending moments for test 05AP2 where a pair of specimens were tested. Only one experimental point is available but it is in reasonable agreement with the predicted lines based on [5.12]. This was the only pair of 5 mm specimens that was gauged on both sides of the plates.

Fig. 5.12 gives the moment distribution for a pair of 15mm specimens. At low loads the experimental data are deviate somewhat from the predicted straight line relationship. For the higher loads the data fall considerably below the predicted straight line indicating a redistribution of moments towards the fixed grip end. This is what would be expected when yielding of the plate near the weld occurs, as was the case.

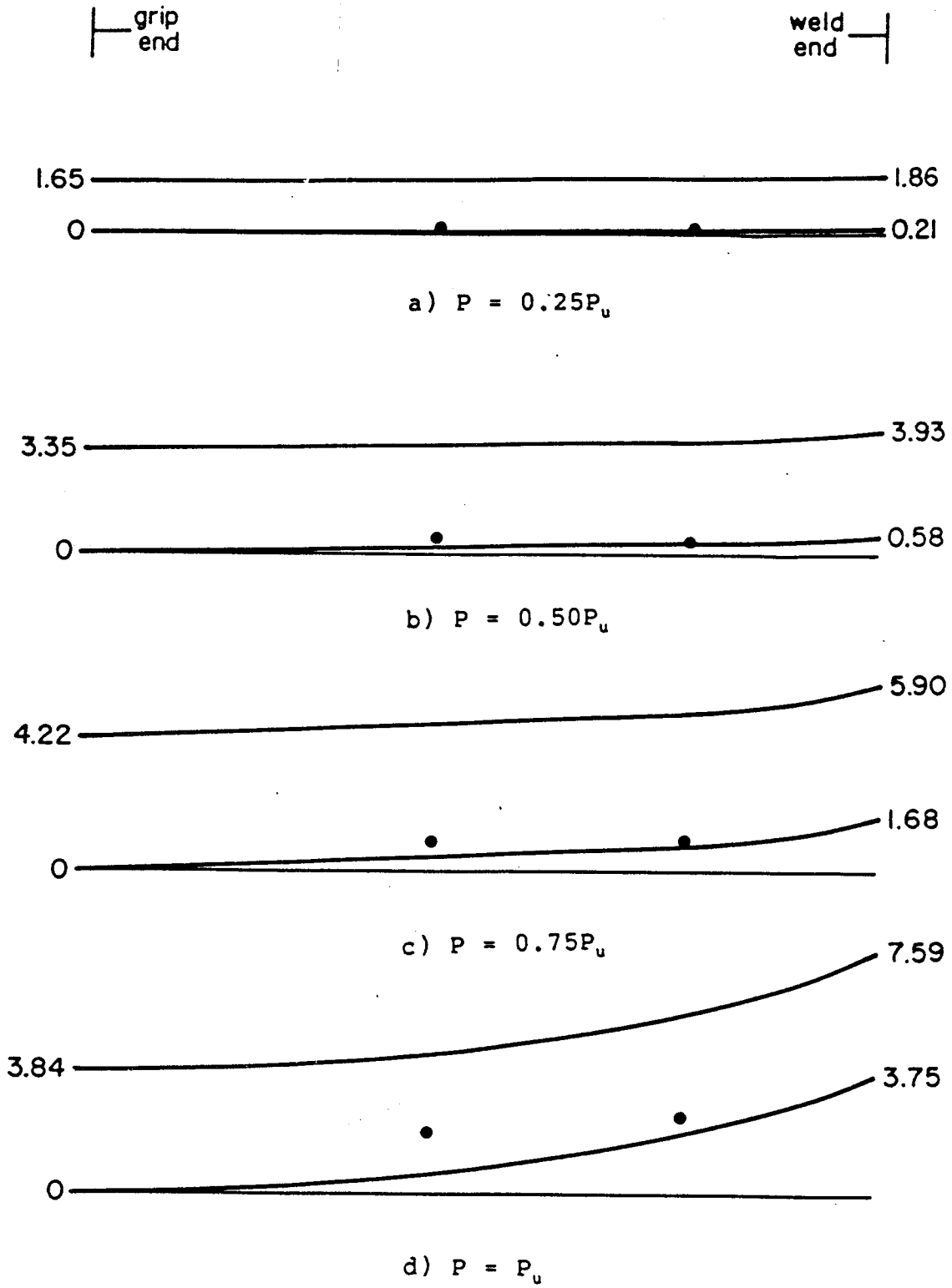

Figure 5.10 Distribution of Bending Moments for Test 15AS2

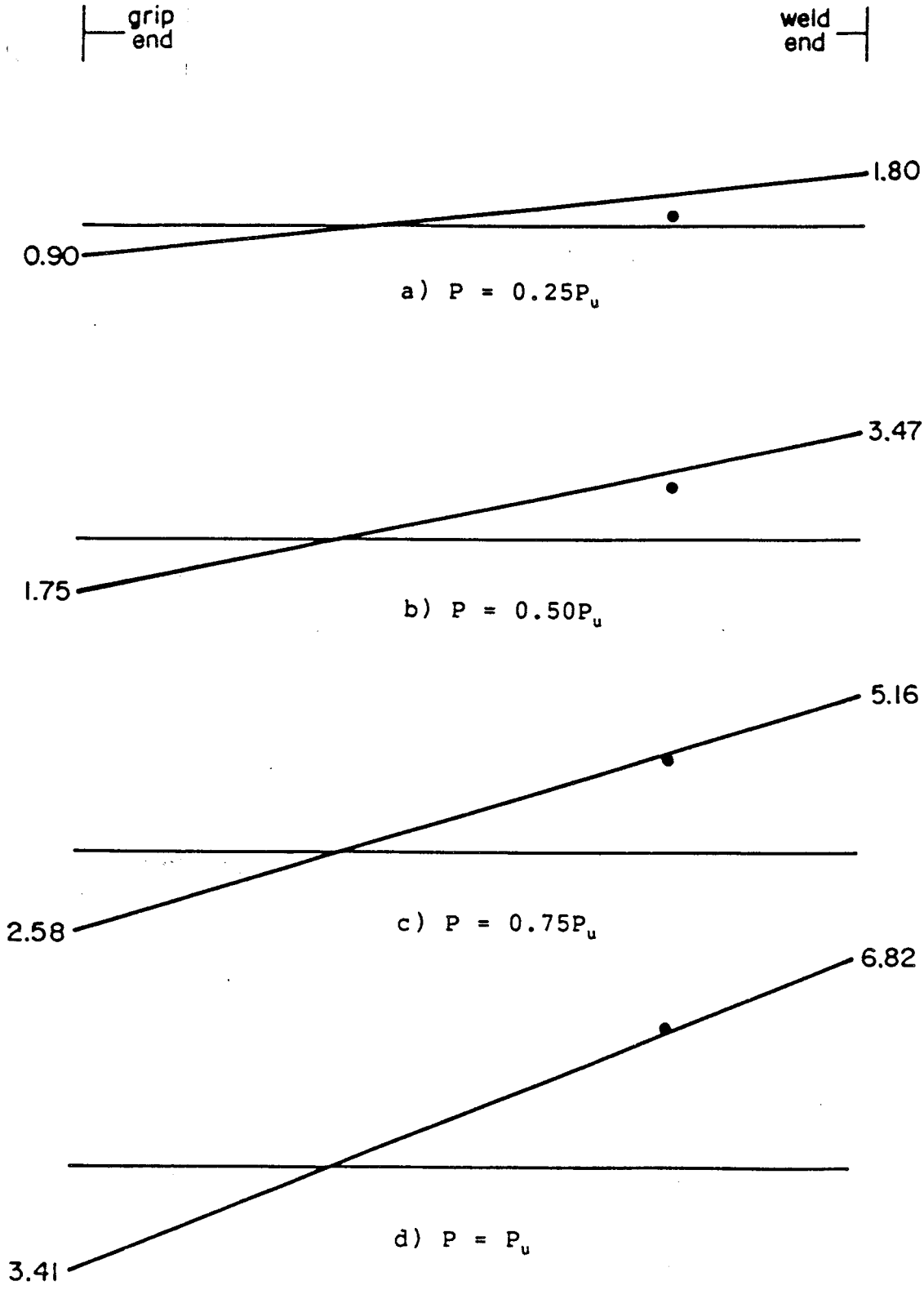

Figure 5.11 Distribution of Bending Moments for Test 05AP2

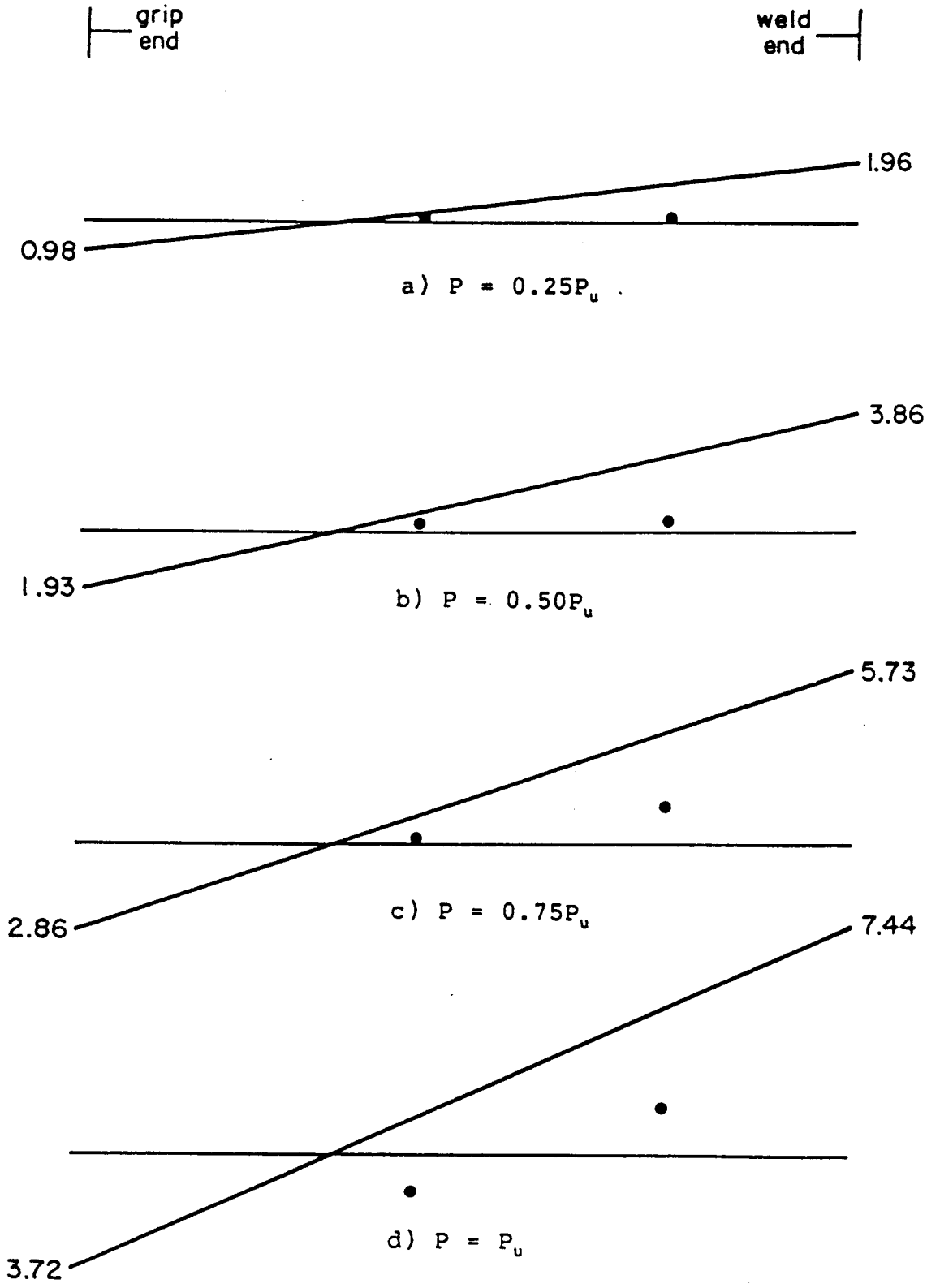

Figure 5.12 Distribution of Bending Moments for Test 15WP3

The 20 mm specimens behaved similarly to the 15 mm specimens but as the plates were fully yielded in tension before the ultimate load was reached no moments could exist in the plate at ultimate.

The test results, as exemplified by the moment distributions in the plates, therefore substantiate the models predicting the behaviour of both single specimens and pairs of specimens. The single specimens deflect sideways at the weld so that the weld tends to align itself with the load. The welds finally yield in tension so that, although considerable rotation has occurred in the weld, no moment exists and the weld fails in tension across the throat. The pairs of specimens are prevented by the test set-up from deflecting laterally at the weld. The welds undergo significant rotation but finally fail in tension as well.

5.2 Weld Equilibrium and Failure Theories

5.2.1 Weld Equilibrium

It will be assummed that the welds are loaded in axial tension only as shown in Fig. 5.13 as the ultimate load is reached.

For any failure plane at an angle θ from the weld throat, and originating at the weld root, the area is

$$[5.14] \qquad A_\theta = \frac{dw}{\cos\theta}$$

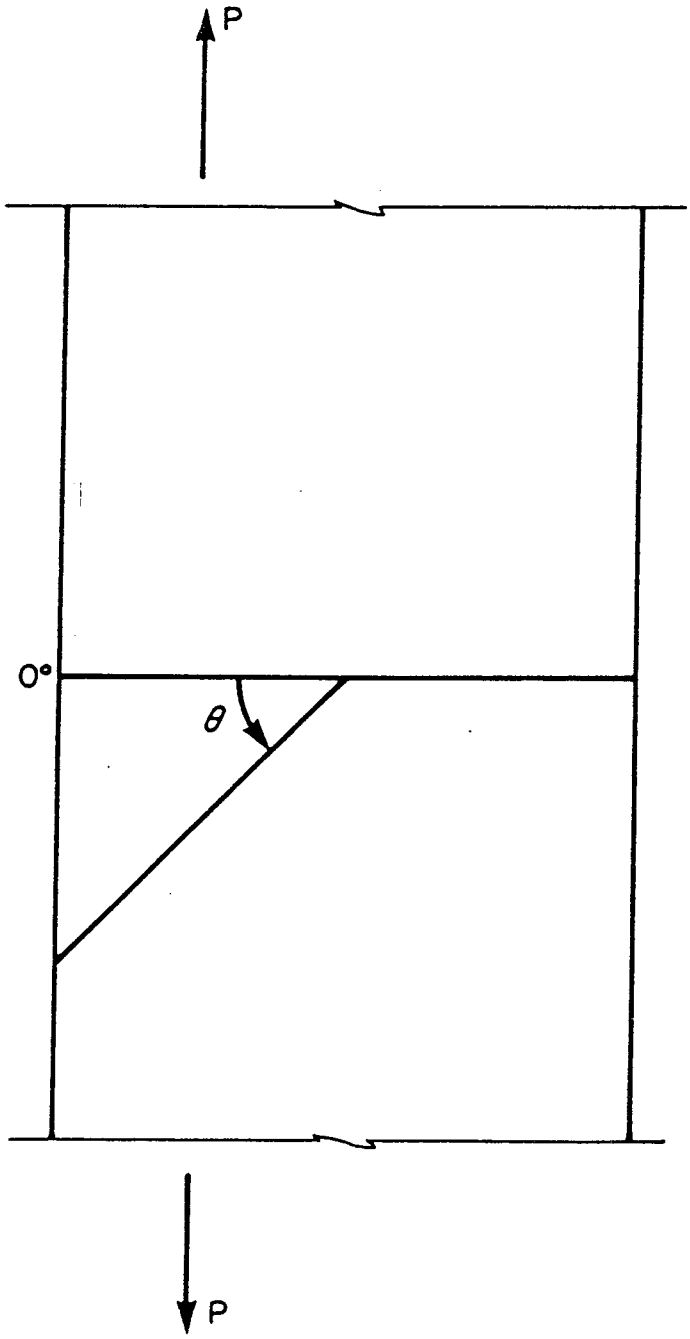

Figure 5.13 Loading on Weld

Resolving the force P normal and perpendicular to the plane and dividing by the area from [5.14] gives average normal and shear stresses of

$$[5.15] \qquad \sigma_\theta = \frac{P \cos^2\theta}{dw}$$

and

$$[5.16] \qquad \tau_\theta = \frac{P \sin\theta \cos\theta}{dw}$$

These expressions can be examined for various failure theories to determine whether the failure theories predict the correct fracture angles.

5.2.2 Maximum Shear Stress Theory

This theory suggests that fracture occurs on the plane of maximum shear stress. Therefore by differentiating [5.16] with respect to θ and setting equal to zero

$$[5.17] \qquad \frac{\partial\tau}{\partial\theta} = \frac{P\,(\cos^2\theta - \sin^2\theta)}{dw} = 0$$

gives $\theta = \pm 45°$.

Setting $\tau_u = \frac{\sigma_u}{2}$ as appropriate for this theory gives for $\theta = 45°$ and rearranging [5.16] gives

$$[5.18] \qquad P = \sigma_u\, d\, w$$

5.2.3 Maximum Normal Stress Theory

Failure is assummed to occur on the plane with the maximum normal stress. Differentiating [5.15] with respect to θ and setting equal to zero,

$$[5.19] \qquad \frac{\partial \sigma}{\partial \theta} = \frac{-2\ P \cos^2\theta \sin\theta}{dw} = 0$$

gives $\theta = 0°$ and $90°$. The $90°$ value is a point of inflection and $0°$ corresponds to a maximum value. Setting $\sigma = \sigma_u$ as is appropriate gives

$$[5.20] \qquad P = \sigma_u\ d\ w$$

the same failure load as for the maximum shear stress theory.

5.2.4 Strain Energy of Distortion Theory

Using the von Mises criterion gives

$$[5.21] \qquad Y = [\sigma^2 + 3\tau^2]^{1/2}$$

and substituting σ and τ from [5.15] and [5.16], then differentiating with respect to θ and setting equal to zero gives

$$[5.22] \qquad \frac{\partial Y}{\partial \theta} = \frac{P}{2}[\cos^4\theta + \sin^2\theta \cos^2\theta]^{-1/2} \times$$

$$[-4 \cos^3\theta \sin\theta + 3(2\cos^3\theta \sin\theta - 2\sin^3\theta \cos\theta)]=0$$

which yields a maximum value when $\theta = \pm 30°$. Using $\theta = 30°$ and σ_u as the comparative stress gives, substituting in [5.21],

$$[5.23] \qquad \sigma_u^2 = \frac{9P^2}{16d^2w^2} + \frac{9P^2}{16d^2w^2}$$

or

$$[5.24] \qquad P = 0.943\ \sigma_u\ d\ w$$

5.2.5 Fracture Surface Observations

The three fracture criteria predict failure angles at 0 to 45° to the weld throat with ultimate loads ranging from 0.943 to 1.000 times the ultimate strength of the throat area. Fracture surface angles were observed between 0 and 45° and varied in appearance from silky smooth to grainy or crystalline, but always occurred in the fusion face on the plate with the square preparation. The angle that this fusion face made with the surface of the plate varied with the degree of penetration. For the 5 mm welds, melting of the base plate caused this fusion face to be on an

approximately 45° plane as shown in Fig. 4.3. However, with increasing penetration this angle reduced because the depth of melting decreased in proportion to the depth of penetration. Failure loads, as discussed subsequently, were generally in excess of the ultimate strength of the throat area when based on the plate strength and varied from 0.88 to 1.43 of the ultimate strength of the throat area when based on the ultimate strength of the weld.

The 5 mm welds had fracture angles from 30° to 45° with the throat and were silky smooth with failure loads from 1.01 to 1.43 of the ultimate strength through the throat. The fracture appearance and angle support the maximum shear stress or von Mises criteria.

The behaviour of the 10 mm welds appears to be a transition between that of the 5 mm welds on the one hand and that of the 15 and 20 mm welds on the other with fracture angles less than 30° but still silky smooth in appearance. Failure loads varied from 0.93 to 1.10 of the ultimate strength of the weld.

The 15 and 20 mm welds fractured on the throat (θ = 0°) and were crystalline in appearance and carried from 0.88 to 1.15 of the ultimate strength of the weld. Few shear lips were present although there was a noticeable reduction in thickness, ranging from 0.74 to 0.96 of the original, in all specimens.

The three theories do not give substantially different ultimate loads. It appears that other conditions, such as

the angle the fusion face makes with the throat and the restraint to lateral and through thickness contraction offered to the welds by the adjoining less heavily stressed plate material, influenced the failure load, fracture surface appearance and failure angle. The restraint is greatest for the 5 mm welds and least for the 20 mm welds.

5.3 Ultimate Strength

5.3.1 General

This section investigates the effects that the percentage of weld penetration, the grade of base metal and eccentricity of the applied load have on the ultimate strength of partial joint penetration groove welds. The data are also compared to the various failure theories and the test results of other researchers.

5.3.2 Effects of Eccentric Loadings

All welds in this investigation were initially loaded eccentrically.

Fig. 5.14 shows the ultimate strength data for specimens tested singly and in pairs. The data are normalized by dividing the ultimate stress that the partial weld carried, based on the full plate area, by the ultimate stress for a full penetration weld again based on the full plate area. The test data give a coeffecient of variation of 5.6%, about the least-squares best fit curve of

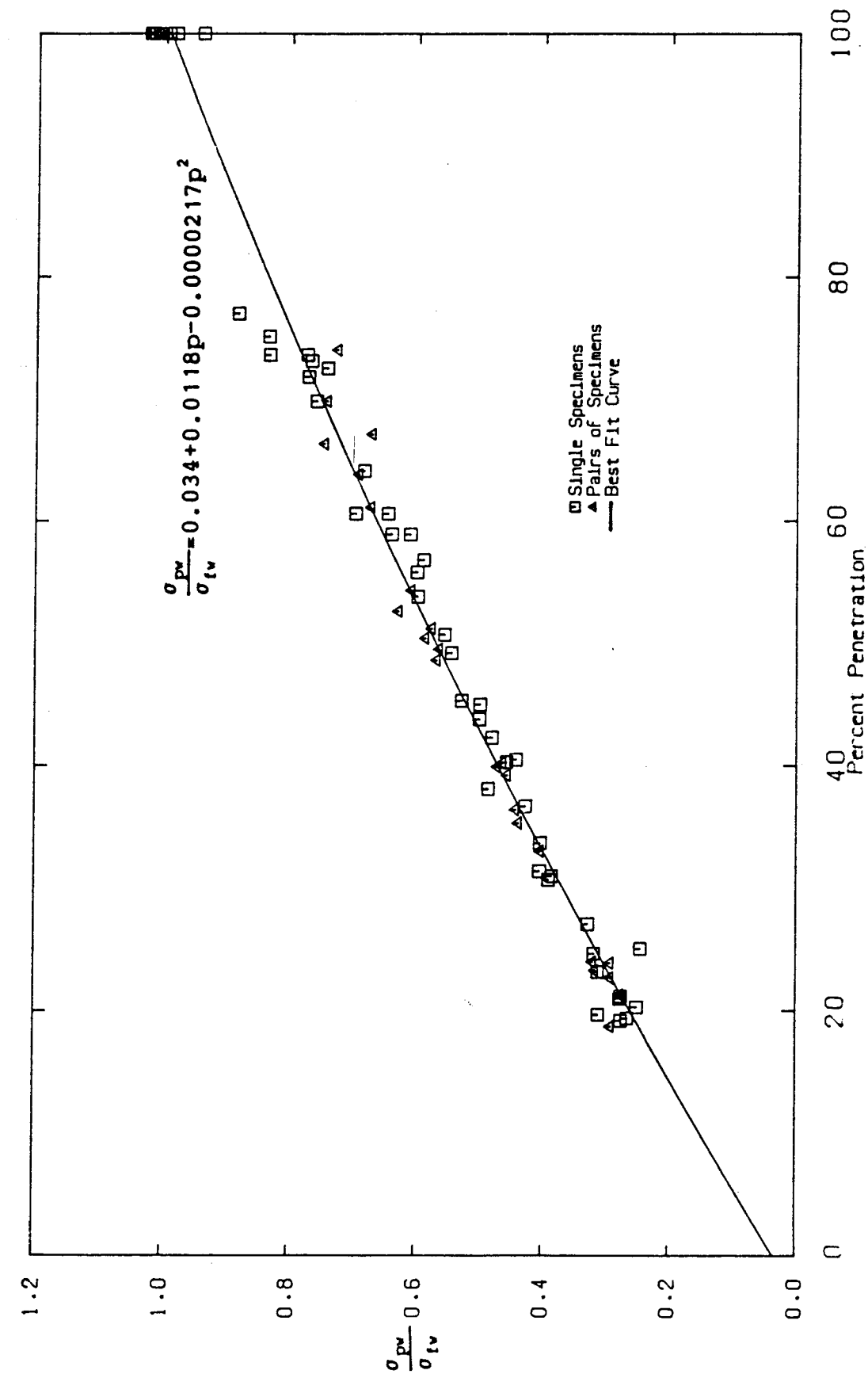

Figure 5.14 Ultimate Strength of Single and Pairs of Specimens

$$[5.25] \qquad \frac{\sigma_{pw}}{\sigma_{fw}} = 0.034 + 0.0118p - 0.0000217p^2$$

There is no apparent difference in the data for the welds tested singly and in pairs. Both types of specimens underwent considerable rotation in the weld. The test data of Popov and Stephen (1977) on concentrically loaded welds, plotted in Fig. 5.15 with the test data from this program show no difference in strengths of concentrically loaded specimens and eccentrically loaded specimens. Although rotations in the weld in the tests reported here cause uneven straining, with the root of the weld being subject to the maximum tensile strains, the relatively flat-top of the stress-strain curve of the weld finally results in a relatively uniform stress distribution across the weld. The final bending moment in the welds approaches zero. The weld fails in tension and there is no effect of the initial bending moments on the strength.

In examining the behaviour of single specimens in section 5.1.2 it was shown that lateral deflections at the weld tended to reduce the moments in the weld. These deflections were increased when the percent penetration was decreased and when the end moment developed in the member was reduced. Testing the specimens in pairs gave satisfactory behaviour when no lateral deflections at the weld could take place. Therefore the tendancy of single specimens to align themselves with the load is not required

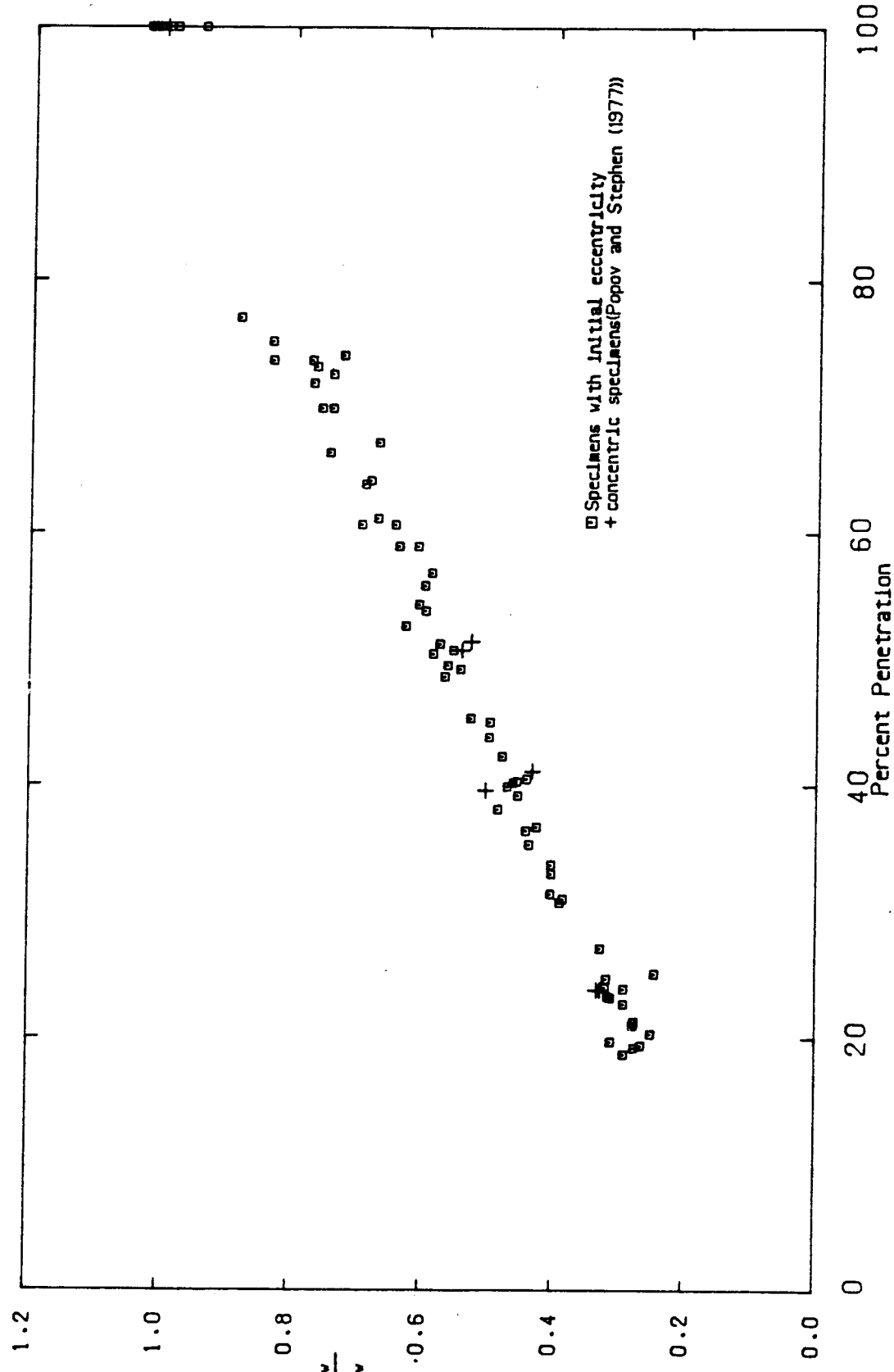

Figure 5.15 Comparison of Initially Eccentric and Concentric Specimens

for the performance to be satisfactory. Fig. 5.6 shows the deflected shape that develops in one-half of one of a pair of specimens when the weld has fully yielded in tension. The total rotation that the weld must accommodate while sustaining the maximum load is

$$[5.26] \qquad 2\omega = \frac{Pe\ell}{2EI}$$

assuming elastic behaviour of the plate, and is four-thirds of this amount if the far ends of the specimen were hinged. For a given length the rotation is directly proportional to the eccentricity, "e". In Fig. 5.16 the normalized stress ratio $\frac{\sigma_{uw}}{\sigma_{fw}}$ is plotted versus the eccentricity for the tests on pairs of welds, the eccentricity e=0.5t(1-p). Clearly not only did the welds have sufficient ductility throughout the range of these tests to accommodate the rotation that occurred but the strength actually increased (as discussed subsequently) as the eccentricity increased. Although the rotations that occur in the weld produce uneven straining, with the root of the weld being subject to the maximum tensile strains, the relatively flat top of the stress strain curve of the weld metal finally results in a relatively uniform stress distribution across the weld. Therefore, the bending moment in the weld is dissipated. The weld fails in tension and there is no difference in strengths between eccentrically and concentrically loaded specimens.

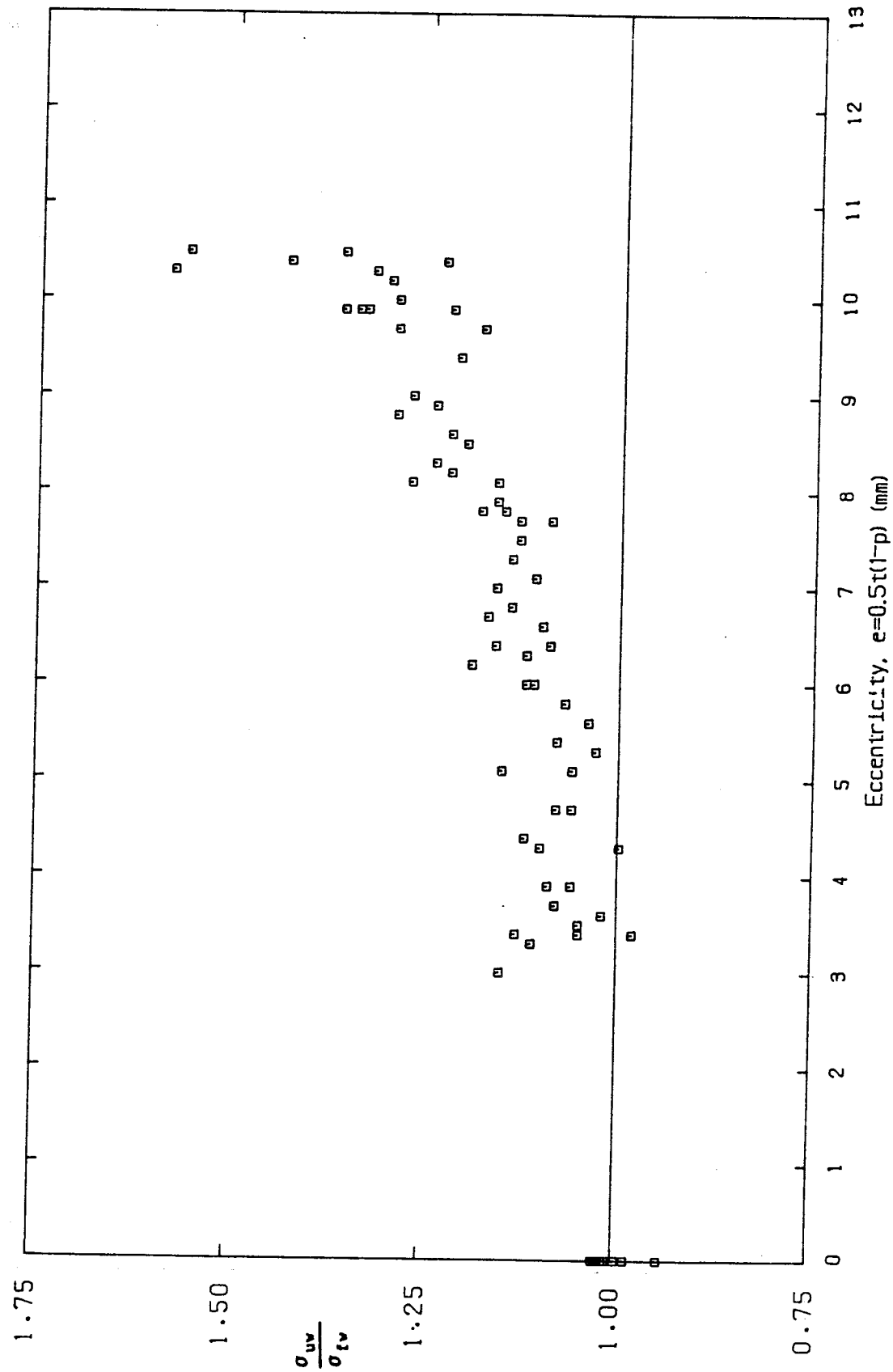

Figure 5.16 Normalized Failure Stress versus Eccentricity

Therefore, the strength of a properly made weld exhibiting ductile behaviour can be based on its tensile capacity.

5.3.3 Factors Affecting Ultimate Capacity and Comparison to Failure Theories

Fig. 5.17 shows that the strength of the partial joint penetration groove welds increases in proportion to the percent penetration, i.e, in proportion to the cross-sectional area of the weld. The ultimate strength data in this figure have been normalized by dividing the ultimate strengths of the partial welds by the mean ultimate strength of the full penetration welds of specimens of the particular grade of base metal. Fig. 5.17 shows that by taking into account the grade of steel that there is no statistical difference in the data. This indicates that the capacity of the joints is directly dependent on the ultimate strength of the base metal. Nearly all the data in Fig. 5.17 fall above the straight line

$$[5.27] \qquad \frac{\sigma_{pw}}{\sigma_{fw}} = p$$

Introducing the plate area, recognizing that the failure stress for fully welded specimens is the ultimate strength of the plate, and that $pA_p=A_w$, [5.27] is equivalent to

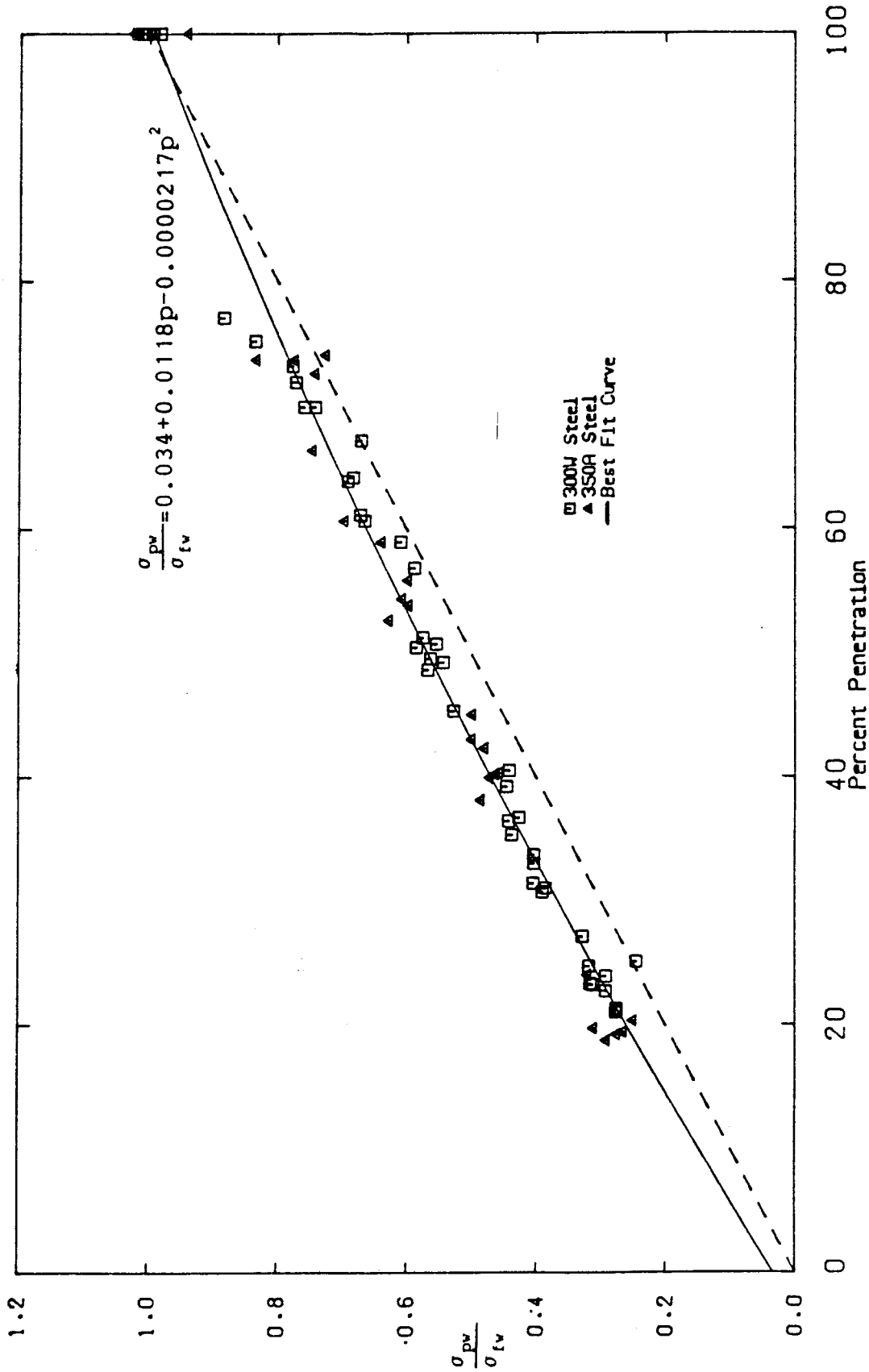

Figure 5.17 Ultimate Strengths of Specimens vs Percent Penetration

[5.28] $$P = \sigma_u A_w$$

Thus the test data exceed that given by identical equations [5.18] and [5.20] for the maximum normal stress theory and maximum shear stress theory and lie considerably above [5.24] for the von Mises criterion. A lower bound criterion for design, consistent with all three failure theories, is that the tensile capacity of a partial joint penetration groove weld be based on the area of the weld and the ultimate strength of the base plate.

5.3.4 Restraint in the Weld

In Fig. 5.18 the strengths of the welds are normalized by dividing the failure load by the actual area of the partial joint penetration groove weld and then dividing this stress by that to cause a full penetration groove weld(in the same plate material) to fail. The horizontal line

[5.29] $$\frac{\sigma_{uw}}{\sigma_{fw}} = 1$$

indicates that a partial joint penetration groove weld is as strong on an unit area basis as a full penetration weld. Fig. 5.18 shows that the ultimate strengths of the specimens increased significantly in a consistent manner as the percent penetration decreased.

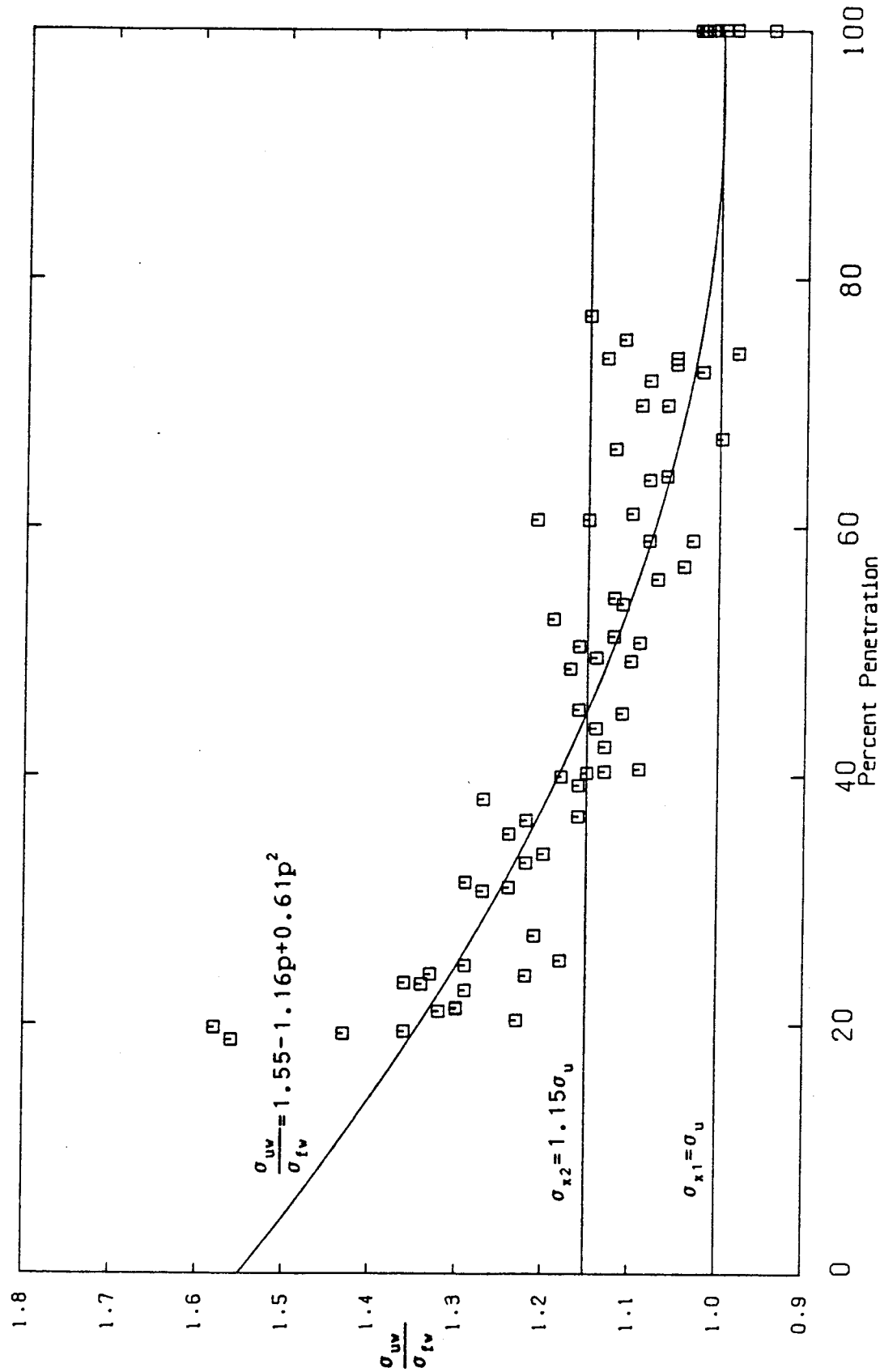

Figure 5.18 Normalized Ultimate Strength vs Percent Penetration

For any partial joint penetration groove weld (Fig. 5.19), loaded in tension, the plate adjacent to the weld is less heavily stressed on the average than the throat of the weld. Therefore as the weld throat attempts to contract laterally the less heavily stressed plate, contracting less, will restrain the weld setting up tensile stresses in the weld on planes normal to the throat of the weld. These stresses will develop, in particular, across the width of the plate. First of all, the unfused "dead area" adjacent to the joint is unstressed longitudinally and does not tend to contract laterally until pulled by the laterally contracting weld. Second, there is a significant distance across the width of the plate in which to develop the restraint.

Through the thickness of the plate, there is less distance in which to develop the restraint. Also there will be through thickness contraction on either side of the weld due to longitudinal stresses, albeit less than in the weld where the longitudinal stresses are higher. Therefore the through thickness restraint is less than that across the width.

The restraint offered by the plate and hence the magnitude of the stresses in planes normal to the throat increases as the percent penetration decreases. This is because, with an increase in the ratio of the average stress on the weld throat to that in the plate, the differences in the free lateral contraction of the weld and the plate are increased.

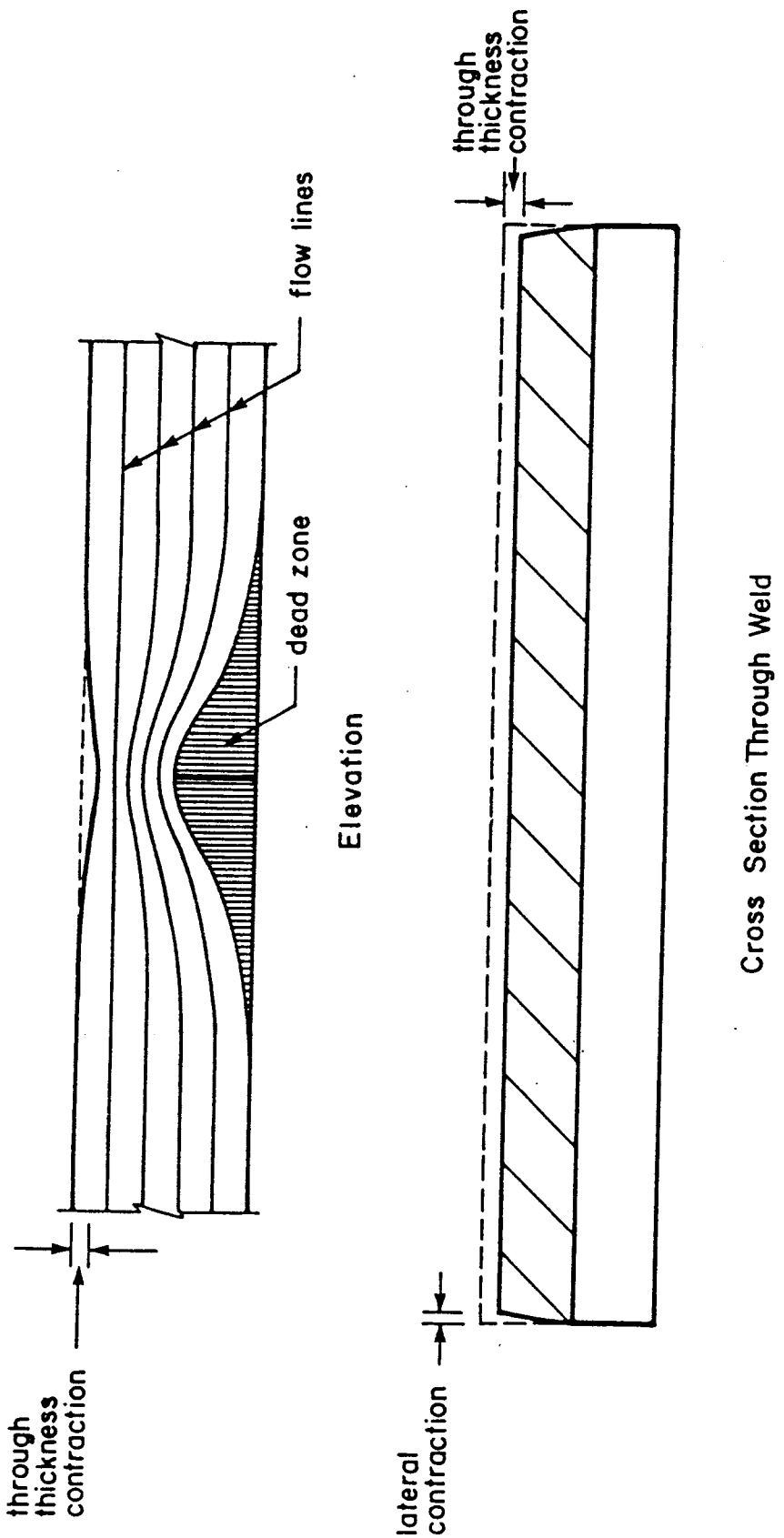

Figure 5.19 Development of Restraint

Consider the three-dimensional element in Fig. 5.20 subject to principal stresses σ_x, σ_y and σ_z. Under elastic conditions the relationships between stress and strain are

[5.30a] $$\epsilon_x = \frac{1}{E}(\sigma_x - \nu(\sigma_y + \sigma_z))$$

[5.30b] $$\epsilon_y = \frac{1}{E}(\sigma_y - \nu(\sigma_z + \sigma_x))$$

[5.30c] $$\epsilon_z = \frac{1}{E}(\sigma_z - \nu(\sigma_x + \sigma_y))$$

The von Mises-Hencky yield criterion in terms of principal stresses is

[5.31] $$(\sigma_1 - \sigma_2)^2 + (\sigma_2 - \sigma_3)^2 + (\sigma_3 - \sigma_1)^2 = 2Y^2$$

Let us consider three different states of stress: case 1, uniaxial tension or plane stress, case 2 biaxial stress state or uniaxial plane strain as defined by Lay (1982), and case 3 triaxial stress state or biaxial plane strain (Lay, 1982).

In case 1, as in a uniaxial tension test substituting $\sigma_1=\sigma_{x1}$ and $\sigma_2=\sigma_y=\sigma_3=\sigma_z=0$ in [5.31] gives

[5.32] $$\sigma_{x1} = Y = \sigma_{yp}$$

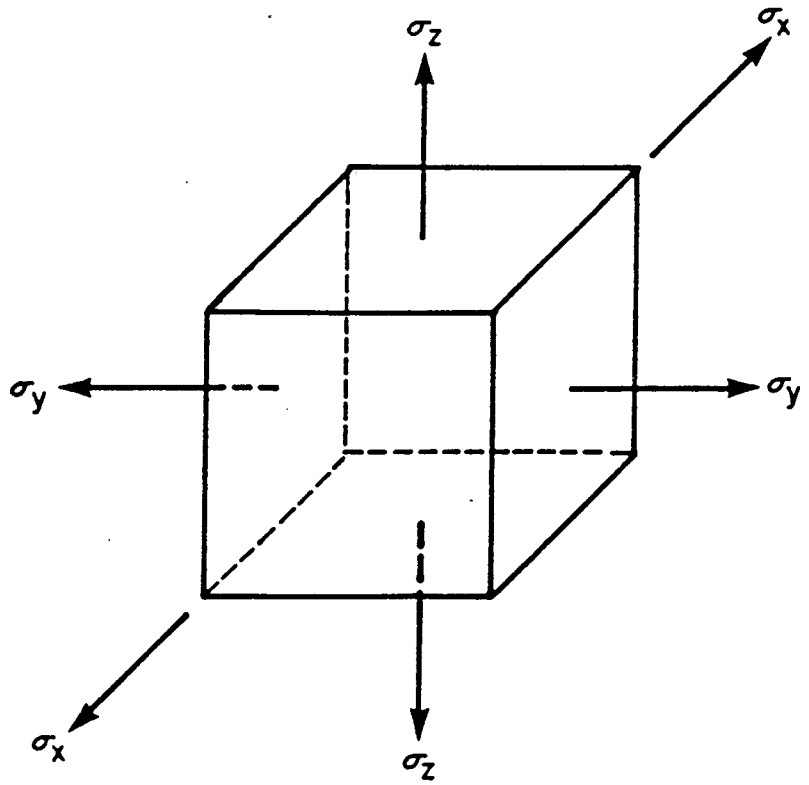

Figure 5.20 Element of Weld

as yielding occurs when $\sigma_{x1} = \sigma_{yp}$.

For case 2 straining in the y direction, say, does not occur but through thickness straining (z direction) can take place with the normal stresses in the z direction equal to zero. Thus $\sigma_x=\sigma_{x2}$, $\sigma_y\neq0$, $\epsilon_y=0$, $\sigma_z=0$ and $\epsilon_z\neq0$. From [5.30b]

$$[5.33] \qquad \sigma_y = \nu\sigma_x$$

Substituting $\sigma_1=\sigma_{x2}$, $\sigma_2=\sigma_y=\nu\sigma_{x2}$, $\sigma_3=\sigma_z=0$ and $Y=\sigma_{yp}$ in [5.31] gives

$$[5.34] \qquad \sigma_{x2} = \frac{\sigma_{yp}}{[1 - \nu + \nu^2]^{1/2}}$$

and yielding is delayed until $\sigma_{x2}=1.125\sigma_{yp}$ when ν is taken to be 0.3.

For case 3 straining in both the y direction and z direction are considered to be zero. Thus $\sigma_x=\sigma_{x3}$, $\sigma_y\neq0$, $\epsilon_y=0$, $\sigma_z\neq0$ and $\epsilon_z=0$. From [5.30]

$$[5.35] \qquad \sigma_y = \sigma_z = \frac{\nu}{(1 - \nu)}\,\sigma_x$$

and substituting appropriately in [5.31] gives

$$[5.36] \qquad \sigma_{x3} = \frac{(1 - \nu)}{(1 - 2\nu)}\,\sigma_{yp}$$

For elastic conditions with ν=0.3 yielding is delayed until $\sigma_{x3}=1.75\sigma_{yp}$.

The groove welds do not fail until ultimate conditions are reached. Therefore the von Mises-Hencky yield criterion is extended to the ultimate with the assumptions that there is an appropriate modulus to replace the modulus of elasticity, the comparative stress is the ultimate tensile strength σ_u rather than the yield stress σ_{yp}, and Poisson's ratio takes on a value consistent with inelastic behaviour. Ratzlaff et al. (in preparation) suggest ν_p=0.42. Under these conditions if restrained across the width only (case 2) a partial joint penetration groove weld would fail when

$$[5.37] \qquad \sigma_{x2} = 1.15\ \sigma_u$$

If complete restraint is offered across the width of the weld and through the thickness (case 3) a partial joint penetration groove weld would fail when

$$[5.38] \qquad \sigma_{x3} = 3.63\ \sigma_u$$

Equation [5.37] is plotted in nondimensional form in Fig. 5.18 together with the test results. A least squares best fit quadratic curve to the test data is

$$[5.39] \qquad \frac{\sigma_{uw}}{\sigma_{fw}} = 1.55 - 1.16p + 0.61p^2$$

indicating that as zero penetration is approached, (in the limit) the strength is increased 1.55 times.

Restraint is present in the partial joint penetration groove welds that increases with decreasing penetration. It is postulated that the across-width restraint probably develops first and is the more significant contributor to the increased strength. The through thickness restraint adds to the strength to a lesser extent but at an increasing rate as the percent penetration decreases.

For welds with greater than 70% penetration in these tests, as the ratio of the yield strength to ultimate is 0.70, yielding would occur in the plate before fracture of the weld. This yielding of the plate would increase its lateral contraction and decrease the restraint to the weld. Therefore increased strength due to restraint would be expected to be less significant above 70% penetration as is the case.

5.3.5 Weld Defects

Weld defects, particularly in the form of porosity, but also as inclusions and lack of fusion, were present in some welds and amounted to up to 5% of the weld area. When this loss of weld area is taken into account the points falling below the line given by [5.29] plot above the line. As the area of weld defects on the average was only 1.4% the data have not been adjusted and have been presented and analyzed

assuming zero weld defects.

5.3.6 Test Results of Others

The data of Popov and Stephen (1977) are in good agreement with the results of these tests as plotted in Fig. 5.21. The strength increases on an unit area basis as the percentage penetration decreases. The data of Lawrence and Cox (1976) show the same trend of increasing strength with decreasing perecentage penetration but appear to lie above these data and those of Popov and Stephen. This is attributed to the higher strengths steels used by Lawrence and Cox. As the yield/ultimate strength ratio was 0.89, yielding of the plate prior to fracture of the weld would only occur at higher percentage penetrations than in the tests reported here. Furthermore, with no sharply defined yield point and the corresponding yield plateau, and with a yield strength closer to the ultimate, local yielding, tending to reduce the restraint would be less than for normal structural steels. Thus the restraint is greater and the partial joint penetration groove welds in the higher strength steels exhibit the increased strength due to restraint even more than normal structual steels with a yield plateau.

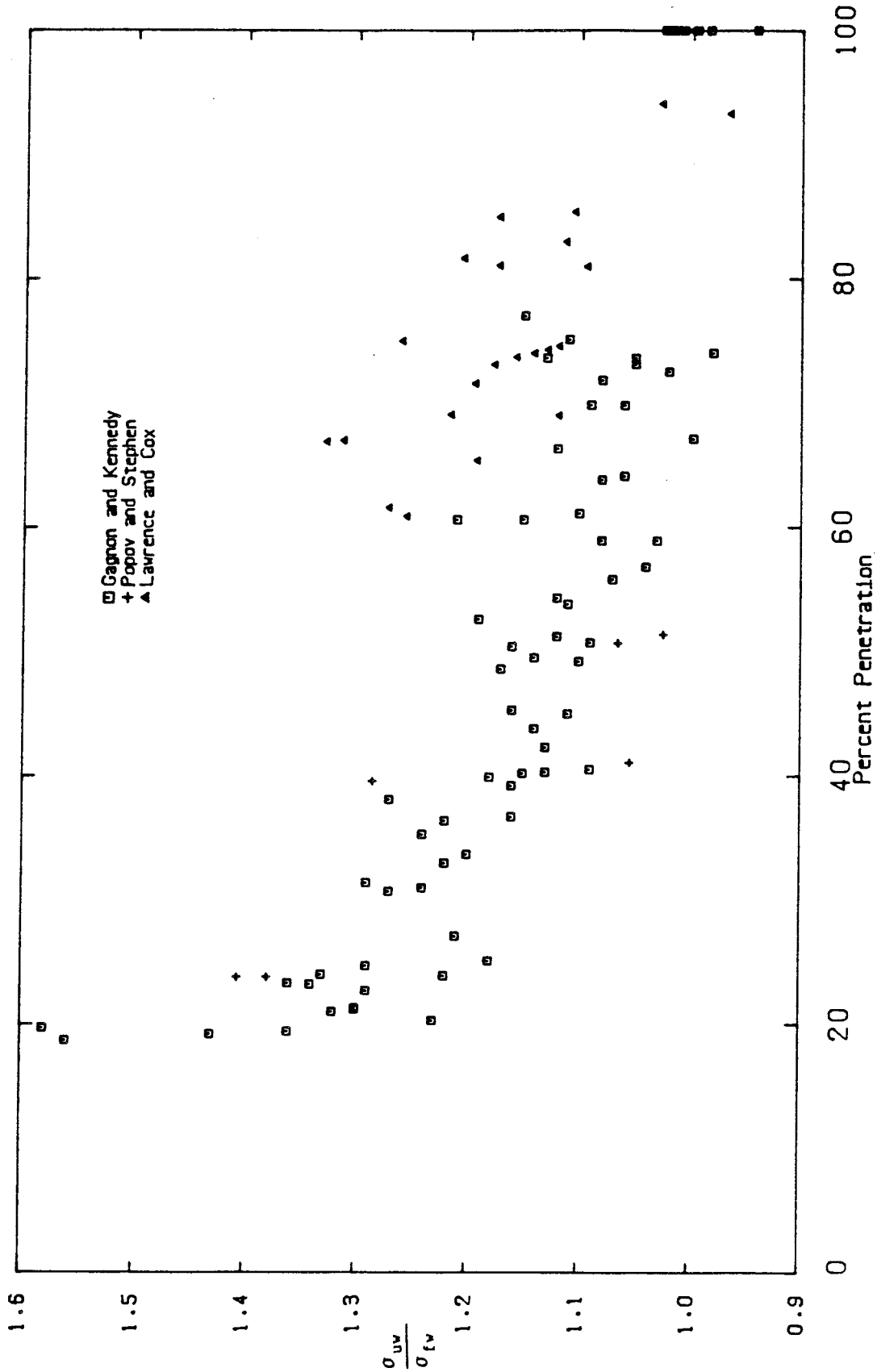

Figure 5.21 Comparison with Test Results of Others

5.4 Ductility of Specimens

The strains measured across the weld, on a 75 mm gauge length, generally increased as the percent penetration increased as shown in Fig. 5.22. In general the deformations were limited in those cases where the ultimate strength of the weld was less than the yield strength of the plate. When the weld did not fracture before the plate yielded the deformations were consistent with yielding of the plate. Therefore to get ductile behaviour of the whole specimen the ultimate strength of the weld must be greater than the yield strength of the plate.

The welds themselves exhibited considerable ductility with even the 5 mm welds straining an average of 1.16% on the 75 mm gauge length at maximum load. Estimating the elastic or inelastic deformations of the plate within the 75 mm gauge length and subtracting from the total deformation the deformation within the weld can be estimated. Dividing this deformation by the weld size gives a non-dimensionalized deformation greater than 4% as shown in Table 5.1. The deformation of the welds, in fact, will be concentrated over a much shorter distance and therefore the ductility is much greater than this 4%. These deformations were sustained in the presence of rotations in the weld of up to 2.8°, as measured for the 5 mm welds, with no loss in strength. Although larger rotations were measured in some larger welds part of the rotation was due to plastic deformation of the plate.

Table 5.1 Non-dimensionalized Deformations in Welds

Specimen	Estimated Deformations in Weld	Specimen	Estimated Deformations in Weld
05WS1	0.193	15WS1	-
05WS2	0.148	15WS2	0.178
05WS3	0.188	15WS3	0.213
05WS4	0.338	15WS4	-
05WS5	0.312	15WS5	0.066
05WS6	0.299	15WS6	0.137
05AS1	0.089	15AS1	0.150
05AS2	0.185	15AS2	0.152
05AS3	0.184	15AS3	0.117
05AS4	0.217	15AS4	0.109
10WS1	0.193	20WS1	0.047
10WS2	0.194	20WS2	0.064
10WS3	0.253	20WS3	0.139
10WS4	0.172	20WS4	0.264
10WS5	0.174	20WS5	0.145
10WS6	0.148	20WS6	0.161
10AS1	0.177	20AS1	0.091
10AS2	0.162	20AS2	0.173
10AS3	0.169	20AS3	0.141
10AS4	0.172	20AS4	0.046

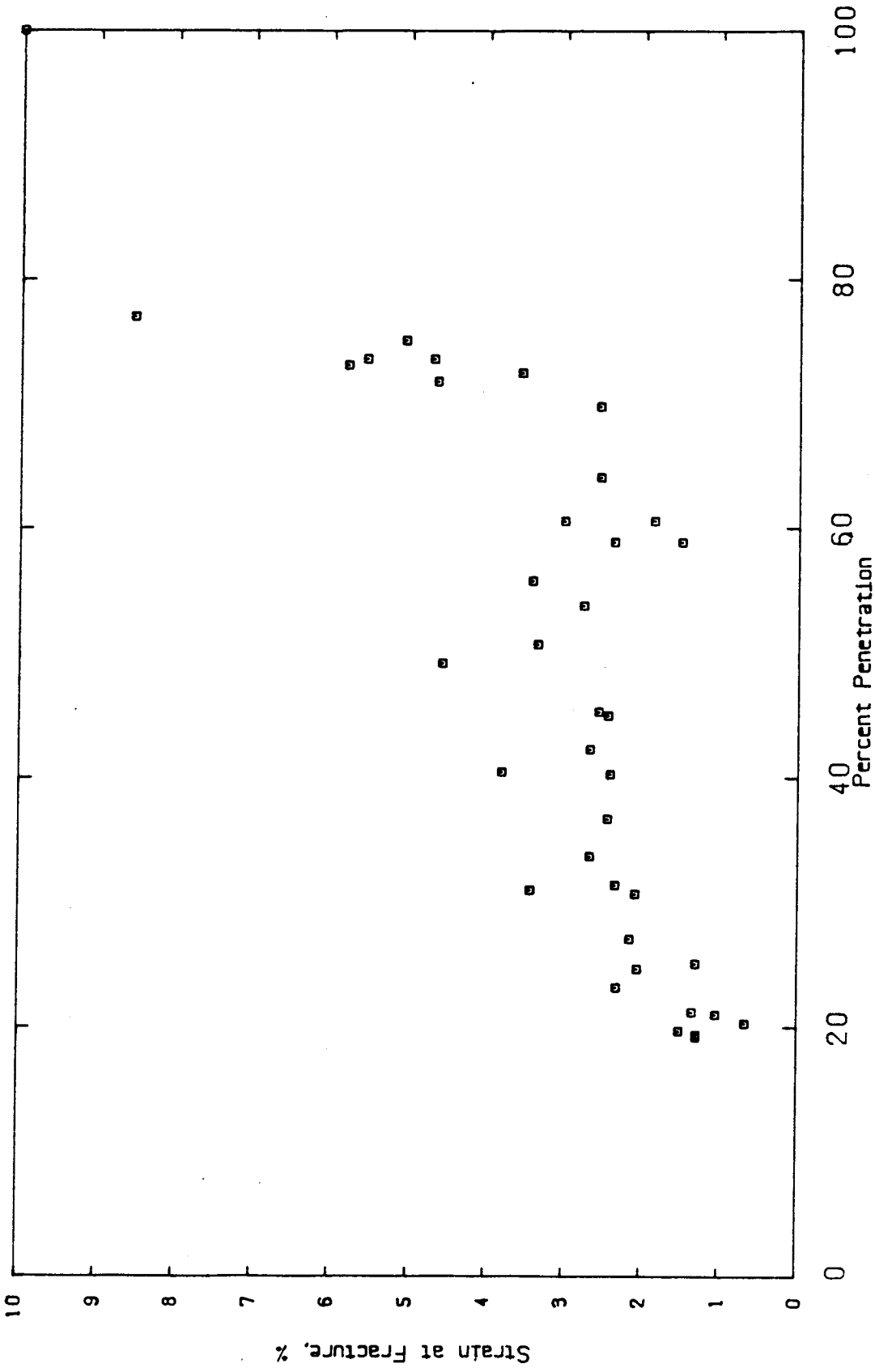

Figure 5.22 Fracture Strain vs Percent Penetration

The welds themselves exhibited considerable ductility but overall specimen ductility only occurs when yielding occurs in the plate before the welds fracture.

6. DESIGN APPLICATIONS

6.1 Design for Strength

The analysis of the test results show that the ultimate tensile strength of a partial joint penetration groove weld can be based on the weld area normal to the load and the ultimate strength of the base metal. The weld area can be expressed as

$$[6.1] \qquad A_w = p\ A_p$$

Thus from Fig. 6.1 a lower bound to the ultimate tensile strength of the weld can be taken as

$$[6.2] \qquad T_{r1} = \phi_1\ p\ A_p\ F_u$$

By fitting a curve to the test data the increasing strength with decreasing penetration can be taken into account and tensile resistance can be written as

$$[6.3] \qquad T_{r2} = \phi_2\ (1.55p - 1.16p^2 + 0.61p^3)\ A_p\ F_u$$

This relationship takes into account the lateral restraint offered to the weld by the adjoined less heavily stressed plate material. It is strictly valid only for steels for which the ratio of ultimate strength to yield strength is

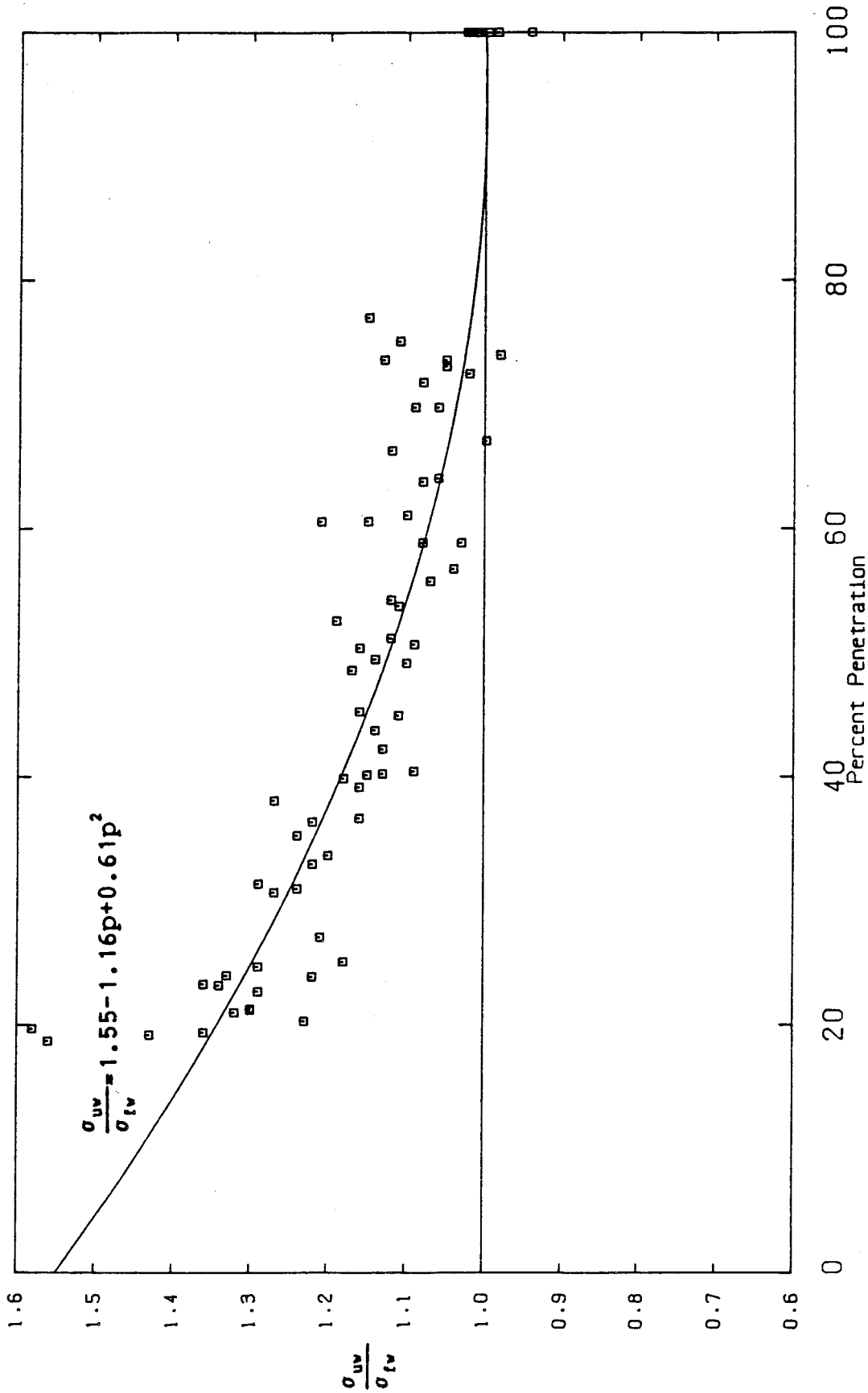

Figure 6.1 Normalized Ultimate Strength vs Percent Penetration

less than about 1.5. Furthermore, the restraint developed in plates with smaller width/thickness ratios may also be reduced. The resistance factors, ϕ_1 and ϕ_2, for [6.2] and [6.3] need to be determined.

6.1.1 Resistance Factors

Galambos and Ravindra (1976) have shown that resistance factors for steel structures can be written in the form

$$[6.4] \qquad \phi = \rho_R \exp(-\beta \alpha_R V_R)$$

while α_R, the separation coefficient can be taken as 0.55 and the reliability index, β, for connections is 4.5. This value of β of 4.5 decreases the probability of failure of the connector as compared to the member as a whole for which a value of β of 3.0 is commonly used for building structures. The ratio of the nominal resistance to the specified resistance ρ_R is, in this case,

$$[6.5] \qquad \rho_R = \rho_M \rho_{G1} \rho_{G2} \rho_P$$

and the associated coefficient of variation is obtained from

$$[6.6] \qquad V_R^2 = V_M^2 + V_{G1}^2 + V_{G2}^2 + V_P^2$$

Two geometric parameters are needed to account for the

variation of the percentage penetration and the variation the area of the plate. Kennedy and Gad Aly (1980) give a mean-to-nominal ratio for the variation in plate thickness of 1.015 with a coefficient of variation of 0.013. From Table 6.1 the corresponding figures for the percentage penetration are 0.985 and 0.134 repectively. Table 6.2 gives the results of 31 tension tests conducted by various graduate students at the University of Alberta in which the ultimate tensile strength was recorded. The measured-to-nominal ratio has a mean value of 1.091 and a coefficient of variation of 0.1013. As [6.2] and [6.3] predict the strength differently these will be different values of the test-to-predicted ratios for them. For [6.2] each test value in Fig. 6.1 is divided by the predicted value of 1.0 and the mean value and coefficient of variation of the resulting test-to-predicted ratios are established. As given in Table 6.3 these are 1.1516 and 0.1720 respectively. Using these data in [6.5] and [6.6] gives

$$\rho_{R1} = 1.091 \times 0.985 \times 1.015 \times 1.1516 = 1.256$$

$$V_{R1}^2 = 0.1013^2 + 0.1339^2 + 0.013^2 + 0.1720^2$$

$$= 0.05794$$

from which

Table 6.1 Mean to Nominal Ratios for Weld Penetrations

Specimen	Mean / Nom.	Specimen	Mean / Nom.
05WS1	1.09	15AS1	0.97
05WS2	1.05	15AS2	0.93
05WS3	1.29	15AS3	1.02
05WS4	1.20	15AS4	0.66
05WS5	1.40	15WP1	0.84
05WS6	1.28	15WP2	0.88
05AS1	1.05	15WP3	0.87
05AS2	0.99	15WP4	0.85
05AS3	1.01	15AP1	0.91
05AS4	1.01	15AP2	0.94
05WP1	1.24	20WS1	0.89
05WP2	1.21	20WS2	0.83
05WP3	1.17	20WS3	0.97
05WP4	1.10	20WS4	1.00
05AP1	0.97	20WS5	0.92
05AP2	1.25	20WS6	0.94
10WS1	1.04	20AS1	0.94
10WS2	0.87	20AS2	0.95
10WS3	0.80	20AS3	0.95
10WS4	0.94	20AS4	0.78
10WS5	0.81	20WP1	0.91
10WS6	0.79	20WP2	0.86
10AS1	1.09	20WP3	0.82
10AS2	1.04	20WP4	0.87
10AS3	1.16	20AP1	0.86
10AS4	1.13	20AP2	0.96
10WP1	1.01	25W1	1.03
10WP2	0.85	25W2	1.02
10WP3	0.91	25W3	1.04
10WP4	0.94	25W4	1.03
10AP1	1.04	25W5	1.02
10AP2	1.03	25W6	1.04
15WS1	0.77	25A1	1.04
15WS2	0.85	25A2	1.03
15WS3	0.98	25A3	1.03
15WS4	1.01	25A4	1.03
15WS5	1.05	25A5	1.04
15WS6	0.88		
		μ	0.985
		σ	0.132
		V	0.134

Table 6.2 Mean to Nominal Ratios for Ultimate Strength of Base Metal

Type of Steel	F_y	F_u	Specified	Mean / Nominal
300W	349	500	450	1.111
300W	332	518	450	1.151
300W	286	474	450	1.053
300W	319	526	450	1.169
300W	306	515	450	1.144
300W	325	497	450	1.104
300W	362	491	450	1.091
300W	363	516	450	1.147
300W	319	476	450	1.058
300W	331	445	450	0.989
300W	334	489	450	1.087
300W	294	488	450	1.084
300W	304	509	450	1.131
300W	351	496	450	1.102
300W	302	488	450	1.085
300W	318	488	450	1.084
300W	342	466	450	1.036
300W	341	474	450	1.054
300W	345	495	450	1.100
300W	348	498	450	1.106
300W	361	476	450	1.057
300W	353	481	450	1.069
300W	340	471	450	1.047
300W	364	522	450	1.160
300W	324	493	450	1.096
300W	346	513	450	1.140
350W	444	499	480	1.040
350W	444	537	480	1.119
350W	392	474	480	0.988
350A	384	539	480	1.123
			μ	1.091
			σ	0.1105
			V	0.1013

Table 6.3 Variation in Ultimate Strength vs Percent Penetration

Test	Test Strength	Equation 6.2		Equation 6.3	
		Predict	Mean / Nominal	Predict	Mean / Nominal
05WS1	1.30	1.00	1.30	1.33	0.98
05WS2	1.32	1.00	1.32	1.33	0.99
05WS3	1.18	1.00	1.18	1.30	0.91
05WS4	1.34	1.00	1.34	1.31	1.02
05WS5	1.21	1.00	1.21	1.28	0.95
05WS6	1.29	1.00	1.29	1.30	0.99
05AS1	1.23	1.00	1.23	1.34	0.92
05AS2	1.43	1.00	1.43	1.35	1.06
05AS3	1.36	1.00	1.36	1.35	1.01
05AS4	1.58	1.00	1.58	1.35	1.17
05WP1	1.22	1.00	1.22	1.31	0.93
05WP2	1.36	1.00	1.36	1.31	1.04
05WP3	1.29	1.00	1.29	1.32	0.98
05WP4	1.30	1.00	1.30	1.33	0.98
05AP1	1.56	1.00	1.56	1.35	1.16
05AP2	1.33	1.00	1.33	1.31	1.02
10WS1	1.09	1.00	1.09	1.18	0.92
10WS2	1.20	1.00	1.20	1.23	0.98
10WS3	1.24	1.00	1.24	1.25	0.99
10WS4	1.16	1.00	1.16	1.21	0.96
10WS5	1.29	1.00	1.29	1.25	1.03
10WS6	1.27	1.00	1.27	1.25	1.02
10AS1	1.13	1.00	1.13	1.17	0.97
10AS2	1.13	1.00	1.13	1.18	0.96
10AS3	1.11	1.00	1.11	1.15	0.97
10AS4	1.14	1.00	1.14	1.16	0.98
10WP1	1.16	1.00	1.16	1.19	0.97
10WP2	1.22	1.00	1.22	1.23	0.99
10WP3	1.24	1.00	1.24	1.22	1.02
10WP4	1.22	1.00	1.22	1.21	1.01
10AP1	1.15	1.00	1.15	1.18	0.97
10AP2	1.18	1.00	1.18	1.19	0.99
15WS1	1.16	1.00	1.16	1.15	1.01
15WS2	1.10	1.00	1.10	1.13	0.97
15WS3	1.04	1.00	1.04	1.09	0.95
15WS4	1.03	1.00	1.03	1.08	0.95
15WS5	1.06	1.00	1.06	1.07	0.99
15WS6	1.09	1.00	1.09	1.12	0.97
15AS1	1.07	1.00	1.07	1.10	0.97
15AS2	1.11	1.00	1.11	1.11	1.00
15AS3	1.08	1.00	1.08	1.08	1.00
15AS4	1.27	1.00	1.27	1.20	1.06

Table 6.3 continued

Test	Test Strength	Equation 6.2		Equation 6.3	
		Predict	Mean / Nominal	Predict	Mean / Nominal
15WP1	1.17	1.00	1.17	1.13	1.04
15WP2	1.12	1.00	1.12	1.12	1.00
15WP3	1.16	1.00	1.16	1.12	1.04
15WP4	1.14	1.00	1.14	1.13	1.01
15AP1	1.19	1.00	1.19	1.11	1.07
15AP2	1.12	1.00	1.12	1.10	1.02
20WS1	1.09	1.00	1.09	1.04	1.05
20WS2	1.06	1.00	1.06	1.06	1.00
20WS3	1.11	1.00	1.11	1.03	1.08
20WS4	1.15	1.00	1.15	1.02	1.13
20WS5	1.08	1.00	1.08	1.04	1.04
20WS6	1.05	1.00	1.05	1.03	1.02
20AS1	1.02	1.00	1.02	1.03	0.99
20AS2	1.13	1.00	1.13	1.03	1.10
20AS3	1.05	1.00	1.05	1.03	1.02
20AS4	1.15	1.00	1.15	1.07	1.07
20WP1	1.06	1.00	1.06	1.04	1.02
20WP2	1.10	1.00	1.10	1.07	1.03
20WP3	1.08	1.00	1.08	1.06	1.02
20WP4	1.00	1.00	1.00	1.05	0.95
20AP1	1.12	1.00	1.12	1.05	1.07
20AP2	0.98	1.00	0.98	1.03	0.95
25W1	0.98	1.00	0.98	1.00	0.98
25W2	1.01	1.00	1.01	1.00	1.01
25W3	1.00	1.00	1.00	1.00	1.00
25W4	1.02	1.00	1.02	1.00	1.02
25W5	1.01	1.00	1.01	1.00	1.01
25W6	0.98	1.00	0.98	1.00	0.98
25A1	1.02	1.00	1.02	1.00	1.02
25A2	1.02	1.00	1.02	1.00	1.02
25A3	1.02	1.00	1.02	1.00	1.02
25A4	0.94	1.00	0.94	1.00	0.94
25A1	1.00	1.00	1.00	1.00	1.00
μ			1.1516		1.0057
σ			0.1981		0.0491
V			0.1720		0.0489

$$\phi_1 = 1.256 \exp(-4.5\times0.55\times0.2407)$$

$$= 0.692,$$

say 0.69 for use with [6.2].

Similarly for [6.3] each test value in Fig. 6.1 is divided by the predicted value given by the best fit curve

[5.39] $$\frac{\sigma_{uw}}{\sigma_{fw}} = 1.55 - 1.66p + 0.61p^2$$

evaluated at the measured penetration. From Table 6.3 the mean value and coefficient of variation are 1.0041 and 0.0488. Using these data in [6.5] and [6.6] gives

$$\rho_{R2} = 1.091\times0.985\times1.015\times1.0041 = 1.095$$

$$V_{R2}^2 = 0.1013^2 + 0.1339^2 + 0.013^2 + 0.0488^2$$

$$= 0.03074$$

from which

$$\phi_2 = 1.095 \exp(-4.5\times0.55\times0.1753)$$

$= 0.710$

say 0.71 for use with [6.3].

6.1.2 Design Equations

The design equations consistent with current practice in CSA Standard S16.1-M84 are therefore

[6.2a] $T_{r1} = 0.69\ p\ A_p\ F_u$ and

[6.3a] $T_{r2} = 0.71(1.55p - 1.16p^2 + 0.61p^3)\ A_p\ F_u$

Equation [6.2a] is the simpler to use while [6.3a] recognizes the greater strength of the welds with small penetrations. On the average they both provide the same reliability but [6.3a] gives a better prediction for different degrees of penetrations. The resistance factors are both slightly in excess of the currently used value of 0.67 in connections. This latter value could be used safely with a 3% and 6% error, both on the safe side, for [6.2a] and [6.3a] respectively.

In Fig. 6.2, [6.2a] and [6.3a] are plotted for partial joint penetration groove welds for a unit area of plate in grade 300W steel made with matching E480XX electrodes. Also plotted in the figure is the strength as given by CSA Standard W59,

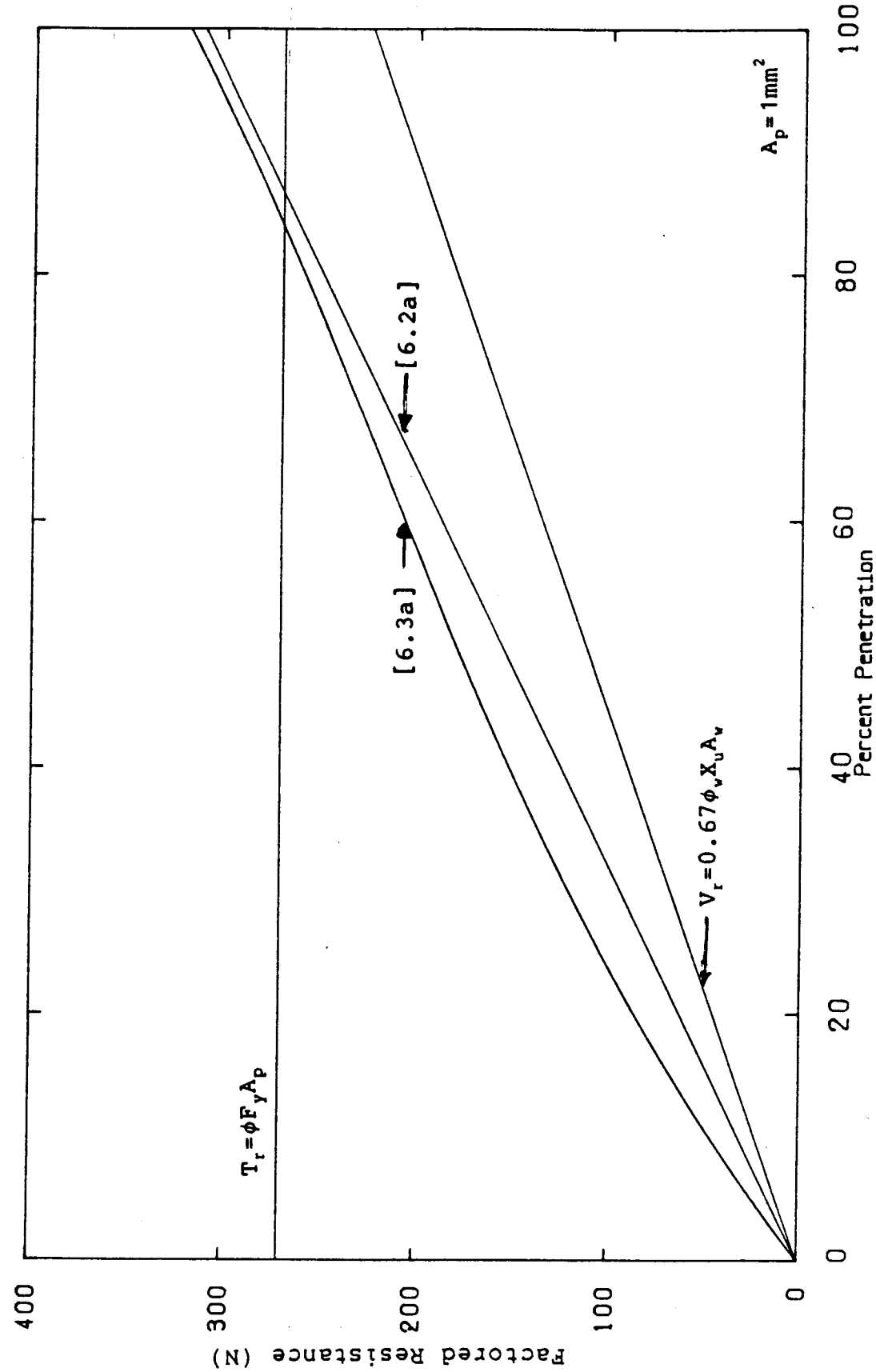

Figure 6.2 Comparison of Proposed and Current Design Equations

[2.14] $V_r = 0.67 \phi_w A_w X_u$

It is seen that [6.2a] gives results 1.39 times that of the current design equation and that [6.3a] is 1.00 to 1.05 times [6.2a]. Beyond 84% penetration for [6.3a] and 87% penetration for [6.2a] the respective equations give strengths greater than the factored resistance of the plate itself and therefore would not be applicable above these respective percentage penetrations.

6.2 Design for Ductility

All partial joint penetration groove welds exhibited considerable ductility in the weld itself as was evident from the significant joint rotations they underwent before failure. However, as the amount of weld metal that can deform is limited, the total deformation of the specimens was small in all those cases where the weld fractured before the plate yielded. To ensure overall ductility of welded members the fracture load on the weld should exceed the yield load on the plate area using [6.2] as the predictor equation gives

[6.7] $p A_p F_u > A_p F_y$, or

[6.8] $p > \frac{F_y}{F_u}$

in deterministic format. Fig. 6.3 shows [6.2], [6.3] and the equation for the tensile resistance

$$[6.9] \qquad T_r = F_y A_p$$

in unfactored form. For ductile behaviour the percent penetration must be greater than 67% when based on [6.2] and 62.5% found from equating [6.3] and [6.9], ie

$$[6.10] \qquad p\,(1.55 - 1.16p + 0.61p^2) > \frac{F_y}{F_u}$$

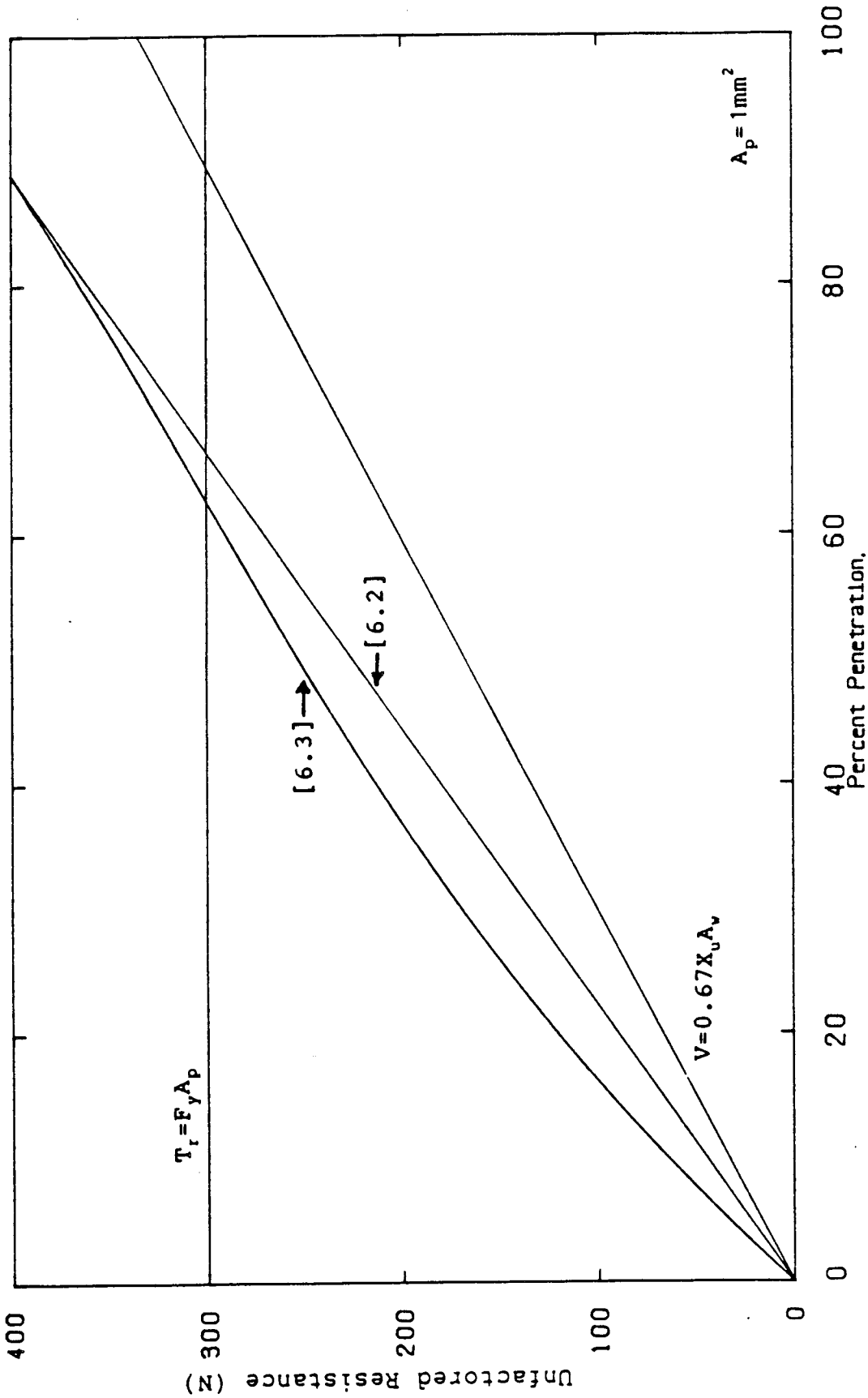

Figure 6.3 Comparison of Unfactored Design Equations

7. SUMMARY AND CONCLUSIONS

7.1 Summary and Conclusions

1. Although the literature review has shown, for the limited number of investigations that have been made, that the strength of partial joint penetration groove welds, loaded in direct tension, is directly related to the tensile strength of the weld material, current Canadian standards base the strength, in part, on the shear strength of the weld. The review also showed that the deformability of these welded members was limited, when the weld fractured before the plate yielded.

2. A total of 75 partial and full joint penetration groove weld specimens made with matching E48018 electrodes in grade 300W and 350A steel were tested. Weld preparation consisted of a 45° single bevel preparation 2-3mm deeper than the specified penetration. Penetrations from 20% to 100%, or complete penetration, were tested.

3. All partial joint penetration groove weld specimens failed in the weld on the fusion face of the specimen with the square preparation. The full joint penetration groove welds failed in the base plate some distance from the weld.

4. The analyses of the behaviour of the specimens, as verified by tests, showed that, though specimens tested singly and in pairs initially had combined axial and bending stresses on the weld, the tensile yielding of the weld dissipated the bending moment and the welds failed in tension.

5. The fracture surface appearances ranged from a silky smooth texture on a plane at approximately 45° to the plate surface for the 5mm welds to a crystalline surface on a plane at about 90° to the plate surface for the 20mm welds. The fracture always followed a fusion face.

6. There was no difference in ultimate strength whether specimens were tested singly or in pairs or with concentric loading.

7. The strength of partial joint penetration groove welds made with matching electrodes is linearly related to the ultimate strength of the base metal and directly, though not linearly, to the degree of weld penetration. The maximum normal and shear stress theories predict weld strengths equally well.

8. The ultimate strength of the joint, based on weld area, increases with decreasing weld penetration due to the development of lateral restraint in the weld arising

because the adjacent base plate is less heavily stressed.

9. Weld defects, based on data from this and other studies, decrease the joint strength in proportion to the area of the defects.

10. All welds had adequate ductility to accommodate the rotations that occurred in them with no loss of strength. The partial joint penetration groove welds thus exhibited considerable ductility. The entire specimen behaved in a ductile manner only if the strength of the weld exceeded the yield strength of the base plate.

11. The factored tensile resistance of partial joint penetration groove welds can be written as either

$$T_r = \phi \; p \; A_p \; F_u$$

where $\phi = 0.69$ or

$$T_r = \phi \; p \; A_p \; F_u \; (1.55 - 1.16p + 0.61p^2)$$

where $\phi = 0.71$ based on a reliability index of 4.5 and a coefficient of separation of 0.55. These equations

provide a minimum of 39% increase in tensile resistance for welds made with E480XX electrodes in 300W and 350A steel as compared to the existing resistance equations in CSA Standard W59-1984. The current resistance factor of 0.67 for welds as used in CSA Standard S16.1 would not be inappropiate. The latter equation based on the increased strength due to lateral restraint is strictly valid only for steels with ultimate strength/yield strength ratios less than about 1.5 and with width/thickness ratios similar to those examined.

12. To insure overall member ductility the plate area must yield before the weld fractures. For the 2 equations giving the tensile resistances this occurs when

$$p > \frac{F_y}{F_u}$$

and $$p(1.55 - 1.16p + 0.61p^2) > \frac{F_y}{F_u}$$

7.2 Areas of Further Research

Useful extensions of this work would be:

1. to investigate experimentally the effect, if any, of other types of weld preparation on the behaviour and ultimate strength of partial joint penetration groove welds,

2. to investigate the strength and behaviour of partial joint penetration groove welds reinforced with fillet

welds as may be used when joining a beam flange to a column flange in the shape of a Tee, and

3. an inelastic 3-dimensional finite element analysis of the stress conditions at failure, taking into account the inelastic values of Poisson's ratio, to assess the effect of restraint on the strength of the partial joint penetration groove weld.

REFERENCES

AMERICAN SOCIETY FOR TESTING AND MATERIAL (ASTM). 1977. Standard Methods and Definitions for Mechanical Testing of Steel Products. ASTM A370-77 Part (1), Philadelphia, Penn.

AMERICAN SOCIETY FOR TESTING AND MATERIAL (ASTM). 1961. Standard Test Method for Young's Modulus at Room Temperature. ASTM E111-61 Part (10), Philadelphia, Penn.

AMERICAN WELDING SOCIETY (AWS). 1979. Structural Welding Code. AWS D1.1-79, Miami, Fla.

BENT, R.M. 1983. Alternative Design of Partial Penetration Groove Welds. Report to W59 SC-1. Stelco Inc. Hamilton, Ont. 22pp.

BISKUP, J.T. 1969. Static Strength of Welded Joints with Defects. Proc. 2nd Conference on the Significance of Defects in Welds. The Welding Institute, London, May 29-30, Paper No. 6, 6pp.

CANADIAN STANDARDS ASSOCIATIONS (CSA). 1974. Steel Structures for Buildings-Limit States Design, CSA Standard S16.1-1974. Canadian Standards Association, Rexdale, Ontario, 114pp.

CANADIAN STANDARDS ASSOCIATIONS (CSA). 1980. Mild Steel Covered Arc Welding Electrodes. W48.1-M1980 Canadian Standards Association. Rexdale, Ontario.

CANADIAN STANDARDS ASSOCIATIONS (CSA). 1981. Structural Quality Steels, Standard CAN3-G40.21-M81. The Algoma Steel Corperation Limited, Sault Ste. Marie, Ontario, Canada.

CANADIAN STANDARDS ASSOCIATIONS (CSA). 1982. Welded Steel Construction (Metal Arc Welding), W59-1982. Canadian Standards Association, Rexdale,Ontario.

CANADIAN STANDARDS ASSOCIATIONS (CSA). 1984. Welded Steel Construction (Metal Arc Welding), W59-1984. Canadian Standards Association, Rexdale,Ontario.

GALAMBOS, T.V. and RAVINDRA, M.K. 1976. Load and Resistance Factor Design Criteria for Steel Buildings. Structural Division, Civil and Environmental Engineering Department, Washington University, St.Louis, MO, Research Report No. 27.

GRAY, T.G.F., and SPENCE, J. 1982. Rational Welding Design - Second Edition. Butterworths, Toronto, 308pp.

KULAK, G.L., ADAMS, P.F. and GILMOR, M.I. 1985. Limit States Design in Structural Steel. Canadian Institute of Steel Construction, Willowdale, Ontario, 321pp.

HONIG, E.M., and CARLSON, K.W. 1976. Tensile Properties of A514 Steel Butt Joints Containing Cluster Porosity. Welding Journal, American Welding Society, April, pp. 103s-107s.

KENNEDY, D.J.L., and GAD ALY, M. 1980. Limit States Design of Steel Structures - Performance Factors. Canadian Journal of Civil Eng., Vol. 7, pp. 45-77.

LAWRENCE, F.V., and COX, E.P. 1976. Influence of Inadequate Joint Penetration on Tensile Behaviour of A514 Steel Welds. Welding Journal, American Welding Society, May, pp. 113s-120s.

LAY, M.G. 1982. Structural Steel Fundamentals - An Engineering and Metallurgical Primer. Australian Road Research Board, Australia.

POPOV, E.P. and STEPHEN, R.M. 1977. Tensile Capacity of Partial Penetration Groove Welds. Jour. Struc. Div., ASCE, 103, ST9, Sept., pp. 1721-1729.

RATZLAFF, K.P., GAGNON, D.P. and KENNEDY, D.J.L. (in preparation). Experimental and Analytical Study of Poisson's Ratio for Inelastic Steel Strains.

SALMON, C.G. and JOHNSON, J.E. 1980. Steel Structures: Design and Behaviour, 2nd Edition. Harper and Row, New York, 1007pp.

SATOH, K., SEO, K., HIGUCHI, G. and YATAGI, T. 1974. Experimental Study on the Mechanical Behaviour and Tensile Strength of Partial Penetration Groove Welded Joint. Trans. Japan Welding Society, 5, No. 2, Sept., pp.198-206.